UNIVERSITÀ
DEGLI STUDI
DI PADOVA

UNIVERSITÀ DEGLI STUDI DI PADOVA

DIPARTIMENTO DI INGEGNERIA ELETTRICA

SCUOLA DI DOTTORATO DI RICERCA IN INGEGNERIA INDUSTRIALE

INDIRIZZO IN INGEGNERIA ELETTROTECNICA

CICLO XXIII

Modeling and Management of Smart Energy Networks

Direttore della Scuola: Ch.mo Prof. Paolo Bariani _____

Coordinatore d'indirizzo: Ch.mo Prof. Giovanni Martinelli _____

Supervisore: Ch.mo Prof. Roberto Turri _____

Dottorando: Loredana Carradore

_____

31 Gennaio 2011

dedicate to *nonna Amelia*

Abstract

"Smart grids" identifies what future electrical network would represent: an intelligent integrated system where every device available to modify their generation/absorption is responsive, awaken of its role, eco-sensitive, flexible and interconnected with others.

In this scenario, smart technologies, such as Information and Communication Technologies and smart meters, will allow interconnections and interactions among these devices that are available to participate in ancillary services; whereas a smart management system would ensure quality, reliability, efficiency, effectiveness in the supply service and the free participation in services for the grid support of these new customers.

However, even if the smart grid scenario seems to be clearly defined, investigation on the management system is still required, in order to efficiently co-ordinate all distributed resources in distribution networks and to exploit the potentiality of new possible participants in the network regulation, such us energy storage devices and electrical vehicles.

By the way, energy markets seem to be ideally suited to support the system operator in the co-ordination of different energy resources, also allowing the exploitation of synergy among different energy carries to increase the overall efficiency and reliability of the system. In fact, energy markets could create suitable price signals able to make responsive devices available to modify their generation/absorption to network requirements. For this reason, it seems reasonable to refer to these devices as customers.

Investigations on smart management procedures for the co-ordination of different resources in energy networks is the main thread of this thesis. In particular, the importance of price signals to obtain a virtuous behavior of customers has been exploited, focusing on co-ordinated management procedures, in order to ensure the management of the complex electrical network system.

In the first chapter a brief introduction to smart grids, energy markets and storage devices is provided, in order to present general background and motivation of this work. The modeling basis of the software environment developed during the PhD and used to investigate management issues in smart energy network are presented in chapter 2. Chapter 3 presents preliminary investigations on energy hub, a generation, conversion and storage center, management based on suitable price signals to optimally manage exchanges of flows among different energy vectors, in order to exploit synergy properties. In chapter 4, investigation on the management of a multi-energy vector systems through price coefficients is presented. In particular, price coefficients

proportional to reference signals, that represents network requirements, have been analyzed in a decoupled management procedure between network and energy hubs with storage devices. In chapter 5, it is described how to exploit this decoupled optimisation procedure, considering aggregators of EVs as flexible distributed storage devices. In chapter 6, an innovative management procedure based on token ring philosophy, aimed to co-ordinate distributed resources, ensuring their free participation in services for the grid support is proposed. The thesis ends with chapter 7, where the most important achievements and suggests in possible future work are summarizes and discusses.

Sommario

Con “smart grids” si può identificare quello che rappresenteranno le reti elettriche del futuro, ovvero un sistema integrato ed intelligente, dove ogni dispositivo disponibile a modificare la propria generazione e il proprio assorbimento, è reattivo, attento ai segnali di prezzo, consapevole del proprio ruolo, sensibile agli aspetti ambientali, flessibile e interconnesso con gli altri.

In questo scenario, tecnologie intelligenti, come i sistemi ICT (Information and Communication Technologies) e gli smart meter, permetteranno le interconnesioni e le interazioni tra questi dispositivi disponibili a partecipare nei servizi ancillari; mentre un sistema di gestione intelligente dovrebbe essere in grado di assicurare qualità, affidabilità, efficienza, efficacia nel servizio di fornitura e la libera partecipazione nei servizi per il supporto della rete di questi nuovi clienti.

Sebbene lo scenario identificato dal termine “smart grids” sembri essere chiaramente definito, risulta ancora necessario lo studio relativo al sistema di gestione fondamentale per coordinare in maniera efficiente le risorse distribuite nelle reti di distribuzione e le potenzialità introdotte da nuovi possibili participanti nella regolazione della rete, come per esempio i sistemi di accumulo e i veicoli elettrici.

A questo proposito, i mercati energetici sembrano ideali per aiutare l’operatore di sistema a coinvolgere tutte le risorse energetiche nella regolazione della rete, permettendo anche lo sfruttamento della singergia tra differenti vettori energetici, allo scopo di incrementare l’efficienza e l’affidabilità generale di tutto il sistema. Infatti, i mercati energetici possono creare appropriati segnali di prezzo in grado di rendere sensibili alle esigenze della rete quei dispositivi disponibili a modificare la loro generazione e il loro assorbimento. È per questo motivo che sembra opportuno identificare questi dispositivi come clienti.

Il principale filo conduttore di questa tesi è stato la ricerca di procedure intelligenti di gestione per la coordinazione di differenti risorse nelle future reti energetiche intelligenti. In particolare, è stata sfruttata l’idea chiave dell’importanza dei segnali di prezzo per ottenere un comportamento virtuoso dei clienti, concentrandosi su metodi di coordinamento in grado di assicurare con meccanismi semplici la gestione di un complesso sistema come quello della rete elettrica.

Nel primo capitolo di questa tesi è presente una breve introduzione alle smart grids, ai mercati energetici e ai sistemi di accumulo, al solo scopo di presentare background e motivazioni di questo lavoro. Il capitolo 2 raccoglie le basi teoriche della modellizzazione dell’ambiente software sviluppato durante il dottorato e usato per studiare la gestione in reti energetiche intelligenti. Il capitolo 3 presenta le prime indagini sulla gestione di un energy hub, un centro di generazione, conversione e

assorbimento, basata su segnali di prezzo adeguati a permettere una gestione ottima di flussi tra differenti vettori energetici, in modo da sfruttare la loro sinergia. Il capitolo 4 riporta quanto studiato per la gestione di un sistema multi-vettore energetico attraverso coefficienti di prezzo. In particolare, è stata analizzata la possibilità di utilizzare termini di prezzo proporzionali ad un segnale di riferimento che rappresenti la richiesta della rete in una gestione disaccoppiata di rete ed energy hub con sistemi di accumulo. Questa precudura di ottimizzazione disaccoppiata è stata applicata nel capitolo 5 a degli agglomerati di veicoli elettrici, intesi come sistemi di accumulo flessibili e distribuiti. Nel capitolo 6, infine, viene presentata un'innovativa procedura di gestione, basata sulla filosofia del token ring, mirata a coordinare risorse distribuite assicurando la loro libera partecipazione nei servizi per il supporto della rete. La tesi si chiude con il capitolo 7, che riassume e discute i più importanti traguardi raggiunti e suggerendo possibili futuri lavori.

List of publications

The work reported in this thesis is basically covered by the following publications:

- L. Carradore, F. Bignucolo, "Distributed Multi-Generation and Application of the Energy Hub Concept in Future Networks", Universities Power Engineering Conference 2008, 1–4 Sept. 2008, Padova (con presentazione poster alla conferenza)
- D. Poli, S. Barsali, L. Carradore, R. Turri, S. Scalari, "Integration of process-side energy storage and active distribution networks: technical and economical optimisation", CIRED 2009, Prague
- L. Carradore, R. Turri, "Modeling and Simulation of Multi-Vector Energy Systems", Bucharest PowerTech'2009
- L. Carradore, R. Turri, "Optimal co-ordinated operation of distributed multi-generation in active distribution networks", Universities Power Engineering Conference 2009, Glasgow, UK, 1-4 Sept. 2009
- L. Carradore, R. Turri, "Gestione coordinata di risorse distribuite in reti elettriche MT", AEIT 2009, Catania, Italia, 27–29 Sept. 2009
- L. Carradore, R. Turri, L.M. Cipcigan, P. Papadopoulos, "Electric Vehicles as flexible energy storage systems in power distribution networks", EVER 2010, Montecarlo, Monaco, 25-28 March 2010
- F. Bignucolo, R. Caldon, L. Carradore, A. Sacco, R. Turri, "Role of storage systems and market based ancillary services in active distribution networks management", CIGRÉ 2010, Paris, France, 22–27 Aug. 2010
- L. Carradore, R. Turri, "Distributed Co-ordinated Power Management in MV Electrical Networks", Universities Power Engineering Conference 2010, Cardiff, UK, 31 Agosto – 3 Sept. 2010
- L. Carradore, R. Turri, "Electric Vehicles Participation in Distribution Network Voltage Regulation", Universities Power Engineering Conference 2010, Cardiff, UK, 31 Agosto –3 Sept. 2010
- S. Skarvelis-Kazakos, P. Papadopoulos, I. Grau, A. Gerber, L.M. Cipcigan, N. Jenkins, L. Carradore, "Carbon Optimized Virtual Power Plant with Electric Vehicles", Universities Power Engineering Conference 2010, Cardiff, UK, 31 Aug. –3 Sept. 2010

- L. Carradore, R. Turri, “A Token Ring Procedure for Distributed Co-ordinated Regulation of Active MV Networks”, ICHQP 2010, Bergamo, Italia, 26 –29 Sept. 2010

Acknowledgment

I'd like to thank my supervisor Prof. Roberto Turri for supporting and trusting me during the last three years. His cooperation and his friendship have really been appreciated.

Thanks to UPEC 2008 held in Padova which was an opportunity to have a unique experience and get to know new people. Thanks a lot to those who made it possible.

I can't help mentioning Maurizio (and Gabriel as well) for his help during my stay in Cardiff, for the Italian coffee he made me in the morning and the weekend "cousine sessions" together.

Many thanks to Valeria who shared many meals and Matteo, my first colleague, who very often liked talking and listening to me also sharing the first months of my "PhD adventure".

I can't forget all my friends, my family (pets included) who have believed in me and Leonardo in particular.

Loredana

Contents

List of Figures

List of Tables

Notation

Symbols and acronyms that occur frequently in this thesis are listed below. Other less frequently used symbols are defined in the text.

Acronyms

CHP, Combined Heat and Power

CSV, Comma-Separated Values

DG, Distributed Generation

DSM, Distribution System Management

ESS, Energy Storage System

EVs, Electric Vehicles

HEVs, Hybrid Electric Vehicles

ICT, Information and Communication Technologies

OOP, Object-Oriented Programming

OPF, Optimal Power Flow

PBT, Pay Back Time

PF, Power Flow

PEVs, Plug-in Electric Vehicles

PHEVs, Plug-in Hybrid Electric Vehicles

RES, Renewable Energy Sources

SOC, Status of Charge

SS, Swapping Station

V2G, Vehicle-to-Grid

pu, per unit

mu, monetary unit

Vectors and matrices

C, coupling matrix

$\dot{\boldsymbol{E}}$, storage energy derivatives vector

J, Jacobian matrix

L, vector of loads

p, pressure vector

P, (active) power vector

Q, reactive power vector

S, storage coupling matrix

tap, tap position vector of the OLTC transformers

V, module voltage vector

x, unknown vector

$\boldsymbol{\Delta p}$, pressure variation vector

$\boldsymbol{\theta}$, phase angle vector

Scalars

c, cost coefficient

$c_{\alpha\beta}$, coupling matrix coefficient between energy vectors α and β

dt, time step

dE, energy variation in dt

E, energy

I, current

p_{th}, pressure (thermal network)

p_{gas}, pressure (natural gas network)

p, price coefficient

P, (active) power

Q, reactive power

S, apparent power

T, time period

tap, tap position of the OLTC transformer

V, module voltage

Δp, price variation

ΔP, active power variation

ΔQ, reactive power variation

ΔV, module voltage variation

$\Delta\theta$, phase angle voltage variation

η, efficiency

ν, dispatch factor

Miscellaneous

f, objective function

n, total number of nodes

n_b, total number of branches

n_{ESS}, total number of ESSs

n_g, total number of generators

n_l, total number of loads

n_{PQ}, total number of PQ nodes

n_{PV}, total number of PV nodes

n_{SL}, total number of SL nodes

n_T, total number of time steps

n_{tr}, total number of OLTC transformers

n_v, total number of control devices

PQ, node with known active and reactive power

PV, node with known active power and module voltage

SL, slack node

Subscripts or superscripts

base, base value

c, converter

CHP, CHP plant

el, electrical

ex, heating exchanger

f, furnace

gas, natural gas

h, the h-th energy hub

in, input

init, initial

max, maximum

min, minimum

opt, optimal

out, output

P, active power

Q, reactive power

ref, reference

t, the t-th time step

th, thermal

w, the w-th ESS

α *and* β, energy carriers

0, starting

1 Introduction

Smart grids will increase opportunities for future distribution networks, thanks to their high level of interconnections. Interactivity among different distributed resources requires investigations on the management procedure, key to ensure the coordination of resources, maximizing benefits of networks, consumers and producers. The importance of energy markets to introduce new opportunities for consumers and producers and energy storage devices to add flexibility to electrical networks completes the scenario of energy networks of the future.

In this following, background and motivation of this work is briefly described.

1.1 Smart grids and smart energy networks

Smart grids concept responds to requirements of renewal and innovation of the electrical grid, due to the increasing of energy consumption and of standards of supplies. Security and sustainability, reliability, efficiency, effectiveness and environmental sustainability are mandatory characteristics for the distribution network of the future, that requires high quality levels of the supply service, at minimum costs and reduced environmental impact [1].

Smart grids will be flexible, to ensure responsiveness in both emergency and standard conditions, accessible to every consumers and producers that should be accommodated disregarding its intrinsic characteristics, reliable, to guarantee quality and security standard for the supply service, and economical, to maximize effectiveness with interesting investments.

However smart grids is not only a concept. Smart grids consist of technologies that create an intelligent framework where smart grid functionalities could be exploited. Electronic controls and smart meters will enforce the involvement of resources, increasing their opportunities, whereas new value will be created for all actors involved in this scenario. In particular, new intelligent Information and Communication Technologies (ICTs) which allow reliable and secure transmission of information to where it is needed on the grid are fundamental to make responsive all distributed resources available in the network.

In fact, the vision of the Internet model inspires the future electrical network: "Every node in the electrical network of the future will be awake, responsive, adaptive, price-smart, eco-sensitive, real-time, flexible, humming and interconnected with everything else" (Source: The Wired). Interactivity will design networks of the future, letting everyone to have access to network; for example ensuring the maximum

penetration level of Distributed Generation (DG) and Renewable Energy Sources (RES) [2]. Each node would take part in the Demand-Side Management (DSM) according to network needs with the possibility of a real-time observability, controllability and process efficiency optimisation.

All these innovations require an equivalent evolution in the management approach [3]. Opportunities introduced by smart grids require to be exploited with innovative and intelligent control systems, that maximizes performance of the overall system and integrates all introduced challenges. In particular, co-ordination could be considered the keyword to understand and make feasible smart grids. Co-ordination of distributed resources, located at different nodes, that exchange information, that interact with other resources, being conscious of their importance in the global system, is key to manage a responsive and adaptive network.

1.1.1 Toward a multi-vector network

Smart grids are important for the development of new opportunities not only in electrical networks. Smart grids technologies could be vehicle of deep changes in the management of all energy systems, exploiting interactions among different energy vectors and their synergy. This means taking advantage from the specific behavior of the energy carrier, ensuring a high level of integration and consciousness of the importance of co-ordination of different contributions.

Energy has an important role in the development of human society. Economy, public health, safety of people and businesses are directly related to energy conditions. In particular, electricity is the main interchangeable energy carrier that could be converted from and to other forms. Furthermore electrical network is the most critical strategic infrastructure in our society. In fact it is a complex widely extended system from which other infrastructures depend. To ensure the functioning of the whole system, a resilient, reliable, secure, quality and convenient electric transmission and distribution grid has to be ensured.

The recent growth of energy consumption concerns not only electrical demand. Thermal and chemical needs grow up and hydrogen technologies are emerging or substituting other fossil fuel based in a long-term vision. These and other different energy carriers are usually considered and managed independently, except for cogeneration and tri-generation plants that have already demonstrated to be the most efficient form of combined generation [4].

Considering different political, social and economical goals as well as the need of differentiate the combustible park, reduction of harmful emissions, economical use of resources, demand supply etc, the effective possibility to evolve towards a multivector network is understandable.

A multi-source multi-product system would be able to add degrees of freedom and flexibility to independent supply infrastructures because a sort of redundancy effect is created. The same amount of power can be delivered from a different combination of energy carriers. The interconnection between different energy carrier means greater levels of reliability of supply and the shortage availability of a resource could be easily handled [5, 6, 7].

Particularly, considering the electrical network and smart grids, integration of different energy vector seems to be a further step towards smart energy networks.

1.2 Energy markets role

Smart grids have been defined "economical". This means to ensure efficiency on deployment of resources and create new opportunities for all resources involved in these challenges, through the energy markets evolution according to smart grids requirements. Liberalised markets will encourage trading opportunities to be identified and developed and will make producers and consumers more aware of their opportunities and more responsive to network needing.

The importance of energy markets are evidenced by the influence of economic aspects in politic decisions. Efficiency, environmental matters and safety affect the market structure since economic considerations influence energy policies, whereas technical-environmental and political decisions are driven by economical conditions in order to provide the necessary incentives for investments. As an example, nowadays resource portfolio, unit commitment and dispatch, technical intervention to increase efficiency or to reduce emissions are evaluated by means of investments and fuel costs. For these reasons, energy markets are yet evolving from a vertical integrated structure to a retail market where both consumers and producers have freedom to choose their production and consumption politics.

In this context, the management of energy networks could not avoid economical considerations. Additionally, the innovation in the control system due to technical improvements requires an equivalent evolution in energy markets. In particular, market based methods seem to be desirable to create added value for all resources and new opportunities, making resources a new actor in the regulation scenario of smart grids [1]. In this way, energy markets will be an important part of the management framework of smart grids.

Energy markets have the important role to increase awareness of the customers of their importance in a smart grids scenario, which aims to achieve high quality standards in the supply service with the participation of all distributed resources in the grid regulation. Their main goal is to activate responsive behaviour of producers and consumers in smart grids, allowing the exploitation of capillary and real-time signals, available thanks to smart installed technologies [8]. At this point, resources could be named customers, referring to all owners of devices (loads, generators and storage devices) available to participate in grid regulation, modifying their actual generation/absorption to support the grid, depending on suitable price signals.

1.3 Energy storage devices

Distributed Energy Storages (DES) will actively participate in grids evolution towards smart grids, due to their ability to supply the stored energy when and where it is critically needed [9]. Energy devices can add flexibility to the electrical grid providing ancillary services, behaving like a load or a generator, improving the stability of the system and the management of the high penetration of distributed generators, reliability of supply and power quality offering a great number of services for the grid support [10, 11]. Storage units can provide load levelling, charging during off-peak load periods when the energy cost is low and discharging during peak periods characterized by higher energy values. In this way it is possible to provide load levelling service and to increase efficiency and life time of generators, which can operate

at more constant and at nearer to optimum output power for longer periods. More efficient generators can be used to reduce the fuel consumption adding environmental benefits, increasing their production during cheaper hours instead of using less efficient plants during peak hours. Storage units can increase both generation capacity, transferring generations during the day and from/to different areas, and transmission capacity, charging during off-peak periods and discharging to reduce loading of lines during peak periods. Energy storages can add value to renewable generators negatively characterized by stochastic behaviour and with low amount of full load hours, as wind and photovoltaic generators, balancing the power fluctuations with a general increase of their availability [9].

Thanks to recent developments in both storage and electronic interface technologies, storage devices can rapidly supply big amount of power, both active and reactive. In this way, it is possible to provide power and frequency regulation for the stability of the system and voltage regulation without the emissions of the conventional plants. Stored energy can also provide black start and power support for uninterruptible resources and energy devices can thus substitute traditional plants for spinning reserve and manage, in a more efficient way, bulk energy resources shifting the energy absorption.

Many technologies are available to provide these services but they are penalized by high investment costs, siting and technical characteristics limitations [12]. Pumped hydroelectric systems are well-developed, traditionally used to discharge the stored water during peak hours, to generate energy when the demand is high. This means to produce electricity during peak periods at lower costs, as Compressed Air Energy Storage (CAES), which uses stored air to produce energy through turbines. Superconducting Magnetic Energy Storage (SMES) is characterized by high efficiency and fast response capability. Flywheel energy storage systems are best suited to short duration, high-power discharges, for example over time periods of several minutes. They have extended cycle lives, higher power to energy ratios than Battery Energy Storage Systems (BESS), which are the most attractive technology, for its cost-effectiveness [12]. The most known battery technologies are Sodium Sulphur batteries (NaS), characterized by high energy density and high cycle life, no emissions during operation and the cost is not so high; Nickel Cadmium batteries (NiCd), a mature technology, that could be scaled into a relatively large systems, but suffering from a memory effect and must be periodically exercised and environmental problems (cadmium is toxic); Lead Acid (PbA), another mature technology, characterized by short life cycle and lowest energy density; and the well-known Lithium Ion (Li-ion) technology, which is continuously under investigation to improve its characteristics, with particular focus on application on electric vehicles, due to high energy density [13].

In this work, energy storage devices have been considered for the importance to provide services for the grid support. The investigation focus on electric batteries, even if all technologies could be employed for network regulation purposes, as can be drawn from table 1.1 [14] due to their promising expectations for the future. Particular focus has been given to Electrical Vehicles (EVs), that recognized as a storage device able to provide ancillary services in table 1.1. EVs that could be plugged into the grid to re-charge their on-board batteries could provide active power regulation, thanks to Vehicle-to-Grid (V2G) technologies, that allow bi-directional flows

Table 1.1: Mapping of Technology to Balancing Service Capability.

	Frequency Response	*Fast Reserve*	*Fast Start*	*STOR*	*Energy Balancing*	*Reactive Power*	*Black start*
Pumped Storage	✓	✓	✓	✓	✓	✓	✓
Compressed air storage	✓	–	–	✓	✓	✓	✓
Flywheel	✓	✓	–	–	–	✓	–
Supercapacitor	✓	–	–	–	–	–	–
Battery technologies	✓	✓	✓	✓	✓	✓	✓
Dynamic Demand	✓	–	–	–	–	–	–
Smart Metering	✓	✓	✓	✓	–	–	–
Electric Vehicles	✓	✓	✓	✓	–	–	–
Large industrial sites	✓	✓	✓	✓	✓	✓	✓
OCGT Generation	✓	✓	✓	✓	✓	✓	✓

between the grid and EVs. However, re-charging infrastructures and electronic interfaces between the grid and EVs (four quadrant converter) could allow the exploitation of the reactive power regulation, that is not usually considered, in particular due to the lack of a suitable remuneration of this service. Promising results could be achieved, considering that the reactive power management does not affect the status of charge of the on-board batteries (no degradation aspects) and that energy markets, and particularly the reactive power price scenario [15], are expected to evolve in the future.

2 The Modeling Basis of the Software Environment

In this chapter, the software program developed during the PhD activities is presented. The Matlab® Object-Oriented Programming and fmincon optimisation tool have been used to develop a software platform, specifically aimed at investigating the role of storage devices in electrical networks. Main features are calculations for electrical, natural gas and thermal networks and the optimisation for stand-alone energy hubs and networks power flow and for networks with energy hubs, whose modeling details are described.

2.1 Introduction

The aim of this chapter is to present the software platform developed in this work for simulating and optimising the operation of multi-energy vectors network and the modeling basis of its main procedures.

A general description of the structure of the software is given, with particular emphasis on the Object-Oriented Programming (OOP) structure used to improve efficiency and effectiveness of the software implementation.

The conceptual scheme of the software is provided, focusing on the multi-level structure used for two main reasons. Firstly, in order to obtain a comprehensive software environment, able to allow investigation of different aspects in a multi-energy vectors network system. This structure enable to activate specific modules depending on the particular needs, in order for example to investigate a specific network or the whole system, a specific virtual utility or energy hub.

Secondly, a multi-level structure better resembles the general concept of problem decomposition, which aims to simplify a complex process decomposing into easier sub-processes. With regard to the management problem of energy networks, the management problem decomposition in different levels would provide a solution very close to the solution available with a centralized management system. Sub-problems should act independently each others focusing on specific purposes, but accounting for others thanks to suitable signals (reference profiles or prices), main thread of this thesis.

The core of the system is represented by the models of the network, energy hub and virtual power plant, which account for all physical devices installed and their

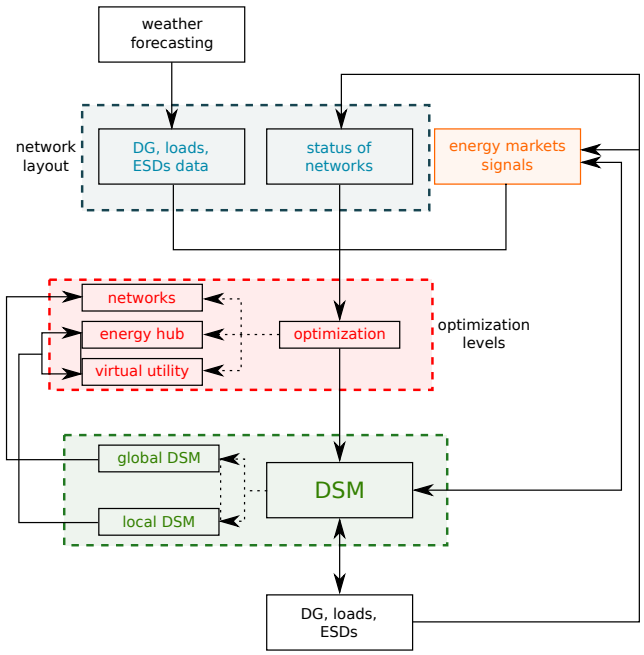

Figure 2.1: Conceptual scheme of multi-vector algorithm. Arrows show one or two-sided interactions, dotted arrows elements.

mutual interactions. In this chapter their modeling are described, representing the general basis for all other chapters.

2.2 Structure of the software environment

2.2.1 Conceptual scheme of the software

A conceptual scheme of the developed software environment is depicted in fig. 2.1. Data represents realistic estimates of generation/consumption curves of all customers (weather forecast data will enable to assess realistic renewable resources production trends) and it is used for defining the initial network status condition. This information is provided as input data to the optimisation section of the algorithm, that aims to provide new set points for all control devices in the networks to define a new optimal network status. In order to achieve different knowledge level, the optimisation section is divided in two sub-levels. The first global level operates on the multi-vector network (or networks in fig. 2.1) in order to satisfy demand and supply side requirements respecting the different technical constraints. The second level is aimed at the economical optimisation of both the multi-vector exchange energy hubs and of the virtual utilities, on the basis of the suitably modulated energy market signals.

The Distribution System Management (DSM) receives new set points provided by the optimisation section for all control devices in networks and exchange information with networks and active devices and with optimisation sections, if it is necessary to

consider different aspects in the management of the global system. New set points are provided by the DSM to the active devices to define the new optimal system status. The DSM, in turn, is considered to operate at two-levels: a global level which interacts with the multi-vector network and a local one with the energy hubs and virtual utilities. The DSM will also dynamically modify the status of the networks and provide up-dated input information to modulate energy markets signals.

Particular attention is given to energy market signals, which represent a key factor to achieve the best result from the technical point of view at minimum cost for system operator managing the energy system. It is foreseen that energy market signals would be suitably modulated on the basis of network needs. For instance, active and reactive power production/consumption nodal prices can be varied depending on local voltage profile, line losses and congestions, environmental issues, etc. in order to provide incentives to the producer/consumer to operate near the network optimal set points, still maximizing its own revenue [8].

2.2.2 Object-Oriented Programming structure

The software environment has been developed with Matlab® using the recent Object-Oriented Programming (OOP), available in Matlab® since R2008a release [16]. OOP is based on objects, data structures with attributes (data fields) and methods to get access and modify them. OOP defines entities and their relationships creating a hierarchical structure based on information hiding, which allows to abstract programming process, representing real entities with objects. In this thesis, OOP has been adopted to improve Matlab® efficiency declaring new data types, to improve the software structure development and to consider similarities among different networks.

The *MultiNetwork* software environment is mainly structured in classes and packages.

In OOP, a class is a template for an object that gives the definition of objects, characterized by methods and attributes (or properties, as called in Matlab®). Attributes are data fields that defines characteristics of objects and methods define operations (functions in Matlab®) available for objects of specific classes.

Packages is a mechanism to organized classes, an abstract container used to define a scope for the contents of the package directory. This means that function and class names need to be unique only within the package. Using a package provides a means to organize classes and functions and to select names for these components that can be reused in other packages. In Matlab® , packages are represented by special directories that can contain class directories, functions, and other packages.

In the software environment, five manly packages are identified as:

- *Systems*, which contains network classes;
- *Elements*, with network components classes;
- *Types*, which contains libraries of network elements classes;
- *Charts*, with libraries of loading profiles classes;
- *Tariff*, with tariff classes.

Network classes in Systems package are:

- *Networks*, a generic class for networks;
- *ElectricalNetwork*, electrical network class;
- *PipelineNetwork*, pipeline network class and its specialized version for thermal network (*ThermalNetwork* class) and natural gas network (*GasNetwork* class).

Attributes of network classes are lists of instances of their components, loaded from a CSV file structure, that allows portability in all operating systems (supported by Matlab®).

Lists are ordered by the software depending on power flow requirements, avoiding pre-processed data in CSV files. As an example, *Bus*, *Branch*, *Transformer*, *Generator* and *Load* instances are listed in *busses*, *branches*, *transformers*, *generators* and *loads* attributes of *ElectricalNetwork* instance. Whereas *Branch*, *Transformer* and *Load* instances are loaded according to the order specified in CSV files, *Generator* instances are ordered depending on their control variables (defined by their typology) due to power flow implementation, which needs to group generators in a specific way; and *Bus* instances are created with regard to data of each component which defines the reference name (*ID*) of connection node, according to generators order, loads order and, finally, to branches and transformers order (nodes where no generators or loads are connected). Any CSV file with a node list is thus required.

In *Elements* packages, each element/component of each network is represented by a class. Generic classes are available

- for nodes, *Bus*, with ID and position attributes;
- for branches, *Branch*, with ID, starting and ending nodes attributes;
- for devices, *Device*, with ID, rate factor, daily, monthly and yearly load profiles, status, abbreviation with library instance, connection bus and prices with *Prices*, a class used to define prices for generation and adsorption of generators and loads, instance attributes, which are the information used to define an element connected to a bus;
- for energy hubs, *EnergyHub*, with an attribute for each device and other technical information about energy hub modeling (matrices, data, coefficients), an attribute for each input energy vector containing energy vector nodes from which the energy hub derives and an attribute with the ID;
- for chp and storages, *CHP* and *Storage*, with ID, hub that belongs to, abbreviation and other specific information.

Specialized version of generic classes are grouped in specific packages for each energy network and inheritates properties and methods of generic "parent" classes, called superclasses, and can introduce their own.

Inheritance property of classes is an interesting feature of OOP, that has enabled to consider similarities among different networks and components and to use handle object properties. In Matlab® *Handle* class allows objects indirectly refer its data, emulating variables by reference available with other programming languages [16]. In fact, passing variables to function causes Matlab® to create and assign or pass a copy

of the original variable. With handle objects, it is possible to refer to the original variable of objects, called instances, and an element network instance could be accessible by its instance or by the list of elements in network attributes. *Handle* class allows to link elements of networks, referring to an unique original variable. For example, a generator is connected to a node. Generator and node instances are listed in generators and busses properties of *ElectricalNetwork* instance. Generator instance contains information about the connecting node in bus property. The contents of bus property is the correspondent node instance. The node instance in busses property of *ElectricalNetwork* instance and in bus property of *Generator* instance is the same variable. A change in that *Bus* in busses list or in bus is the same. For this reason, all classes are subclasses of *Handle* class.

Types package contains packages for each energy vector, which contains libraries for each elements in networks. In this way, for each element is possible to specify an *abbreviation* associated with an element type, which identifies some technical characteristics not dependent on specific element. For example, a branch type loads kilometers resistance, inductance, capacitance, susceptance and maximum current values; A generator type loads nominal powers, nominal voltage and constraints (capability curve) etc.

Charts objects in *Charts* package represent daily, monthly and yearly power profiles. Each profile represents a typology of profile (industrial, commercial, residential and tertiary loads, for example, wind, photovoltaic, hydro and fuel generators).

Tariff package contains Tariff superclass and two subclasses that describes electrical and thermal tariffs, with their coefficients costant and proportional to power and energy.

All classes are characterized by a constructor method, the method that creates new instances, and methods that represent the available operations for those specific instances. All *Elements* are characterized by methods for attributes updating, *EnergyHub* by methods for its optimisation, network classes by methods to load all attributes, to execute power flow and optimisation etc. In the next sections, the modeling basis for the main methods are presented. In particular:

- energy hub modeling, used to model *Storage* and *EnergyHub* instances;
- electrical and pipeline network power flow modeling, used in power flow methods in classes for electrical and pipeline network respectively;
- energy hub optimisation modeling, used in optimisation methods in class for energy hubs;
- electrical network optimal power flow modeling, used in optimal power flow methods in class for electrical networks;
- multi-energy carrier optimal power flow modeling, used in optimal power flow method of *Networks* class.

2.3 Energy hub concept

The energy hub is an interface between different types of energy vectors, aimed at efficiently transferring multiple energy flows [17]. Its usefulness is the simplicity of

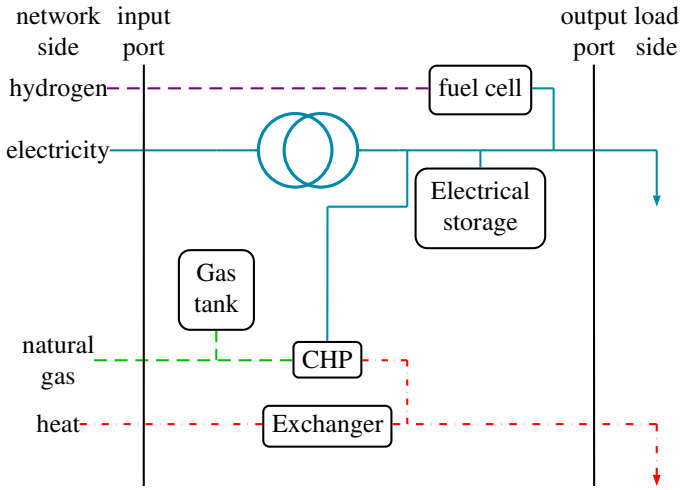

Figure 2.2: Example of energy hub.

its generalized matrix model for network (in particular for a multi-vector network) modeling which may describe whatever configuration of generation, conversion and storage element. In this perspective, the energy hub is like a *black box* for the system wherein energy carriers flow in different energy forms to satisfy network needs.

Typical elements composing an energy hub are power electronic converters, (micro) gas turbines, fuel cells, heat exchangers, batteries, gas tanks, etc, as schematically represented in figure 2.2.

2.3.1 Energy hub modeling

With reference to a generic energy hub (figure 2.2), energy carriers from an output port m (vector $\boldsymbol{L}$) to an input port n (vector $\boldsymbol{P}$) are related by a forward coupling matrix $\boldsymbol{C}$.

$$\underbrace{\begin{bmatrix} L_\alpha \\ L_\beta \\ \vdots \\ L_\omega \end{bmatrix}}_{\boldsymbol{L}} = \underbrace{\begin{bmatrix} c_{\alpha\alpha} & c_{\beta\alpha} & c_{\gamma\alpha} & \dots & c_{\omega\alpha} \\ c_{\alpha\beta} & c_{\beta\beta} & c_{\gamma\beta} & \dots & c_{\omega\beta} \\ \vdots & \vdots & \vdots & \ddots & \vdots \\ c_{\alpha\omega} & c_{\beta\omega} & c_{\gamma\omega} & \dots & c_{\omega\omega} \end{bmatrix}}_{\boldsymbol{C}} \underbrace{\begin{bmatrix} P_\alpha \\ P_\beta \\ \vdots \\ P_\omega \end{bmatrix}}_{\boldsymbol{P}} \tag{2.1}$$

The coefficients of coupling matrix $\boldsymbol{C}$ represent the relationships between each pair of energy carriers (for instance $c_{\alpha\beta}$ is the relationship between the energy carriers α and β). They consider both the conversion efficiency of the converters, depending on the converted power, and the internal partition of an input energy carrier into several converters each.

Each coefficient of the coupling matrix ($c_{\alpha\beta}$) is subject to conservation of power physical law, which ensures no power could be gained from a conversion and the output of a single energy carrier has to be equal or less than its input. Equations 2.2 and 2.3, representing these constraints in a mathematical form, have to be verified for each energy carrier.

$$0 \leq c_{\alpha\beta} \leq 1 \quad \forall \alpha, \beta \in \epsilon = \{\text{energy carriers whole}\} \tag{2.2}$$

$$0 \leq \sum_{\beta \in \epsilon} c_{\alpha\beta} \leq 1 \quad \forall \alpha \in \epsilon \tag{2.3}$$

Dispatch factors $v_{\alpha\beta}$ represent the internal-hub partition of an energy carrier, that could feed different converters (or a converter and the output port, as depicted in fig. 2.2 for the natural gas). Similarly to coefficients of coupling matrix constraints, every branch carrier is a part of the energy total input flow and the sum of dispatch factor in a junction is equal to unity as shown in eqs. 2.4 and 2.5.

$$0 \leq v_{\alpha k} \leq 1 \quad \forall \alpha \in \epsilon, k \in \mathcal{C}_\alpha \tag{2.4}$$

with $\mathcal{C}_\alpha = \{1, 2 \ldots, \text{total number of converters}\}$

$$\sum_{k \in \mathcal{C}_\alpha} v_{\alpha k} = 1 \quad \forall \alpha \in \epsilon \tag{2.5}$$

In addition to efficiencies and dispatch factors, other terms can be considered in the coupling matrix, depending on the purpose of the investigation. For example, emission coefficients is introduced in environmental and cost emissions studies and power factor ($cos\varphi$) coefficients to exploit reactive power in electrical devices (in eq. 2.6, β is electricity and the converter between α and β energy carriers, with efficiency $\eta_{\alpha\beta}$, generates both active and reactive power, with j imaginary unit).

$$c_{\alpha\beta} = \eta_{\alpha\beta} v_{\alpha\beta} (cos\varphi_\beta + j sin\varphi_\beta) \tag{2.6}$$

Further information can be found in [18, 19, 20].

2.3.2 Energy storage devices

In the energy hub modeling, the presence of Energy Storage Systems (ESSs) modifies equation (2.1) adding a new term:

$$\boldsymbol{L} = \boldsymbol{CP} - \boldsymbol{S\dot{E}} \tag{2.7}$$

where $\boldsymbol{\dot{E}}$ is the vector of internal power flow and $\boldsymbol{S}$ is the storage coupling matrix.

For steady-state consideration power is approximated as the change in energy ΔE during the period dt. Consequently, the energy stored after a certain period t depends on energy stored at previous time step $t-1$, change in energy and any power stand-by losses E_{losses} (eq. 2.8).

$$E_t = E_{t-1} + \dot{E}_t - E_{losses} \tag{2.8}$$

Coefficients $s_{\alpha\beta}$ represent relation between α and β energy carriers, if a conversion is provided, and how much the power exchanged with the system affects the stored energy, with charge and discharge efficiencies of the storage device [21].

Fig. 2.3 shows the exchanging flows between input and output side of energy hub that converts α in β [22]. The power provided at output side P_β by storage devices is proportional to the flow affecting the storage devices at input and output side respectively $\dot{E_{in}}$ and $\dot{E_{out}}$, thought storage coupling matrix coefficients. The storage at output side is influenced only by charge and discharge efficiency, whereas the storage at input side depends on conversion efficiency $\eta_{\alpha\beta}$ too. Eq. 2.9 shows the

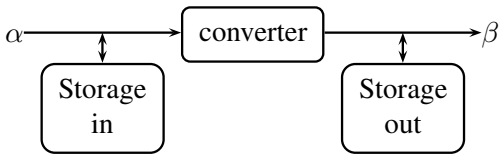

Figure 2.3: Flows in an energy hub between two energy carriers (α and β), with energy storage devices.

storage coupling matrix of fig. 2.3, where e_α^{in} and e_α^{out} represent charge and discharge efficiencies.

$$P_\beta = \begin{bmatrix} \frac{\eta_{\alpha\beta}}{e_\alpha^{in}} & \frac{1}{e_\alpha^{out}} \end{bmatrix} \begin{bmatrix} \dot{E_{in}} \\ \dot{E_{out}} \end{bmatrix} \tag{2.9}$$

Their values depend on e_α^+ and e_α^-, forward and reverse energy efficiencies of the interface, respectively, and Q_α, the amount of power exchanged for vector α, according to eq. 2.54,

$$e_\alpha = \begin{cases} e_\alpha^+ & \text{if} \quad Q_\alpha \geq 0 \\ \frac{1}{e_\alpha^-} & \text{else} \end{cases} \tag{2.10}$$

2.3.3 Example of energy hub

As an example, referring to fig. 2.2, eq. 2.11 represents the energy hub equation, with η_{fc}, η_t, $\eta_{CHP,el}$, $\eta_{CHP,th}$, η_{ex} respectively fuel cell, transformer, electrical and thermal CHP and heat exchanger efficiencies; P_h, P_{el}, P_{gas}, P_{th} respectively hydrogen, electrical, natural gas and thermal input powers; L_{el}, L_{th} electrical and thermal loads, $\dot{E}_{el}$, $\dot{E}_{gas}$ electrical and natural gas power variations.

$$\begin{bmatrix} L_{el} \\ L_{th} \end{bmatrix} = \begin{bmatrix} \eta_{fc} & \eta_t & \eta_{CHP,el} & 0 \\ 0 & 0 & \eta_{CHP,th} & \eta_{ex} \end{bmatrix} \begin{bmatrix} P_h \\ P_{el} \\ P_{gas} \\ P_{th} \end{bmatrix} - \begin{bmatrix} \frac{1}{e_{el}} & \frac{\eta_{CHP,el}}{e_{gas}} \\ 0 & \frac{\eta_{CHP,th}}{e_{gas}} \end{bmatrix} \begin{bmatrix} \dot{E}_{el} \\ \dot{E}_{gas} \end{bmatrix} \tag{2.11}$$

2.4 The power flow problem

The power flow problem is formulated as a system of non-linear algebraic equations as

$$f(\boldsymbol{x}) = 0 \tag{2.12}$$

where $\boldsymbol{x}$ is a vector with the n unknown variables. Iterative methods, like the Newton-Raphson method, can solve these problems [23, 24]. Starting from initial values vector $\boldsymbol{x_0}$, the i-step solution vector $\boldsymbol{x_i}$ can be improved by a $\boldsymbol{\Delta x_i}$ quantities vector until a desired accuracy is achieved ($|\boldsymbol{\Delta x_i}| \leq \epsilon$). In Newton-Raphson method, the Taylor expansion defines

$$\boldsymbol{f}(\boldsymbol{x_i} + \boldsymbol{\Delta x_i}) \simeq \boldsymbol{f}(\boldsymbol{x_i}) + \boldsymbol{J}(\boldsymbol{x_i})\boldsymbol{\Delta x_i} \tag{2.13}$$

considering only the first derivative terms, where $\mathbf{J}$ is the Jacobian matrix of the system, formed by the partial derivates $\partial f / \partial x$.

The improved approximated solution $\boldsymbol{x_{i+1}}$

$$\boldsymbol{x_{i+1}} = \boldsymbol{x_i} + \boldsymbol{\Delta x_i} \tag{2.14}$$

can be calculated adding the vector $\boldsymbol{\Delta x_i}$ (eq. 2.15) to the original guess $\boldsymbol{x_i}$.

$$\boldsymbol{\Delta x_i} = -\boldsymbol{J}(\boldsymbol{x_i})^{-(1)}\boldsymbol{f}(\boldsymbol{x_i}) \tag{2.15}$$

2.4.1 The electrical power flow

In electrical networks, the non-linear algebraic equations $f(x)$ represent the power flow equations

$$P_j = \sum_{j=1}^{n_{PQ}+n_{PV}} |V_j||V_k|(G_{jk}cos\theta_{jk} + B_{jk}sin\theta_{jk}) \tag{2.16}$$

$$Q_j = \sum_{j=1}^{n_{PQ}+n_{PV}} |V_j||V_k|(G_{jk}sin\theta_{jk} - B_{jk}cos\theta_{jk}) \tag{2.17}$$

in j-node, with G_{jk} and B_{jk} conductance and susceptance between j-bus and k-bus, θ_{jk} phase angle difference between V_j and V_k (voltages at j-bus and k-bus). Active P_j and reactive Q_j power, module V_j and phase angle θ_j of voltage at j-node are known and unknown variables, depending on node type.

In fact, in a n busses network, n_{PQ} nodes are characterized by known active and reactive power (PQ nodes), n_{PV} by known active power and module voltage (PV nodes) and n_{SL} by known module and angle voltage (SL nodes, usually 1), which represents the angle reference and the power balance for accounting of both powers and losses. SL, PV and PQ nodes inherit this attribute by connected generators and loads.

The $\boldsymbol{\Delta x_i}$ is the active and reactive power changes vector at i-iteration, used to update the $\boldsymbol{x_i}$ solution. The Jacobian matrix is the partial derivatives of eqs. 2.16 and 2.17 with respect to module and phase voltages, computed at each iteration, until convergence $|\boldsymbol{f_i}(\boldsymbol{x_i})| \leq \epsilon$ is achieved for each $i \in \{1, \ldots, n-1\}$. Eq. 2.18 represents eq. 2.15 ($n_{PVPQ} = n_{PV} + n_{PQ}$) [25].

$$\begin{bmatrix} \Delta P_1 \\ \vdots \\ \Delta P_{n_{PVPQ}} \\ \Delta Q_1 \\ \vdots \\ \Delta Q_{n_{PQ}} \end{bmatrix} = \begin{bmatrix} \frac{\partial P_1}{\partial \theta_1} & \cdots & \frac{\partial P_1}{\partial \theta_{n_{PVPQ}}} & \frac{\partial P_1}{\partial V_1} & \cdots & \frac{\partial P_1}{\partial V_{n_{PV}}} \\ \vdots & \ddots & \vdots & \vdots & \vdots & \vdots \\ \frac{\partial P_{n_{PVPQ}}}{\partial \theta_1} & \cdots & \frac{\partial P_{n_{PVPQ}}}{\partial \theta_{n_{PVPQ}}} & \frac{\partial P_{n_{PVPQ}}}{\partial V_1} & \cdots & \frac{\partial P_{n_{PVPQ}}}{\partial V_{n_{PV}}} \\ \frac{\partial Q_1}{\partial \theta_1} & \cdots & \frac{\partial Q_1}{\partial \theta_{n_{PVPQ}}} & \frac{\partial Q_1}{\partial V_1} & \cdots & \frac{\partial Q_1}{\partial V_{n_{PV}}} \\ & \ddots & & & & \\ \frac{\partial Q_{n_{PQ}}}{\partial \theta_1} & \cdots & \frac{\partial Q_1 n_{PQ}}{\partial \theta_{n_{PVPQ}}} & \frac{\partial Q_{n_{PQ}}}{\partial V_1} & \cdots & \frac{\partial Q_{n_{PQ}}}{\partial V_{n_{PV}}} \end{bmatrix} \begin{bmatrix} \Delta\theta_1 \\ \vdots \\ \Delta\theta_{n_{PVPQ}} \\ \Delta V_1 \\ \vdots \\ \Delta V_{n_{PQ}} \end{bmatrix} \tag{2.18}$$

2.4.2 Pipeline network power flow

Pipeline networks, as thermal and natural gas networks, are represented by nodal balances and line flow equations similarly to an electrical network [26]. A dualism between electrical and pipeline networks could be observed for:

- potential (voltage ≡ pressure)
- flux (current ≡ flow)
- power (≡ pressure*flow)
- power loss ($\Delta pressure * flow \equiv \Delta voltage * current$)
- resistance (impedances ≡ friction factor).

The power flow problem in pipeline networks requires to evaluate node pressures and flow rates in pipelines for known values of source pressure and of gas injections at load nodes. In particular, node could be identified as known-injection node, with known net injection L and unknown pressure p, and known-pressure/slack node, with nodal pressure p specified and net injection Lm unknown [27, 28, 29].

For any pipeline, the flow equation from node k to node j can be expressed in terms of pressure difference:

$$f_{kj} = S_{kj} M_{kj} \sqrt[m]{S_{kj} \Delta p_{kj}} \tag{2.19}$$

where f_{kj} is the line flow [m^3/h], M_{kj} is proportional to the rate between a given power of the diameter (D, [m]) and length (L, [m]) of the pipeline, Δp_{kj} [Pa] is the pressure gap between busses k and j, S_{kj} indicates the direction of the flow ($S_{kj} = sign(\Delta p_{kj})$), and m depends on the network pressure level. This equation is valid for both gaseous and liquid fluids and Δp_{kj} and M_{kj} change according to the hypothesis.

From Kirchhoff's first law, the nodal equations

$$\boldsymbol{L} - \boldsymbol{A} \boldsymbol{f}(\boldsymbol{p}) = 0 \tag{2.20}$$

where $\boldsymbol{A}$ branch-nodal incidence matrix, $\boldsymbol{f}$ is the flow in branches vector and $\boldsymbol{L}$ the loads vector.

The Newton-Raphson nodal method could be applied to solve pipeline power flow [27, 30]. Starting from an initial solution with known and assumed pressures, at each iteration a pressure changes $\boldsymbol{\Delta p}$ is evaluated, with the $\boldsymbol{J(p_i)^{-1}}$ Jacobian matrix with partial derivatives with respect to pressures. The nodal pressure is thus updated for a new flow mismatches check (eq. 2.20).

$$\boldsymbol{\Delta p_i} = \boldsymbol{J(p_i)^{-1}}(-\boldsymbol{f(p_i)}) \tag{2.21}$$

The procedure stops when all flow mismatches are less than a specific tolerance.

A preliminary pipeline network modeling has been introduced in the software environment, in order to have a simple but exhaustive energy-vector modeling that would allow investigation on the potentiality of synergy among different energy vectors in a multi-energy vector network. Focus is always given to the electrical network, whereas other energy networks could exchange power through energy hubs, improving electrical reliability and efficiency, reducing economical and emission costs, for examples.

For this reason the system has been kept simple and compressors, valves, turbines and other specific devices are not considered and a single circuit has been modeled for pipeline network.

2.5 The optimisation problem

The goal of an optimisation problem is to find values of variables that minimize or maximize the objective function while satisfying the constraints. Constraints, as

- equality and inequality linear constraints and
- equality and inequality non-linear constraints,

describe relations among controlled and uncontrolled variables, that affect and does not affect the objective function value respectively. The generic optimisation problem formulation is shown in eq. 2.22, where $\boldsymbol{x}$ is the vector of control variables, $\boldsymbol{g}(\boldsymbol{x})$ and $\boldsymbol{h}(\boldsymbol{x})$ represent vectors of equality and inequality constraints respectively.

$$min \quad f(\boldsymbol{x}) \quad \text{such that} \begin{cases} \boldsymbol{g}(\boldsymbol{x}) & = & \boldsymbol{0} \\ \boldsymbol{h}(\boldsymbol{x}) & \leq & \boldsymbol{0} \end{cases} \tag{2.22}$$

The objective function returns always a scalar value [16].

Usually, maximization problems are transformed in a minimization problem by considering the opposite of the objective function as shown in eq. 2.23.

$$max \quad f(\boldsymbol{x}) = -min \quad (-f(\boldsymbol{x})) \tag{2.23}$$

2.5.1 The multi-period optimisation

In the multi-period optimisation, multiple time periods are considered in the optimisation problem, increasing the complexity of optimisation tools which need to compute the solution for each considered time step.

The problem in eq. 2.22 becomes as shown in eq. 2.24, where objective function is usually the sum of objective functions in the time period and constraints must be satisfied for each time step $t \in \{1, \ldots, n_T\}$, with n_T total number of time steps.

$$min f(\boldsymbol{x}) = \sum_{t=1}^{n_T} (f_t(\boldsymbol{x})) \quad \text{such that} \begin{cases} \boldsymbol{c_t}(\boldsymbol{x}) & \leq & \boldsymbol{0} & & & \forall t \\ \boldsymbol{c_{t,eq}}(\boldsymbol{x}) & = & \boldsymbol{0} & & & \forall t \\ \boldsymbol{A_t x_t} & \leq & \boldsymbol{b_t} & & & \forall t \\ \boldsymbol{A_{t,eq} x} & = & \boldsymbol{b_{t,eq}} & & & \forall t \\ \boldsymbol{lb_t} & \leq & \boldsymbol{x_t} & \leq & \boldsymbol{ub_t} & \forall t \end{cases} \tag{2.24}$$

$\boldsymbol{c_t}(\boldsymbol{x_t})$ and $\boldsymbol{c_{t,eq}}(\boldsymbol{x_t})$ are inequality and equality non-linear constraints, $\boldsymbol{A_{t,eq} x_t} = \boldsymbol{b_{t,eq}}$ and $\boldsymbol{A_t x_t} \leq \boldsymbol{b_t}$ are inequality and equality linear constraints (with $\boldsymbol{A_{t,eq}}$ and $\boldsymbol{A_t}$ coefficient matrices) and $\boldsymbol{lb_t}$ and $\boldsymbol{up_t}$ are lower and upper boundary constraints, which define the range of the solution, at period t [16].

2.5.2 Optimisation problems and techniques

Different commercial optimisation tools are available to solve problems represented by eq. 2.22 and 2.24, which implement different strategies. Some solution techniques are more appropriated for certain types of problems, which are classified according to the characteristics of the objective function, the constraints, and the controllable decision variables [24]. For example, we can recognize:

- linear programming problems, if both constraints and objective function are linear;
- non-linear programming problems, if both constraints and objective function are non-linear, which represents the most complex case;
- quadratic programming problems, if constraints are linear and the objective function is a quadratic function;
- convex programming problems, if the objective function and the feasible region are convex called separable if objective function and constraints are equivalent to sum of functions;
- non-convex programming problems if they are not convex programming problems, that means it is not possible to ensure the global optimum;
- etc.

The general behavior of the most of solution techniques is to find a feasible solution and improving it obtaining a better minimum function value. Usually, solvers require a guess x_0 as starting point to find a feasible solution.

Linear programming based methods are devoid of any non-linearity and simplex method is the basic algorithm. This solution technique and its variants transform all inequality constraints in equality constraints adding slack variables.

Some non-linear programming based methods are:

- sequential quadratic programming, usually used to solve quadratic programming or quadratic programming approximation problems, splitting a complex problem in a sequence of simpler problems;
- successive linear programming, which solves non-linear problem with sequential liberalizations of simpler sub-problems;
- generalized reduced gradient, that uses equality constraints to eliminate a subset of decision variables in order to make easier the original problem;
- interior point methods, used to solve convex problems, which could be applied both to linear and non-linear problems with a successive linear programming technique.

Dynamic programming aims to transforms simplex problem into a sequence of simpler problems and it is usually used to solve decision problems. This technique decomposes a multi-stage problem as a sequence of single-stage decision problems, which are easier to solve sequentially.

Genetic algorithms are based on search techniques that mimics the process of natural evolution, the Darwin thinking of natural selection and natural genetics. Genetics algorithm start from a population, a set of feasible random solutions (chromosomes), and use search operations with probabilistic rules of selection of new generation in the evolution process, ensuring their improvement. The major advantage of evolutionary algorithms is the search techniques that allows to achieve a global optimum, whereas other methods ensure it only if some convex properties of the problem are satisfied. The no starting point dependency and the ability to specialize

the problem formulation makes genetic algorithms very interesting for engineering application, ensuring an high probability to find a global optimum.

Mixed-integer programming methods are used to solve mixed-integer linear or non-linear programming problems, which considers integer control variables, requiring specific solving methods due to discontinuity of these variables. For example, the branching and bounding algorithm solves these problems, identifying (branching) and enumerating in a logic sequence (bounding), that identifies goodness of the best solutions in each subset, sub-problems.

In this thesis, the fmincon optimisation function available in Matlab® has been mainly used, in order to solve constrained non-linear non-convex problems. Alternatively, Knitro, an optimisation software library for finding solutions of both continuous (smooth) optimisation models (with or without constraints), as well as discrete optimisation models with integer or binary variables (i.e. mixed integer programs), has been used in few applications, compatibly with the limitations of the student version (by Ziena-Optimization Inc.).

2.6 Optimisation of energy hubs

Optimisation of energy hubs concerns three main problems:

- the optimal hub layout,
- the multi-carrier optimal dispatch
- and the optimal hub coupling [22].

The optimal hub layout is a mixed-integer optmisation problem which aims to define the best configuration of energy hubs, choosing among different types of converters and storage devices (size, efficiency, costs differences) to minimize the total cost. Usually, the objective function consists of two terms (eq. 2.25): the total cost due to operational costs (a cost function proportional to powers $f_c(P)$) and to investment cost, a function f_{ic} proportional to a coefficient which accounts for investment costs $c_{ic,i}$, that are considered depending on the associated decision variable (I_i, the integer variable representing if i-elements is used, 1, or not, 0).

$$f(P) = \sum_i f_c(P_i) + \sum_i f_{ic}(c_{ic,i}, I_i) \tag{2.25}$$

The multi-carrier optimal dispatch aims to identify the optimal dispatch of converters and storage devices in the energy hub in order to minimize costs or emissions. Eq. 2.26 provides two examples of objective function usually used, respectively, where a_α and b_α are cost coefficients of a quadratic cost function and c_α emission coefficients of a linear function.

$$f(P) = \begin{cases} \sum_{\alpha \in \epsilon} a_\alpha P_\alpha^2 + b_\alpha P_\alpha \\ \sum_{\alpha \in \epsilon} c_\alpha P_\alpha \end{cases} \tag{2.26}$$

Finally, the optimal hub coupling aims to optimise the coupling matrix of the energy hub equation which is introduced in the objective function in order to consider the technological features of the coupling.

In this thesis, the optimal hub layout and the optimal hub coupling problems have not been considered, whereas the multi-carrier optimal dispatch has been investigated in order to perform an optimal management of devices in energy hubs.

2.6.1 Optimal management of energy hub problem

The reduction of supply costs for end users is the base goal to identify the best energy mix, although emissions and losses minimization could be implemented and suitably weighted on an economical basis [31, 32].

Particularly, eq. 2.27 shows the general form of the objective function used to perform the best energy mix obtained taking advantages of synergy among energy carriers connections in the energy hub. The objective function is always a cost function with constant, or proportional to a value, cost coefficients or a function that mimics a cost function. Cost coefficients $c_{t,\alpha}$ are market price signals, used by the system operator to incentivate a desired the correct behavior to devices in the energy hub, because suitable signals as price and cost coefficients are key to incentive a virtuous behavior that means the optimal behavior from the network point of view. Objective function in eq. 2.27 is a summation of functions for both multi-period optimisation ($t \in \{1, \dots, n_T\}$) and single-step optimisation ($n_T = 1$).

$$f(P) = \sum_{t=1}^{n_T} \sum_{\alpha \in \epsilon} f_{t,\alpha}(P_{t,\alpha}) = \sum_{t=1}^{n_T} \sum_{\alpha \in \epsilon} c_{t,\alpha} P_{t,\alpha} \tag{2.27}$$

As mentioned above in the energy hub modeling section, the multi-period optimisation is required when storage devices are present in the energy hub. In such cases, it is important to known the storage status over the whole time period, due to relation among energy stored at different time steps (eq. 2.8), to optimal manage a storage device which has the key role to free power generation/consumption from instant balance.

If storage devices are present, $\forall t \in \{1, \dots, n_T\}$, problem constraints are:

- the energy hub equation, to ensure the power balance:

$$\boldsymbol{L_t} - \boldsymbol{C_t P_t} + \boldsymbol{S_t \dot{E}_t} = 0 \tag{2.28}$$

- boundary constraints on input powers for each energy vector, to respect input lines constraints:

$$P^{in}_{min,t} \leq P^{in}_{t} \leq P^{in}_{max,t} \quad \forall\, in \in \epsilon \tag{2.29}$$

- boundary constraints on devices (size constraints), required to prevent the converter -c from generating more than its maximum capacity:

$$P^{c}_{min,t} \leq P^{c}_{t} \leq P^{c}_{max,t} \quad \forall\, c \in \{1, \dots, \mathcal{C}_\alpha\} \tag{2.30}$$

- boundary constraints on the n_{ESS} (total number) storage devices, $\forall w \in \{1, \dots, n_{ESS}\}$, such us maximum and minimum stored energy, charging power (dt=1h in this work so $\dot{E} \equiv P$), to prevent from charging more than its maximum capacity:

$$\begin{array}{rcccl} E_{min,w} & \leq & E_{s,w} & \leq & E_{max,w} \\ P_{min,w} & \leq & P_{s,w} & \leq & P_{max,w} \end{array} \tag{2.31}$$

- charging power constrains, taking into account the stored energy at the end of previous hour and charging efficiency (defined according to eq. 2.54), used to prevent the storage system from charging more than its maximum capacity:

$$P_{w,t} = (E_{w,t} - E_{w,t-1} + E_{w,t,loss})/e_{w,\alpha} \tag{2.32}$$

- energy balance along time period T, required in order to ensure identical starting and final stored energy of each ESS:

$$E_{w,n_T} = E_{w,0} \tag{2.33}$$

  where the starting energy $E_{w,0}$ could be an unknown variable which needs to satisfy storage capacity constraint

$$E_{min,w} \leq E_{0,w} \leq E_{max,w} \tag{2.34}$$

If no storage devices are in the energy hub, the third term in eq. 2.28 is zeroed and $t = 1$ in order to perform a single-step optimisation, because no integral constraints are required. With only a single time step, the optimisation problem is easily solved by fmincon or knitro solvers, due to the small number of constraints and unknown quantities. In fact, increasing the total considered time steps n_T and the number of ESSs, n_{ESS}, the number of unknowns increases, enlarging the problem size. Additionally, the energy balance along the time period T constraint makes hard the optimum search for both fmincon and knitro solvers, which have to perform a huge number of iterations before to stop in an optimum, which could not be the global one and that could be strongly dependent on starting point $\boldsymbol{x_0}$, required by fmincon and knitro solvers.

Considering a coupling matrix with only efficiency and dispatch factor coefficients, the vector $\boldsymbol{x_t}$ expresses the unknown variables at time step t: powers at input side for each energy vector at input side, dispatch factors for each internal partition and charging powers of each ESS.

$$\boldsymbol{x_t} = [\boldsymbol{P^{in}} \quad \boldsymbol{v} \quad \boldsymbol{P^w}]' \tag{2.35}$$

In this thesis, the number of unknown variables has been reduced considering that eq. 2.28 is a system of linear equations with m equations and n unknowns and it is normally rectangular ($n > m$). However, input power and energy derivatives, power factors which could be present in matrices coefficients [33] and non-constant coefficients of matrices (power and energy dependent) are variables, whereas only $n - m$ free variables are real unknown quantities. If the optimisation tool allows calculation during the optimal feasible solution search, variables could be derived by the system of linear equations. In such way, the total number of unknown variables is reduced.

2.7 Optimisation of energy networks

The management of n_v control devices in a n nodes network is performed with an optimal problem solution.

The Optimal Power Flow (OPF) represents the system operator tool to obtain the best technical and/or economical participation in services for the grid support of elements available to vary their generation and/or adsorption [24]. The OPF could ensure sustainability and a more rational use of energy, increasing efficiency usage of resources, reducing costs, losses and emission costs, ensuring an efficient and high quality service. Additionally, the OPF could allow to co-ordinate different devices to reduce their potential negative impact in to the grid. For example, in distribution electrical networks, Distributed Generation (DG) with stochastic behavior due to aleatory nature of renewable resources and Electric Vehicles (EVs) are two examples of devices which need to be suitably involved in network management in order to avoid critical situations, such us line overloading and voltage limits violations, in high penetration scenarios.

The OPF is usually a non-linear problem, which aims to minimize:

- losses;
- power costs, a polynomial functions used to minimize the economic dispatch of generators as

$$\sum_{l=1}^{n_v} c_1 P_l^2 + c_2 P_l + c_3 \tag{2.36}$$

- emissions, polynomial or exponential functions of the source's power output, used to minimize the emission dispatch;
- and the voltage root mean square deviation from reference voltage values $V_{ref,j}$, which are usually the nominal value (1pu), for the electrical network:

$$\sum_{j=1}^{n} \sqrt{\frac{(V_j - V_{ref,j})^2}{n}} \tag{2.37}$$

Constraints are:

- limits on all control variables (powers, pressure and voltage at nodes etc.)

$$\boldsymbol{x_{min}} \quad \leq \quad \boldsymbol{x} \quad \leq \boldsymbol{x_{max}} \tag{2.38}$$

- power flow equations, in order to ensure the nodal balance among injections at each node (vector P_l) and incoming and outgoing flows in each node, defined by incidence matrix network I and flows in branches (f):

$$\boldsymbol{P_l} - \boldsymbol{I f} = 0 \tag{2.39}$$

- generation/load balance (with n_g and n_l total number of generators and loads, P_{losses} the total losses):

$$\sum_{g=1}^{n_g} P_{gen,g} - \sum_{l=1}^{n_l} P_{load,l} - P_{losses} = 0 \tag{2.40}$$

- branch flow limits for all n_b branches:

$$f_j \leq f_{max,j} \quad \forall j \in \{1, \ldots, n_b\} \tag{2.41}$$

- generators and loads limits, such us boundary constraints

$$\begin{array}{lllll} P_{min,g} & \leq & P_g & \leq P_{max,g} & \forall g \in \{1,\ldots,n_g\} \\ P_{min,l} & \leq & P_l & \leq P_{max,l} & \forall l \in \{1,\ldots,n_l\} \end{array} \tag{2.42}$$

  or more specific constraints that defines capability curves.

2.7.1 Optimisation in electrical networks

In a n busses electrical network, the OPF defines n_v control devices (generators and loads) behavior, in order to improve the electrical network efficiency, under normal operating conditions, and to solve critical situation, as line overloading and voltage violations, under abnormal conditions [24, 34, 35].

Unknown variables of this problem are listed in vector x_t: voltage phase angles (θ) for each PV and PQ bus (total number respectively n_{PV} and n_{PQ}), voltage amplitude for each PQ bus, active and reactive power (P and Q) for each variable generator, load and transformer ratio for each on-load-tap-changer transformer (total number n_{tr}), as shown in (2.43).

$$\boldsymbol{x_t} = \begin{bmatrix} \theta_{j,t} \\ V_{k,t} \\ P_{l,t} \\ Q_{l,t} \\ tap_{tc,t} \end{bmatrix} \begin{array}{l} \forall j \in 1,\ldots,n_{PV}+n_{PQ} \\ \forall k \in 1,\ldots,n_{PQ} \\ \forall l \in 1,\ldots,n_{SL}+n^v \\ \forall l \in 1,\ldots,n_{SL}+n^v \\ \forall tc \in 1,\ldots,n_{tr} \end{array} \tag{2.43}$$

Maximum and minimum constraints (2.44) are defined for these variables,

$$\begin{array}{lllll} \theta_{min,j,t} & \leq & \theta_{j,t} & \leq & \theta_{max,j,t} \\ V_{min,k,t} & \leq & V_{k,t} & \leq & V_{max,k,t} \\ P_{min,l,t} & \leq & P_{l,t} & \leq & P_{max,l,t} \\ Q_{min,l,t} & \leq & Q_{l,t} & \leq & Q_{max,l,t} \\ tap_{min,tc,t} & \leq & tap_{tc,t} & \leq & tap_{max,tc,t} \end{array} \tag{2.44}$$

whereas, as listed below, network constraints are power flows equations, generation/load balance, active and reactive power reserves, current limits and capability curves constraints (not explicated in 2.45).

$$\begin{array}{ll} P_{i,t} - f_t(\boldsymbol{\theta_t}, \boldsymbol{V_t}) = 0 & \forall i \in \{1,\ldots,n-1\} \\ Q_{i,t} - f_t(\boldsymbol{\theta_t}, \boldsymbol{V_t}) = 0 & \forall i \in \{1,\ldots,n-1\} \\ \sum_{g=1}^{n_g} P_{gen,g,t} - \sum_{l=1}^{n_l} P_{load,l,t} - P_{losses,t} = 0 & \\ \sum_{g=1}^{n_g} Q_{gen,g,t} - \sum_{l=1}^{n_l} Q_{load,l,t} - Q_{losses,t} = 0 & \\ \sum_{i=1}^{n_g} P_i \leq P_{reserve} & \\ \sum_{i=1}^{n_g} Q_i \leq Q_{reserve} & \\ I_{b,t} \leq I_{max,b,t} & \forall b \in \{1,\ldots,n_b\} \end{array} \tag{2.45}$$

All variables and their constraints must be satisfied $\forall t \in \{1,\ldots,n_T\}$, where n_T is equal to 1 if no ESSs are available in the network.

It should be noticed, the tap position (tap) of the On Load Tap Changer (OLTC) transformer is a discrete variable, used to define its admittance transmission matrix given by 2.46 [25].

$$\begin{bmatrix} m & \dot{Z}/m \\ 0 & 1/m \end{bmatrix} \tag{2.46}$$

Its variation due to changes in m according to eq. 2.47 modifies the admittance transmission matrix 2.46 and the admittance matrix of the network with no continuous variations.

$$m = 1 + \Delta tap \tag{2.47}$$

To avoid any discrete variable, tap changer is modeled as a continuous variable between tap_{min} and tap_{max} as shown in 2.44. The optimal solution tap^* identifies a lower and an upper tap value ($tap_{low} \leq tap^* \leq tap_{up}$). Either tap_{low} and tap_{up} define a sub-optimal "real" solution, but only one minimizes the objective function. This one is the optimal solution.

If n_{ESS} storage devices are in the network, a multi-period OPF is required. To the $\boldsymbol{x_t}$ vector, the active and reactive power affecting the network at input side of the ESS have to be added in the unknown variable vector 2.48. Additionally, unknowns of ESSs have to be considered: starting energy $E_{O,w}$, maximum capacity (E_w) and charging power (P_w) for each ESS $w \in 1, \ldots, n_{ESS}$ (2.49).

$$\boldsymbol{x_t'} = \begin{bmatrix} x_t \\ P_{s,w,t} \\ Q_{s,w,t} \end{bmatrix} \begin{matrix} \\ \forall w \in 1, \ldots, n_{ESS} \\ \forall w \in 1, \ldots, n_{ESS} \end{matrix} \tag{2.48}$$

$$\boldsymbol{x} = \begin{bmatrix} \boldsymbol{x_t'} \\ E_{0,w} \\ E_{w,t} \\ P_{w,t} \end{bmatrix} \begin{matrix} \forall h \in 1, \ldots, T \\ \forall w \in 1, \ldots, n_{ESS} \\ \forall w \in 1, \ldots, n_{ESS} \\ \forall w \in 1, \ldots, n_{ESS} \end{matrix} \tag{2.49}$$

Constraints introduced in section 2.6 (from 2.31 to 2.33) have to be considered in the OPF problem formulation, to completely define ESSs.

$$\begin{array}{rcccl} E_{min,w} & \leq & E_w & \leq & E_{max,w} \\ P_{min,w} & \leq & P_w & \leq & P_{max,w} \\ E_{min,w} & \leq & E_{0,w} & \leq & E_{max,w} \\ E_{w,n_T} & = & E_{w,0} & & \end{array} \tag{2.50}$$

The relation between $P_{s,w,t}$ and $Q_{s,w,t}$ and $P_{w,t}$ depends on converter and on charge and discharge efficiencies (eq. 2.51) between storage device and network side.

$$\begin{array}{rcll} P_{w,t} & = & (E_{w,t} - E_{w,t-1} + E_{w,t,loss})/e^+_{w,\alpha} & \text{if charging} \\ P_{w,t} & = & (E_{w,t} - E_{w,t-1} + E_{w,t,loss})e^-_{w,\alpha} & \text{if discharging} \end{array} \tag{2.51}$$

In fact, if $P^c_{w,t}$ is the flow affecting the electronic interface between the storage device and network side, power factor of a four-quadrant converter defines the apparent power $P_{s,w,t} + jQ_{s,w,t}$ at network side, whereas $P_{w,t}$ is the flow affecting the storage device. Relations between these power values are defined in equations 2.52.

$$\begin{array}{rcl} P_{s,w,t} + jQ_{s,w,t} & = & P^c_{w,t}(cos\varphi + jsin\varphi_{w,t}) \\ P_{w,t} & = & P^c_{w,t}cos\varphi/e_{w,\alpha} \end{array} \tag{2.52}$$

n^v is the total number of controllable generators and loads. Potentially, the total number of controllable active and reactive power variables (for both generators/loads and ESSs) could be different and vary each hour depending on availability and/or management decisions (e.g. ESS could regulate their active power only).

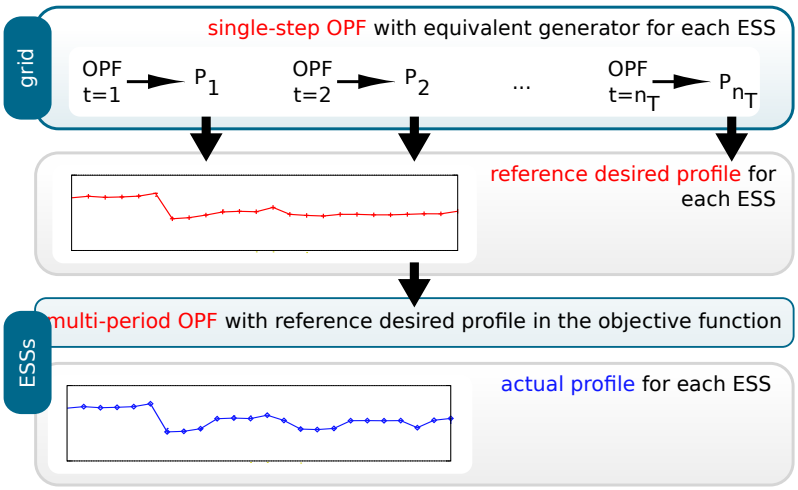

Figure 2.4: Conceptual scheme of the decoupled procedure for the optimisation of electrical networks with storage devices.

Decoupled procedure for MPO

The problem stated above is characterized by a large number of variables and constraints.

For this reason a decoupled procedure has been proposed and implemented in the software environment. The main idea is to consider separately problem constrains to MPO and to single-step optimisation. In this way, it is possible to consider separately the optimisation of the ESSs and the optimisation of the electrical network.

Referring to fig. 2.4, the proposed procedure considers:

1. single-step OPFs to evaluate a desired power profile at the connection node of each ESSs;

2. a multi-period optimisation which aims to obtain the desired power profile provided by the network optimisation

Storage devices at nodes where they are connected are substituted by equivalent generators in the electrical network. These generators are control devices that the system operator ideally desires to optimally manage for a specific purpose (minimize losses, voltage spread etc.). The execution of n_T OPF provides an optimal active power profile (n_T $P_{ref,w,t}$ values), which represents that profile the system operator would like to obtain by the storage devices. However, these values are evaluated without considering the real availability of the ESS, in particular without considering the constraint of energy balance along the time period T, and the ability to shift adsorption and generation during the day.

For this reason, achievement of the desired power profile is the primary goal of the optimal management of the ESS and thus it is suitably catered for in the objective function of the optimisation problem. These terms could represent suitable price signals provided by the system operator, requesting the ESS's owner a service for the grid support against a specific remuneration.

The feasible optimal solution of the MPO is the optimal profile the ESS would provide to the network. Depending on signals sent by the system operator when requiring a service (coefficient terms of the objective function) for the grid support and on its constraints, the optimal profile supplied by the storage device could be different from the expected desired profile required by the grid (particularly if it is not compatible with ESS constraints).

A critical aspect of the decoupled procedure is that provisions must be taken to ensure the power profile so obtained does not worsen the network status, since the ESS management has not any information about network status. The decoupled procedure requires a method to ensure any optimal profile able to make worse the network status, seeing that any information about the network is known by the management tool of the ESS. In particular, network constraints are key to avoid new violations. Solution could be to:

- provide a minimum and a maximum desired profile as constraints, in order to consider network constraints in the MPO;
- iteratively perform single-step optimisation and MPO with mean root square objective functions until a convergence is obtained.

The first method aims to obtain a solution with a one-step procedure: the coefficients introduce in the objective function of the MPO incentive the ESS's owner to supply the desired power profile, whereas minimum and a maximum desired profile constraints add information about the grid.

The second method performs sequential exchanges of information (suitable signals) among network, control devices available to participate in services for the grid regulation (namely ESS or energy hub with ESS) and energy markets (suitable price signals), as schematically represented by network, market and DSM levels in the conceptual scheme of the software environment described in this chapter. A network computes a request, markets translate a technical data in an economical signal and the DSM trades between markets, control devices and networks.

2.7.2 Optimisation of multi-energy vector networks

All different energy carriers are usually considered and managed independently, except for co-generation and tri-generation plants that have already demonstrated to be the most efficient form of combined generation. In this perspective a multi-vector network is a natural consequence to achieve energy efficiency needs, to ensure sustainability and a more rational use of energy. A hybrid system facilitates the management of such energy resources which need of energy carriers conversion, as well as storage facilities [32, 18, 36].

The interactions among different energy networks take places at the nodes. A node could be a real physical node or a virtual node, where different devices are aggregated and can exchange/generate/convert different forms of energy, suitably represented by energy hubs. In addition to energy hubs, devices of the various networks could be aggregated in virtual utilities [8, 6, 37].

Consequently each node takes a greater importance in the system in the Demand-Side Management (DSM) and the possibility of a real-time observability, controllability and process efficiency optimisation becomes a key need.

The optimisation problem of the multi-energy vector system requires to satisfy eqs. from 2.38 to 2.42 for each energy network in the system (eq. 2.53, 2.57 $\forall \alpha \in \epsilon$)

$$\boldsymbol{x_{min,\alpha}} \leq \boldsymbol{x_{\alpha}} \leq \boldsymbol{x_{max,\alpha}} \tag{2.53}$$

$$\left.\begin{array}{lcl} \boldsymbol{\theta_{min}} \leq \boldsymbol{\theta} \leq \boldsymbol{\theta_{max}} \\ \boldsymbol{V_{min}} \leq \boldsymbol{V} \leq \boldsymbol{V_{max}} \\ \boldsymbol{P_{min}} \leq \boldsymbol{P} \leq \boldsymbol{P_{max}} \\ \boldsymbol{Q_{min}} \leq \boldsymbol{Q} \leq \boldsymbol{Q_{max}} \\ \boldsymbol{tap_{min}} \leq \boldsymbol{tap} \leq \boldsymbol{tap_{max}} \end{array}\right\} \alpha = \text{electrical} \tag{2.54}$$

$$\left.\begin{array}{lcl} \boldsymbol{p_{th,min}} \leq \boldsymbol{p_{th}} \leq \boldsymbol{p_{mth,ax}} \\ \boldsymbol{P_{th,min}} \leq \boldsymbol{P_{th}} \leq \boldsymbol{P_{th,max}} \end{array}\right\} \alpha = \text{thermal} \tag{2.55}$$

$$\left.\begin{array}{lcl} \boldsymbol{p_{gas,min}} \leq \boldsymbol{p_{gas}} \leq \boldsymbol{p_{gas,max}} \\ \boldsymbol{P_{gas,min}} \leq \boldsymbol{P_{gas}} \leq \boldsymbol{P_{gas,max}} \end{array}\right\} \alpha = \text{natural gas} \tag{2.56}$$

$$\begin{array}{llll} \boldsymbol{P_{l,\alpha}} - \boldsymbol{I_{\alpha} f_{\alpha}} = 0 & & & \\ \sum_{g=1}^{n_{g,\alpha}} P_{gen,g,\alpha} - \sum_{l=1}^{n_{l,\alpha}} P_{load,l,\alpha} - P_{losses,\alpha} = 0 & & & \\ f_{j,\alpha} \leq f_{max,j,\alpha} & & & \forall j \in \{\dots, n_b\} \\ P_{min,g,\alpha} \leq P_{g,\alpha} & & \leq P_{max,g,\alpha} & \forall g \in \{1,\dots,n_g\} \\ P_{min,l,\alpha} \leq P_{l,\alpha} & & \leq P_{max,l,\alpha} & \forall l \in \{1,\dots,n_l\} \end{array} \tag{2.57}$$

and energy hub equations described in section 2.6 (eq. 2.58 $\forall h \in \{1,\dots,n_H\}$, with n_H energy hubs in the multi-energy vector system), in order to minimize an objective function, that involves terms of all energy carriers in the system.

$$\begin{array}{llllll} \boldsymbol{L_{t,h}} & - & \boldsymbol{C_{t,h} P_{t,h}} & + & \boldsymbol{S_{t,h} \dot{E}_{t,h}} & = 0 \\ P^{in}_{min,t,h} & \leq & P^{in}_{t,h} & \leq & P^{in}_{max,t,h} & \forall\, in \in \epsilon \\ P^{c}_{min,t,h} & \leq & P^{c}_{t,h} & \leq & P^{c}_{max,t,h} & \forall\, c \in \{1,\dots,\mathcal{C}_{\alpha}\} \\ E_{min,w,h} & \leq & E_{s,w,h} & \leq & E_{max,w,h} & \\ P_{min,w,h} & \leq & P_{s,w,h} & \leq & P_{max,w,h} & \\ P_{w,t,h} & = & (E_{w,t,h} & -E_{w,t-1,h} & +E_{w,t,h,loss}) & / e_{w,\alpha} \\ E_{w,n_T,h} & = & E_{w,0,h} & & & \\ E_{min,w,h} & \leq & E_{0,w,h} & \leq & E_{max,w,h} & \end{array} \tag{2.58}$$

Unknowns are electrical unknowns (phase and module voltages, active and reactive powers, tap positions, pressure in pipeline networks, powers at input side of energy hubs, dispatch factors etc.

Application of the optimisation problem of multi-energy vector system is in chapter 4.

3 Optimisation of Energy Hubs

This chapter is primarily aimed at demonstrating how energy tariffs with a significant price difference between day and night can make energy storage systems more profitable for an active customer. An optimisation procedure, based on the "energy hub" concept, has been devised and applied for a co-ordinated operation of local generation and process-side electric and thermal storage devices. The optimised integrated management of these systems enables an efficient use of primary sources, largely resorting to co-generation (CHP) and an optimal use of production and storage devices. Different case studies show how supply and distribution tariffs can influence the cost-effective operation of a CHP system, assuming the presence of various kinds of process-side storages.

3.1 Introduction

Electricity is a very special good: it can be very hardly stored and it needs to be generated at exactly the same time it is consumed. This requires a continuous control of the power system, for ensuring the on-line balance between generation and demand. Usually the energy demand is regarded as possible to be forecasted but not to be controlled, while generators have to follow the load profile, although working at low efficient operating points.

Recent developments in the generation scenario and the need for a higher level of power quality, as well as the possibility of exploiting renewable energy sources and co-generation, are strongly pushing forward the amount of generation directly connected to the distribution level. A continuously increasing share of this Distributed Generation (DG) has a stochastic behavior, thus increasing the need for regulation and reserve margins.

The use of various forms of storage facilities eases the operation of the power system. Pumping storage plants, for instance, are being used for "peak shaving" and "valley filling" in the bulk power system. At the distribution level, balancing has never been a real issue; in fact the upstream transmission system has always been considered as an "infinite bus" able to balance the load and distributed generation fluctuations, then resulting in an implicit storage resource. Energy storage opportunities on the process-side have rarely been exploited, although several processes

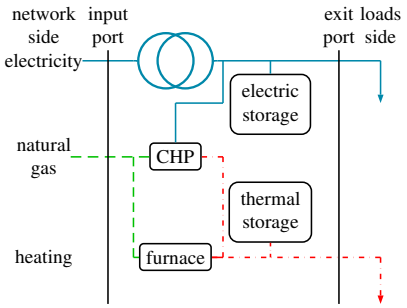

Figure 3.1: Energy hub example.

have significant energy and/or mass storage, the larger usually being thermal and potential energy.

Today, the resort to energy storage systems for coping with the issues posed by the new grid paradigm and for really exploiting the possibilities offered by a large diffusion of distributed generation has become unavoidable. But, due to the relatively large cost of the most commonly used storage systems, a really effective solution must not only exploit grid-side resources, but also the demand side potential.

In this chapter the "energy hub" concept [20] is applied for a co-ordinated operation of local generation, process-side storages and final-use energy systems. Strategies for the integrated management of these systems are proposed to achieve an efficient use of primary sources and the optimal operation of production and storage devices. The effective management of the distribution system (quality of supply, power flows, energy losses) and the increase of the feasible DG share are other important issues which can be suitably improved by the widespread use of storage systems, but, for the sake of clarity, they are not treated in this chapter.

Well-calibrated energy tariffs can induce positive behaviors in active and passive customers, because they can provide economic signals which stimulate power profiles consistent with a rational use of the energy grid resources. Moreover, the price difference between day and night can significantly affect the cost-effectiveness of a storage system, whose presence can reduce the peak demand, or at least shift it to off-peak hours.

3.2 The energy hub optimisation

As shown in chapter 2, the energy hub is an interface between different types of energy vectors, aimed at efficiently transferring multiple energy flow. Its easy mathematical representation with the matrix relation $L = CP - S\dot{E}$, which couples powers at input and output side and internal power variation of storage devices, allows to easy modeling a multi-energy local system. For example the local system shown in fig. 3.1, where a Combined Heat and Power generator (CHP) and a furnace have been considered complemented by a thermal and an electrical storage device.

When suitably managed, the storages can be used to maximize the power production in CHP plants (and tri-generation plants) when power price is high and they can also be used to minimize the use of plants with higher operational costs, since storage devices can store the produced energy during cheap periods and release the

stored energy during expensive periods [38]. For the sake of clarity, in this work any generation and control of reactive electrical power on the output port have been neglected.

The optimisation problem aims to identify the optimal dispatch of converters and storage devices, minimizing the following objective cost function over 24 hours:

$$C = \quad f(E_{el}, P_{el}, mc_{gas}) + \quad f_{sto}(E, P) \tag{3.1}$$

The first term represents the total operational costs due to import and export costs:

$$f(E_{el}, P_{el}, mc_{gas}) = \begin{array}{ll} \sum_{t=1}^{24}(c_{t,el}^{imp} E_{t,el}^{imp} + c_{t,el}^{exp} E_{t,el}^{exp}) + & c_{el}^{p} max(\boldsymbol{P_{el}}) + c_{el}^{fix} + \\ + \sum_{t=1}^{24}(c_{t,gas}^{imp} mc_{t,gas}^{imp}) & c_{gas}^{c} max(\boldsymbol{mc_{gas}}) + c_{gas}^{fix} \end{array} \tag{3.2}$$

where:

- $c_{t,el}^{imp}$ [€/MWh] and $c_{t,gas}^{imp}$ [€/m^3] are imported electrical energy and natural gas flow costs;
- $c_{t,el}^{exp}$ [€/MWh] is the exported electrical energy cost;
- c_{el}^{p} [€/kWp/day] is the electrical peak-power cost;
- c_{gas}^{c} [€/day/(m^3/day)] is the peak gas-flow cost;
- c_{el}^{fix} [€/day] and c_{gas}^{fix} [€/day] are electrical and natural gas fix costs;
- $E_{t,el}^{imp}$ [MWh] is the imported electrical energy;
- $mc_{t,gas}^{imp}$ [m^3] is the imported gas natural flow;
- $E_{t,el}^{exp}$ [MWh] is the exported electrical energy;
- $max(\boldsymbol{mc_{gas}})$ [m^3] is the imported peak-flow;
- $max(\boldsymbol{P_{el}})$ [kW] is the peak-power.

The second term $f_{sto}(E, P)$ in eq. 3.1 is the investment cost of storage devices, given by the value:

$$f_{sto}(E, P) = \begin{cases} \frac{k_{el}}{365 years}(300P^{0.6} + 300P(\frac{E}{P})^{0.8}) & \text{electrical} \\ \frac{k_{th}}{365 years}E & \text{thermal} \end{cases} \tag{3.3}$$

where E is the energy size of the storage (MWh), P is its rated power (MW), k_{el} and k_{th} are appropriate cost coefficients and $years$ is the expected life time of the device; in this way, eq. 3.3 represents the daily equivalent investment cost.

In previous chapter, the optimisation of energy hub has been formulated. To be noted that in this optimisation problem , starting energy E_0 is not a decision variable, whereas the size of each storage device is a problem variable, automatically set to the maximum value of stored energy reached during the period of time of the optimisation. It is thus possible to assess the optimal size of storage devices, since their investment costs are part of the objective cost function.

3.3 Energy tariffs

Tariffs for energy transport and supply (particularly for electricity and gas) are an important tool that Regulators can use to induce power profiles coherent with a rational use of the energy grid resources [39]. For example, end-use tariffs not depending on the time of consumption do not provide any economic signal to stimulate a flat load profile or to encourage a peak-power reduction. In analogy, in the lack of electricity multiple tariffs with a significantly variable rate, usually a CHP plant will follow the thermal load profile, while using the electric system as an implicit and improper storage of huge capacity; in fact, the power grid is able to accept the exceeding electric generation, as well as to provide the lacking energy and just the tariff leverage can mitigate this behaviour.

Furthermore, multiple tariffs with substantial rate difference between day and night can make the end-use energy storage systems more cost-effective for an active customer. Since electric networks are sized on the peak-power demand, transmission and distribution companies are particularly interested to the techniques of Demand Side Response, in particularly the ones allowed by the recent introduction of variable-rate electronic meters. Hence transport tariffs, set by such companies or by electricity Regulators, represent a primary instrument to make the customer power profiles more flat, or at least to shift their maximum consumption to off-peak hours.

For what concerns the supply tariffs, in a deregulated market the hourly price of electricity is set by a Power Exchange or by bilateral contracts, then it cannot be managed by the Regulator. Anyway, the Energy Authorities usually continue to set the supply tariffs for ineligible customers and for the service of "last resort". Then our simulations have assumed that the entire electric tariff can be manipulated by a Regulator.

Under the base case scenario, the electricity and gas tariffs have been calibrated on the Italian situation (medium voltage/pressure client). In particular:

- the tariff for selling exceeding generation to the grid is proportional to the energy volume and differentiated between day and night;
- the tariff for consuming gas is constituted by a fix term [€/year], a peak-flow term [€/year/(m^3/day)] and a term proportional to gas volume [€/m^3], invariable along the 24 hours;
- the tariff for consuming electricity is constituted by a fix term [€/year], a peak-power term [€/kWp/month] and a term proportional to energy consumption [€/MWh], fairly dependent on the time of consumption (F1="peak", F2="off-peak" and F3="shoulder" time slot).

While the base case represents the present Italian tariff, three different scenarios (A, B and C) have been proposed to analyse the impact of regulation on the cost-effectiveness of end-use energy storages:

- in A, B and C, the price of purchased electricity is more and more differentiated between day and night, multiplying the F1 price by a term k and consequently

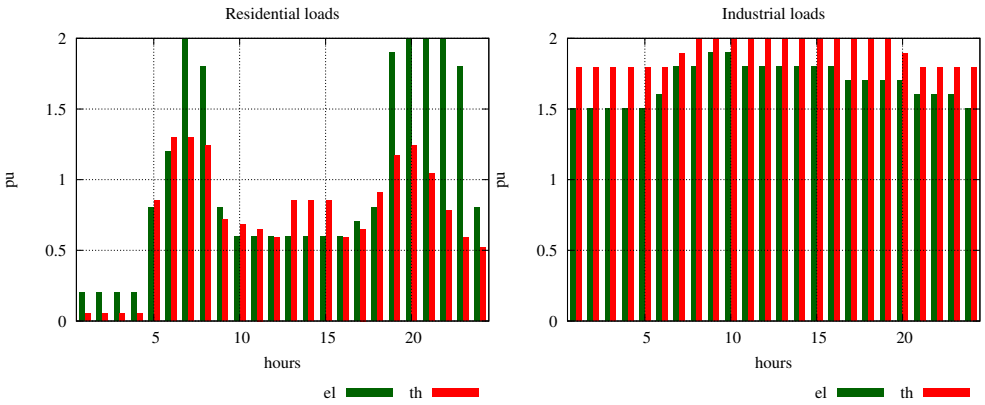

(a) Residential loads **(b)** Industrial loads

Figure 3.2: Residential and industrial electrical and thermal loads.

reducing F2 and F3

$$\begin{array}{lcll} c_{F1,s} & = & kc_{F1} & \forall s \in \{A,B,C\} \\ c_{F2,s} & \leq & c_{F2} & \forall s \in \{A,B,C\} \\ c_{F3,s} & \leq & c_{F3} & \forall s \in \{A,B,C\} \end{array} \tag{3.4}$$

to impose the invariance of the average electricity price for the reference load profile (supplied by the network):

$$\begin{array}{l} C_{tot} = \sum_{t\in F1} c_{F1} P_t + \sum_{t\in F2} c_{F2} P_t + \sum_{t\in F3} c_{F3} P_t \quad \simeq \\ \simeq \sum_{t\in F1_s} c_{F1_s} P_t + \sum_{t\in F2_s} c_{F2_s} P_t + \sum_{t\in F3_s} c_{F3_s} P_t \quad \forall s \in \{scenarios\} \end{array} \tag{3.5}$$

- in all scenarios, in order to penalize the day/night modulation of gas flow, a further term $0.04[€/m^3](PF-1)$ is added to fuel tariff, where the peak factor PF is the ratio between peak and average gas flow

$$m = \left(\frac{max(\boldsymbol{mc})}{average(\boldsymbol{mc})} - 1 \right) 0.04 \tag{3.6}$$

3.4 Applications

In this considered energy hub natural gas and electricity are coupled by a CHP plant and completed by thermal and electrical storage devices. The multi-energy vector local system supplies two scenarios of electrical and thermal load profiles, residential and industrial load profiles respectively (fig. 3.2), thanks to devices shown in fig. 3.1, characterized by:

- transformer efficiency: 98%;
- CHP electrical and thermal efficiencies: 35% and 45% respectively;
- furnace efficiency: 90%;

Table 3.1: Price coefficients for each scenario of import electrical tariff (residential load).

Scenario	k	F1 (peak) 8–19	F3 (off-peak) 7–8,19-23	F3 (shoulder) 0–7,23–24
Caso base	1	152	126	90
A	1.33	202	126	16.89
B	1.66	252	20.25	0
C	2	304	0	0

Table 3.2: Price coefficients for each scenario of import electrical tariff (industrial load).

Scenario	k	F1 (peak) 8–19	F3 (off-peak) 7–8,19-23	F3 (shoulder) 0–7,23–24
Base case	1	152	126	90
A	1.33	202	126	24
B	1.66	252	91	0
C	2	304	48	0

- charge and discharge efficiencies of electrical and thermal storages: 70% and 90% respectively;
- losses of electrical and thermal storages: 0 and 0.3pu respectively (and both null for industrial loads scenario);
- import and export electrical input limits: $\pm 4pu$;
- import and export natural gas input limits: $0 \div 4pu$ (and $0 \div 4pu$ for industrial loads scenario);
- import natural input for the CHP plant: 3.5pu (and 4.5pu for industrial loads scenario);
- import natural input for the CHP plant: 4pu (and 5pu for industrial loads scenario)

(base power 1MW).

As discussed above, the tariff for selling exceeding generation to the grid is assumed to be 90€/MWh from 8am to 8pm, otherwise 45€/MWh in the "Base case". The tariff for consuming gas is assumed to be 1850€/year, 2.96€/year/(m^3/day) and 0.358€/m^3. The tariff for consuming electricity is 1218€/year and 2.58€/kWp/month, plus the term proportional to energy consumption [€/MWh] shown in tables 3.1 and 3.2 for residential and industrial load profiles respectively. As expected, a tariff that aims to promote overnight electricity import imposing the invariance of the average electricity price for the reference load profile means different price coefficients for different load profiles.

Table 3.3: Residential loads: main technical-economical results.

Storage	Operational costs [€/day]	Total costs [€/day]	Max E_{el} [pu]	Max E_{th} [pu]	Exported electricity [years]	PBT [k€]	Expense savings
Scenario Base							
without	2835	2835	–	–	0.17	–	–
E_{el}	2835	2835	0	–	0.17	–	–
E_{el}+E_{th}	2783	2785	0	0.28	1.58	0.4	183
E_{th}	2783	2785	–	0.28	1.58	0.4	183
Scenario A							
without	2855	–	–	0.17	–	–	
E_{el}	2855	2855	0	–	0.17	–	–
E_{el}+E_{th}	2716	2845	0.92	1.77	2.47	8.4	80
E_{th}	2780	2786	–	0.85	2.03	0.8	252
Scenario B							
without	2662	2662	–	–	0.17	–	–
E_{el}	2473	2627	1.54	–	0.09	8.2	128
E_{el}+E_{th}	2444	2591	1.09	2.11	3.50	6.7	259
E_{th}	2575	2583	–	1.01	2.40	0.9	288
Scenario C							
without	2547	2547	–	–	0.17	–	–
E_{el}	2221	2392	1.75	–	0.03	5.3	566
E_{el}+E_{th}	2241	2395	1.35	1.82	3.40	5.0	555
E_{th}	2407	2444	–	4.58	5.56	2.6	376

3.4.1 Residential load scenario

Table 3.3 reports the main technical and economical results of the simulations for residential loads.

Four cases have been considered for each scenario: without storage devices (without), with electrical storage (E_{el}), with thermal storage (E_{th}) and with both electrical and thermal storage devices ($E_{el} + E_{th}$). The costs are reported in €/day: the total cost is given by the operational cost plus the storage investment, spread over a 10 years lifetime period. The maximum stored energy, corresponding to the adopted storage size resulting from the optimisation, and the daily exported electricity are expressed in pu (base power = 1 MW $dt = 1hour$). PBT is the Pay Back Time period of the storage devices, resulting from their investment costs and the expense savings they make possible in CHP operation.

It may be observed for residential loads: electrical storage alone results convenient only with the tariffs with a higher day/night price difference (B and C), although with scenario B the PBT is close to the device lifetime. Combination of electrical and thermal storage is cost-effective in all cases, with interesting PBT only with tariff scenarios B and C due to electrical storage high investment costs (assumptions: $k_{el} = 665$ and $k_{th} = 30000$ in eq. 3.3). As expected, the presence of thermal storage significantly enhances the electrical energy exported to the network, highlighting the

Table 3.4: Industrial loads: main technical-economical results.

Storage	Operational costs [€/day]	Total costs [€/day]	Max E_{el} [pu]	Max E_{th} [pu]	Exported electricity [years]	PBT [k€]	Expense savings
Scenario Base							
without	4522	4522	–	–	0	–	–
Scenario A							
without	4418	4418	–	–	0	–	–
Scenario B							
without	4088	4088	–	–	0	–	–
E_{el}	3698	3964	2.94	–	0	7	453
E_{el}+E_{th}	3630	4002	4.25	1.10	0.24	7.7	314
E_{th}	4055	4062	–	0.6	0	1.5	102
Scenario C							
without	4118	4118	–	–	0	–	–
E_{el}	3505	3804	3.39	–		4.8	1146
E_{el}+E_{th}	3700	3922	2.31	0.26	0.08	5.3	715
E_{th}	4081	4102	–	2.55	0	5.7	58

synergy among energy carriers. In particular, the possibility to provide services for the electrical network support using other networks. In this case, the CHP plant is key to couple networks.

To be noticed, with the "Base case" tariff, the electrical storage is not interesting and the energy hub optimisation with both electrical and thermal storage devices provides an optimal solution that means the electrical storage doesn't improve the objective function value.

The benefits of adopting tariffs with a higher day/night price difference may be better demonstrated by analyzing the daily behavior of the energy hub. As an example, fig. 3.3 shows the multi-period (24 hours) optimal dispatch of the energy hub, equipped with both electrical and thermal storage devices for tariff B scenarios and with any storage device for "Base case". It can be noted that in the former case the CHP production (and thus the natural gas input) tends to follow closely the electric load curve. With the incentive tariff (Scenario B) the optimisation procedure leads to a much greater exploitation of both electric and thermal storage devices, whose energies are suitably modulated resulting in a more uniform natural gas input and CHP production during the "peak" time period. It is also worth noting how the electric energy exchange with the grid is improved, with a greater import during the "off-peak" and "shoulder" periods and a significant export during the "peak" period (when the selling tariff is higher). This behavior, besides lowering the overall operating costs for the consumer, results useful to the supply network, by reducing the daily peak demand.

The electrical storage is an interesting option when the difference between peak and off-peak prices increases, even if the PBT with tariff B represents a value very close to the assumed expected life time of the storage device. Electrical storage devices are penalized by investment costs, even with a positive assumption to halve

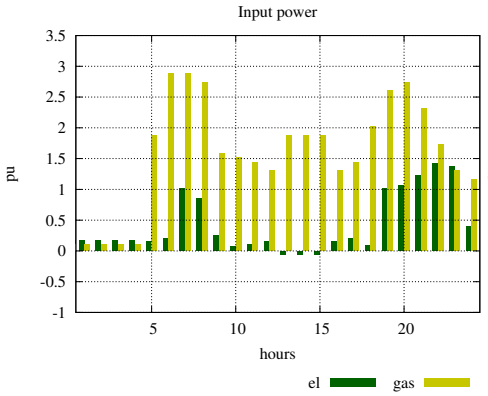

(a) B.c. tariff - without storage - input power

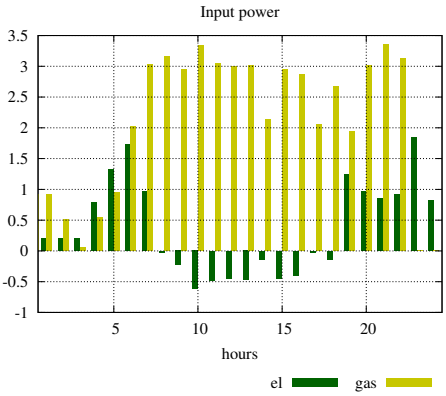

(b) Tariff B - with both storage - P_{el}^{CHP}, P_{th}^{f}

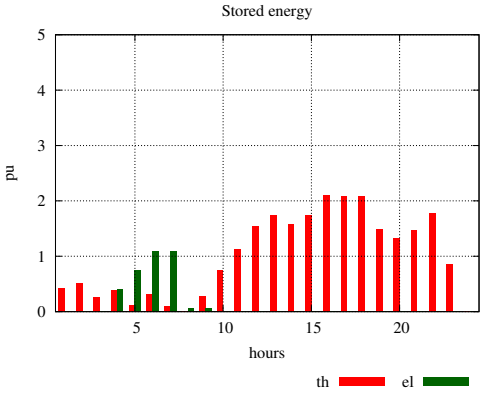

(c) B.c. tariff - without storage - stored energies

(d) Tariff B - with both storage - P_{el}^{CHP}, P_{th}^{f}

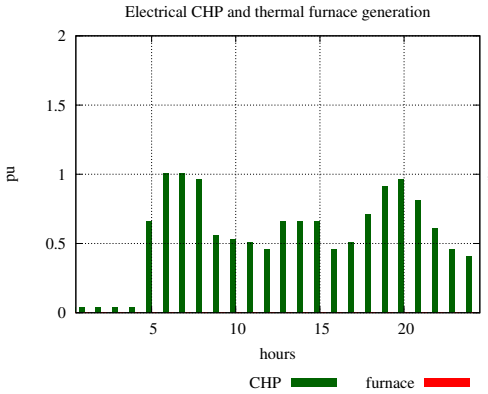

(e) B.c. tariff - without storage - P_{el}^{CHP}, P_{th}^{f}

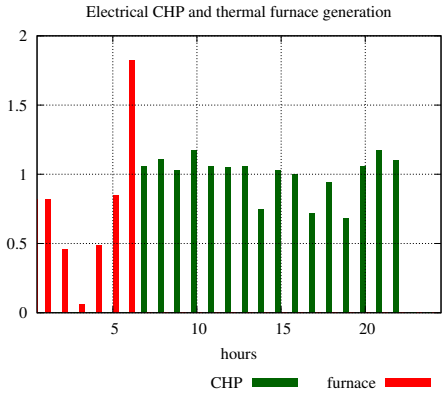

(f) Tariff B - with both storage - P_{el}^{CHP}, P_{th}^{f}

Figure 3.3: Left hand side: "Base case" (B.c.) tariff scenario and no storage devices in the energy hub (consequently A.1c is missing). Right hand side: tariff B scenario and both storage devices. From the top to he bottom: input powers, stored energies and CHP electrical and furnace generation profiles.

actual investment costs.

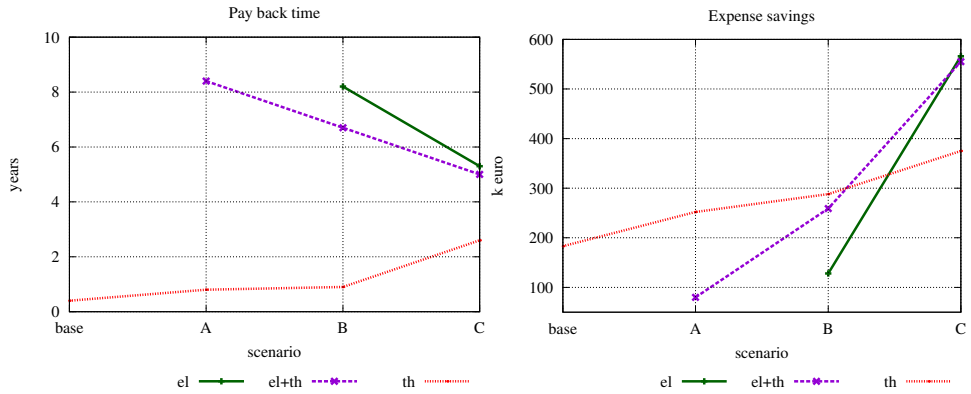

(a) PBT **(b)** Expense saving

Figure 3.4: Pay-back-time and expense saving curves.

This is clearly highlighted in the diagrams of figs. 3.4a and 3.4b. In fig. 3.4a the PBT trend is drawn: this value decreases with an high slope for electrical storage devices when the difference of price coefficients between day and night increases; whereas the thermal storage device is characterized by an opposite behavior, even if values are always lower and more interesting. As expected, the ability of the storage to shift adsorption and generation benefits of the proposed tariff scenario, but assumed investment cost function for storage devices (equations in 3.3) makes thermal storage devices more interesting. The exponential relation between cost coefficients and energy/power capacity of electrical storage creates a strong barrier to their penetration.

Fig. 3.4b shows the expense saving trend with an high slope and high values for the electrical storage. Even if the PBT penalizes the electrical storage due to investment costs, the expense saving increases with incentives as expected. That means the expected new energy markets and reduction of investment costs for electrical storage devices in the next future makes them a very promising technology. With the proposed tariff, expense saving of thermal device is negatively affected both by the day/night modulation factor for natural gas imports and the more day/night price difference for electricity.

All obtained daily profiles are shown in appendix A.

Comparing results of "Base case", the thermal storage device allows to exploit exports during more remunerative hours ("peak" hours), thanks to the efficiently coupling among energy vectors, even if the tariff doesn't incentive large amount of electricity exports, similarly to tariff A.

With tariff A, import profiles are generally improved. In particular, the natural gas modulation factor affects natural gas imports, reducing changes also in CHP generation. However, tariff A doesn't allow an effective use of storage devices and the optimisation doesn't provide interesting results.

With tariff B, the natural gas imports and the CHP plant generation profiles are generally more constant, in particular when both storage devices are available and the electrical one supports the thermal one. In this storage scenario, exports of elec-

tricity significantly increase thanks to interaction between storage devices which allow to better exploit the CHP plant.

Similar considerations could be drawn for tariff C, that enforce results of tariff B thanks to a greater difference between day and night price coefficients. However, the high prices of tariff C may not be a realistic scenario. In particular, with industrial loads it is not possible to impose the invariance of the average electricity price for the reference load profile.

3.4.2 Industrial loads scenario

Similarly to residential loads scenario, table 3.4 shows the main technical and economical results for electrical and thermal industrial loads, used to compare the different behavior of the proposed energy tariffs.

PBT and expense saving values are consistent with the results achieved for the residential load scenario, even if the modulation factor for natural gas imports and the difference between day and night prices for electricity imports and exports are not suitable price signals. In particular, the natural gas constant imports are not due to the day/night modulation factor but to supply requirements of industrial loads (compare graphs in fig. A.9 in appendix A: with tariff A the natural gas import profile is less constant than "Base case").

On the other hands, in this load scenario the electrical storage device has a key role to minimize the objective function, in particular with great difference between day and night price coefficients (tariff C), when the PBT is interesting. Charge and discharge profiles of storage devices behave like with residential loads: charge occurs during cheaper hours and discharge during more expensive hours. However, tariff C does not verify the invariance of the average electricity price for the reference load profile due to specific load profiles.

3.5 Further investigations

Some other investigations on how energy tariffs can make energy storage systems more profitable for an active customer have been carried out. In particular, it has been analyzed the MPO as presented before, which is a complex problem for the optimisation tools used (both fmincon and knitro have been used achieving similar results).

The complexity of the problem depends on the parameters which defines the optimal solution:

- unknown size of storage devices makes the feasibility solution research a complex operation, due to investment costs and operational costs functions (linear and exponential functions, with discontinuous values depending on price slots) and to boundary constraints which depends on storage capacity;
- import and export electricity price coefficients are different: import electricity prices are greater than export electricity prices and hour slots are different. This causes some discontinuity during the evaluation of each term in the objective function, increasing search difficulty for the solvers, which identify optimal path direction to perform a feasible solution.

- The modulation factor for natural gas trying to incentive a constant import profile adds another parameter that affects the final value of the objective function;

- the energy balance constraint ($E_0 = 0 = E_{24}$ in these applications) influences solvers search direction and the resulting daily profiles.

In order to overcome such difficulties, some simplifying hypotheses have been applied, in particular assuming the price coefficients of electricity exports equal to import coefficients. In this way, hour slots for electricity import and export are not different, reducing decision factors in the objective function. In particular, a more suitable signal is provided to incentive export actions: if high difference between day and night price coefficients makes more interesting absorption during nightly time, higher export tariffs enforce this purpose.

Additionally, the tariff C has been substituted with hourly price coefficients calculated trying to impose the price invariance of the average electricity price for the reference load profile.

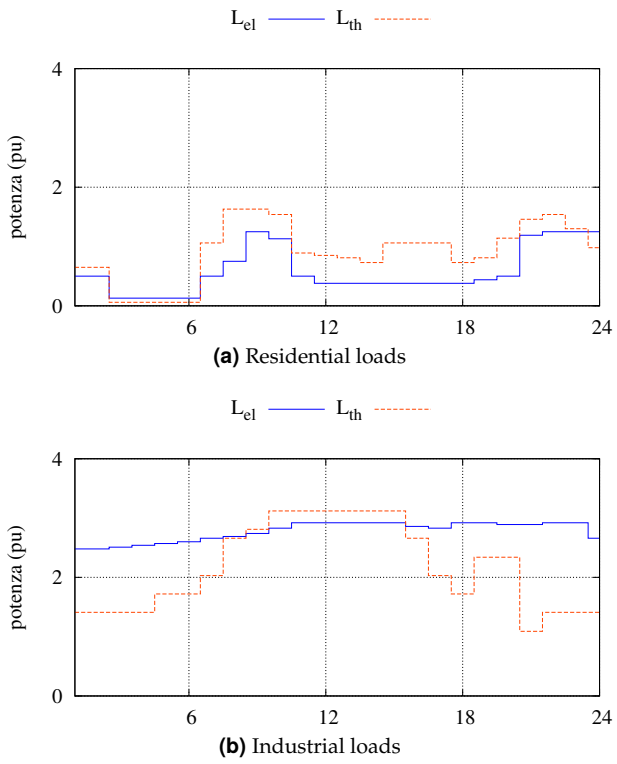

(a) Residential loads

(b) Industrial loads

Figure 3.5: Daily residential and industrial electrical and thermal loads profiles (L_{el} and L_{th} respectively, $P_{base} = 1MW$, $dt = 1h$.

According to load profiles shown in fig. 3.5, values of price coefficients are in table 3.5, whereas the natural gas modulation factor has been increased to 0.10 €/m^3.

Table 3.5: Price coefficients for each scenario of import and export electrical tariff (€/MWh).

Scenario	k	F1	F2	F3
Base case	1	152	126	90
Residential loads				
A	1.33	202	88	61
B	1.66	252	50	33
Industrial loads				
A	1.33	202	84	46
B	1.66	252	34	0
scenario C				

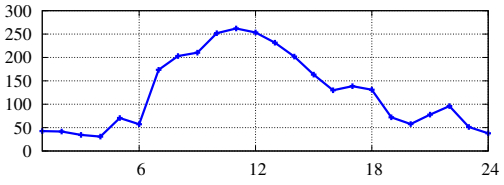

3.5.1 Results and discussions

Figs. 3.6 and 3.7 show electrical and natural gas input powers, CHP plant electrical generation, thermal generation of the furnace and the stored energy for the electrical storage profiles.

The thermal storage is an investment characterized by low investment costs and considerations have been already presented in the previous section. Even with tariff C, even substituting the exponential investment cost function of the electrical storage device with a linear function, with a $k_{el} \simeq 10k_{th}$, the thermal storage is more interesting than the electrical one. However, increasing price coefficients for electricity exports increases electrical storage devices key role, even considering an actual investment cost.

Focusing on electrical storage devices, only tariff A is not interesting and it is not shown in figs. 3.6 and 3.7.

For the residential loads scenario, 22% of expense saving thanks to electrical storage presence comparing "Base case" and tariff B could be obtained with an optimal management of devices in the energy hub. The PBT is 4.16 years considering 5 years of expected lifetime. For industrial loads, 4.86 is the PBT, whereas the expense saving is almost null. In both cases, the capacity of the storage device is 10pu, due to more interesting price signals that incentive export during peak hours and to the new objective function.

These tariffs depend on load profiles. However, it is possible to obtain interesting results using a tariff for both residential and industrial loads, using hourly prices obtained trying to achieve the invariance of electricity cost for reference load profile. In this way, the best compromise with different foreseeable load profiles is achieved. Electrical imports are in the first half of the day, when prices are lower. However, this behavior depends on load profiles and on energy balance constraints. The expense saving for the residential load is 14% with PBT=4 years, whereas expensive saving

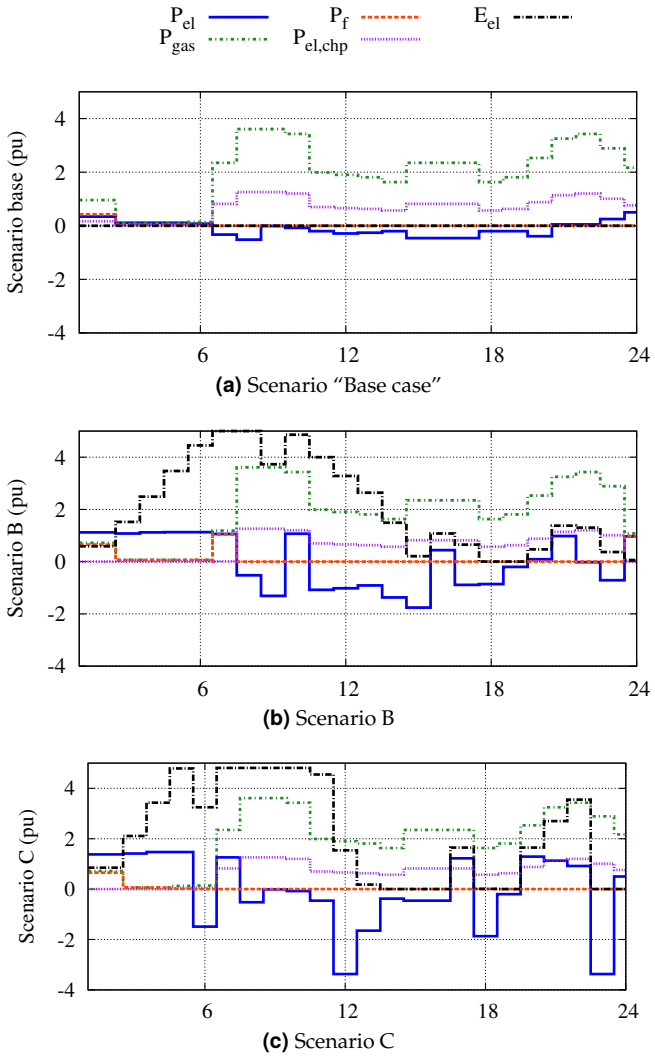

(a) Scenario "Base case"

(b) Scenario B

(c) Scenario C

Figure 3.6: Daily profiles of the residential loads scenario: input powers (electrical $_{el}$, natural gas $_{gas}$), CHP electrical ($_{el,CHP}$) and furnace power generation ($_{f}$) and stored electrical energy (refer to the legend on the top, $P_{base} = 1MW$, $dt = 1h$).

and PBT for industrial loads are 4% and 4.1 years respectively in comparison with "Base case" scenario. An unique hourly tariff appears to be more feasible than a load-depending tariff.

This application demonstrates the importance of some specific parameters in the optimisation problem definition. Firstly, if the global goal of a tariff scenario is to decrease import increasing export at specific node where multi-energy local system are available for an optimal management of energy carriers, both import and export tariffs need to be considered to provide suitable signals both to imports and exports. Secondly, terms of the objective function differently weight on the optimal value. In particular, the exponential investment cost function used in the first application, even if more realistic being derived from empirical measurements, creates

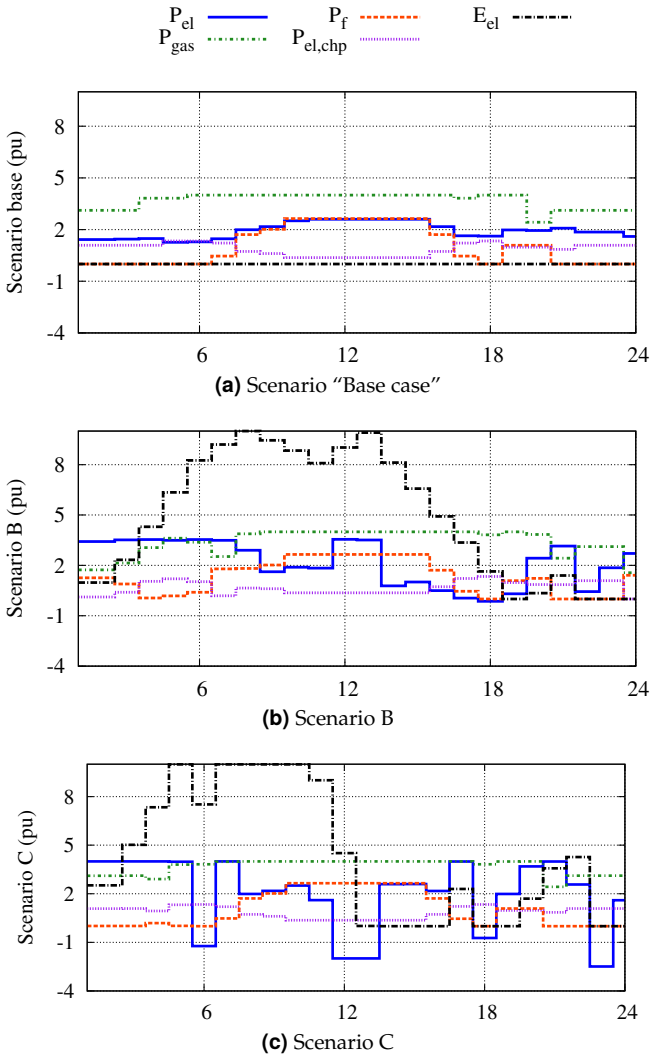

(a) Scenario "Base case"

(b) Scenario B

(c) Scenario C

Figure 3.7: Daily profiles of the industrial loads scenario: input powers (electrical $_{el}$, natural gas $_{gas}$), CHP electrical ($_{el,CHP}$) and furnace power generation ($_{f}$) and stored electrical energy (refer to the legend on the top, $P_{base} = 1MW$, $dt = 1h$).

no-homogeneity in the objective function. Linear terms have to be compared with exponential terms by the optimisation solvers and this could adversely affect the optimal path direction search.

3.6 Conclusion

A multi-period optimisation procedure based on the energy hub concept is applied to optimise the efficient operation of a CHP plant with electric and thermal end-use storage devices, from the strict point of view of the active customer. The case study clearly shows how the optimal dispatch strategy and the Pay Back Time of storage devices are strongly dependent on the energy tariffs applied to CHP. In

particular, in case of supply and distribution electricity tariffs with a higher price difference between day and night, the cost-effectiveness of end-use storage devices significantly increases. In any case, storage devices result in a lower impact on the upstream network, in terms of peak hours power flows. Then Distribution Companies could be directly interested in their installation, or to incentive their adoption by the final users; in this case, the proposed method could help the Distributors or the Regulator in calibrating a proper tariff leverage.

4 Optimisation of Energy Networks

The energetic scenario shows ever growing energy consumptions and the need of an optimal management of different types of energy distributed resources. In particular, the ever growing connection of different types of Distributed Generation (DG) in electrical distribution networks makes the issue of regulation and co-ordination more stringent. In this chapter, the synergy among different energy carriers has been exploited to achieve a more efficient use of resources, with particular focus on reactive power regulation for voltage regulation in electrical distribution networks and on suitable market price signals.

4.1 Introduction

The ever increasing growth of energy consumptions, which concerns not only electrical demand, sets against the needs to respect economical, political and environmental constraints due to different goals, as well as the reduction of harmful emissions, the need to differentiate the combustible park, economical use of resources, demand supply etc. Distributed resources have demonstrated the potentiality to achieve these goals. The availability of new technologies (i.e. microturbines, fuel cells and hydrogen based solutions) combined with traditional ones (like internal combustion engines) make small-scale environmentally compatible generators more suitable than traditional vertical structures for energy production and distribution to end users.

These different types of Distributed Generation (DG) will characterize the electric system in the next future. Small-scale generators, except off-shore wind farms, and renewable generators influence the operation and management of the network and different models of generation and supply approaches have to be developed. In particular, problems as the no optimal location and the partial unpredictability and not dispatchability of many types of DGs require some investigation.

Considering the great diffusion of multi-generation plants like co-generation and trigeneration plants that exploit the synergy between different energy carriers, future networks will be characterized by the optimal integration of different energy carriers [4, 40]. Additionally, energy storage devices could compensate the intermittent nature of renewable sources, smooth load curves, ensuring power availability on

peak periods and providing an economic storage during off-peak period etc. Thanks to the interface converters of these new elements, the system operator could attempt to exploit their flexibility for ensuring the required network voltage profile and enhance supply quality [41, 42].

With particular focus on electrical networks, Combined Heat and Power plants (CHP) could participate in voltage regulation too. In particular, they could play an important role if combined with storage devices (electrical, thermal or both) which may relieve electrical and thermal generation constraints [43].

To reach regulation and co-ordination, system operator may act on energy markets whose key role has been already recognized [43]. With suitable price signals, the system operator may incentive distributed active elements to contribute at satisfying technical network requirements. In particular, only a new energy market system has the capacity to prompt for an optimal management of these degrees of freedom added by multi-source multi-product energy system. Free energy markets will drive the consumers-producers management of their own installations in a multi-vector network where each node is important for the management.

Focusing on electrical network which is the most complex energy system, complex active power markets already exist to ensure power balance, whereas reactive power generation is treated only in ancillary service markets. Reactive power plays an important role in power system reliability and security (to prevent damage such as overheating of generators and motors, to reduce transmission losses and to maintain the ability of the system to withstand disturbances and prevent voltage collapse) and it's the main support for maintaining a specified voltage profile. However, the importance of reactive power management does not match with the general lack of transparent standards and payment structures [15]. Usually not adequate remuneration is provided. For example, DG could not participate in reactive management due to their small size even if they provides reactive power locally, often at site of large loads, reducing losses in the supply lines [44].

In this chapter, synergy among multi-energy vector networks, the role of storage devices, CHP plants participation in voltage regulation and price signals are investigated with two applications. Firstly, an electrical network has been coupled with a thermal network at nodes with CHP plants in energy hubs, mainly to focus on CHP potentiality. Constant cost coefficient and a single-step optimisation has been performed. Secondly, an electrical network with energy hubs has been optimally managed, providing signals proportional to reference "technical" values, in order to remunerate the reactive power proportionally to the required reactive power quantity. In this application, a decoupled procedure has been adopted to manage storage devices present in energy hubs (refer to chapter 2).

4.2 Electrical and thermal network optimal management

Energy management could be more efficient by making more extensive use of energy conversion, e.g. considering chemical conversion and hydrogen potentiality that years ago has been expected to increase significantly. CHP plants are interesting devices which could allow coupling interactions between electrical and thermal networks with an improvement of overall efficiency, as demonstrated in the following.

In this case, price coefficients are used both to make homogeneous different ob-

jectives and to assign more or less importance to each one (weight coefficients). The economical objective function shown in eq. 4.1 represents the minimization of the overall operational cost of energy hubs, which may thus be considered as a sort of virtual utility, expressed as the sum of import/export power costs for each energy hub $h \in \{1, \dots, n_H\}$ (n_H total energy hubs number)

$$\sum_{h \in H} (c_{gas} P_{gas,h} + c_{th} P_{th,h} + c_{el} P_{el,h} + c_{el,Q} Q_{el,h}) \tag{4.1}$$

with c_{gas} natural gas energy cost, c_{th} thermal energy cost, used for both thermal import/export flows of the unknown-injection bus, $c_{el,active}$ active electrical energy cost and $c_{el,reactive}$ electrical reactive energy cost. No time summation has been considered, since no energy storage devices are installed in the energy hub.

Referring to an electrical network coupled with a thermal one though energy hubs, unknown quantities are voltage phase angle for each electrical PV and PQ bus ($\boldsymbol{\theta}$ vector, total number n_{PV} and n_{PQ} respectively), voltage amplitude for each electrical PQ bus ($\boldsymbol{V}$ vector), active and reactive power for each variable generator and load ($\boldsymbol{P}$ and $\boldsymbol{Q}$ vectors, total number $n_v + n_{SL}$ slack nodes), pressure for each unknown-pressure bus ($\boldsymbol{p_{th}}$ vector, total number n_{up}), flow for each unknown-injection bus ($\boldsymbol{P_{th}}$ vector, total number n_{ui}), input powers, dispatch factor and power factor for each energy hub ($\boldsymbol{P_H^{in}}$, $\ni$ and $[\boldsymbol{cos\phi}]'$ vector respectively).

$$\boldsymbol{x} = [\boldsymbol{\theta} \quad \boldsymbol{V} \quad \boldsymbol{P} \quad \boldsymbol{Q} \quad \boldsymbol{p_{th}} \quad \boldsymbol{P_{th}} \quad \boldsymbol{P_H^{in}} \quad \boldsymbol{\nu} \quad \boldsymbol{cos\varphi}]' \tag{4.2}$$

Constraints for energy hubs (4.3), electrical (4.4) and thermal (4.5) network are summarized here below (all details in chapter 2).

$$\left.\begin{array}{rcccl} P^{in}_{min} & \leq & P^{in} & \leq & P^{in}_{max} \\ P^{c}_{min} & \leq & P^{c} & \leq & P^{c}_{max} \\ 0 & \leq & \nu & \leq & 1 \\ 0 & \leq & cos\phi & \leq & 1 \\ \boldsymbol{L} & = & \boldsymbol{CP} & & \end{array}\right\} \boldsymbol{en.hub} \tag{4.3}$$

$$\underbrace{\begin{array}{rcccll} \theta_{i,min} & \leq & \theta_i & \leq & \theta_{i,max} & \forall i \in \{1, \dots, n_{PV} + n_{PQ}\} \\ V_{i,min} & \leq & V_i & \leq & V_{i,max} & \forall i \in \{1, \dots, n_{PQ}\} \\ P_{i,min} & \leq & P_i & \leq & P_{i,max} & \forall i \in \{1, \dots, n_{SL} + n_v\} \\ Q_{i,min} & \leq & Q_i & \leq & Q_{i,max} & \forall i \in \{1, \dots, n_{SL} + n_v\} \\ I_{b,min} & \leq & I_{b,max} & & & \forall b \in \{1, \dots, n_b\} \\ P_i & = & f(\boldsymbol{V}, \boldsymbol{\theta}) & & & \forall i \in \{1, \dots, n\} \\ Q_i & = & f(\boldsymbol{V}, \boldsymbol{\theta}) & & & \forall i \in \{1, \dots, n\} \end{array}}_{\boldsymbol{electrical}} \tag{4.4}$$

$$\left.\begin{array}{rcccll} p_{th,u,min} & \leq & p_{th,u} & \leq & p_{th,u,max} & \forall u \in \{1, \dots, n_{u-p}\} \\ f_{th,bp} & \leq & f_{th,bp,max} & & & \forall bp \in \{1, \dots, n_b^{th}\} \\ P_{th,ui} & = & f(\boldsymbol{p_{th}}, \boldsymbol{f_{th}}) & & & \forall ui \in \{1, \dots, n_{u-i}\} \end{array}\right\} \boldsymbol{thermal} \tag{4.5}$$

4.2.1 Case study system

The integrated electrical and thermal case study network is shown in fig. 4.1. The electric network is a 20 kV 9-bus radial network, connected to the bulk grid (slack bus

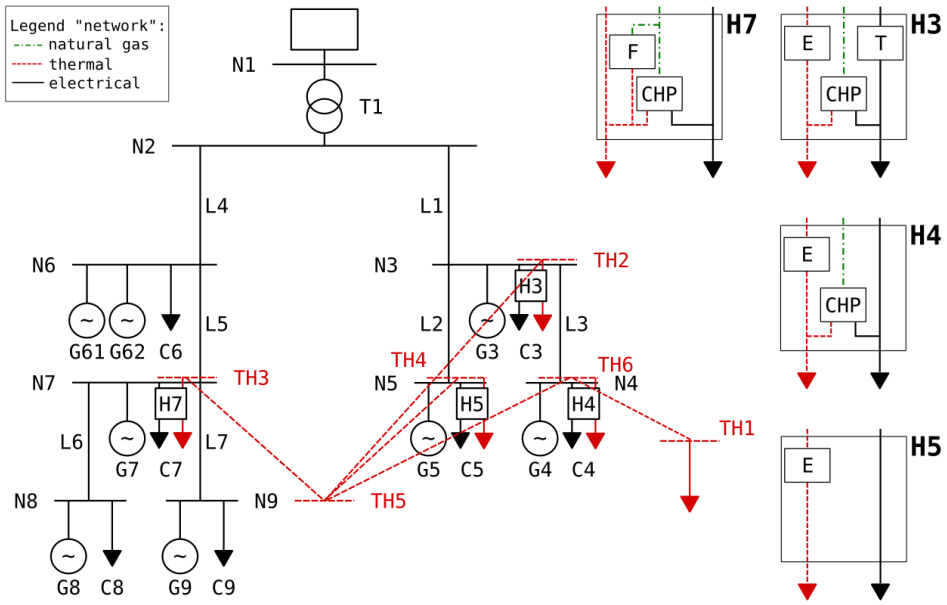

Figure 4.1: Example of multi-vector network with energy hubs.

N1) through a on-load tap-changer (OLTC) transformer. The 6-bus thermal network represents a portion of a district heating system ("slack" known-pressure bus TH5, pressure 14.5 bar). The two networks are coupled through the four energy hubs H3, H4, H5 and H7.

As shown in fig. 4.1, the hubs differ each other by the constituting elements (T = transformer, CHP = combined heat and power generator, E = thermal exchanger) and this is reflected by the values assumed by the coefficients of the coupling matrix in the energy hub equation (4.6), as listed in table B.1 in Appendix B (the size of the CHP units in hubs H3, H4 and H7 is $3.5 MW_{el}$ while in H5 there is no conversion between electrical and thermal energy vectors).

$$\begin{bmatrix} L_{el} \\ L_{th} \end{bmatrix} = \begin{bmatrix} \eta_t & 0 & \nu\eta_{CHP,el}(cos\varphi + jsin\varphi) \\ 0 & \eta_{ex} & \nu\eta_{CHP,th} + (1-\nu)\eta_f \end{bmatrix} \begin{bmatrix} P_{el} \\ P_{th} \\ P_{gas} \end{bmatrix} \tag{4.6}$$

All the electric and thermal network data are reported in Appendix B. In the case study all loads are kept constant, whereas two distributed generation settings have been considered, a low generation (I) and a high generation (II) scenario respectively.

In this study the following cost coefficients have been assumed: 3.741 [€/(kWh)] has been adopted as natural gas cost, assuming Italian purchase tariff (0.358 [$€/m^3$]) [43]. Thermal cost (4.489 [€/(kWh)]) has been supposed 20% higher than natural gas cost to account for efficiencies and other thermal generation costs.

The electrical active energy cost has been considered equal to 8.2 [c€/(kWh)], while the reactive energy cost has been assumed equal to 80% of electrical active energy cost (6.56 [c€/ (kVARh)]). Remuneration of reactive energy has been considered in order to incentivize hub generators to produce also reactive power when required

Table 4.1: Energy hubs and network results without (1.a. 2.a) and with (1.b. 2.b) hubs participation to voltage regulation (negative sign indicates export values).

		Scenario I (tap=-1)		Scenario II (tap=1)	
		1.a	1.b	2.a	2.b
H3	P_{el}	0.609	0.983	0.609	0.914
	Q_{el}	0.826	0.818	0.826	0.836
	P_{th}	-1.447	-0.899	-1.448	-0.775
	P_{gas}	2.952	1.905	2.952	2.098
H4	P_{el}	2.151	1.193	2.151	0.910
	Q_{el}	1.012	-0.199	1.012	-0.531
	P_{th}	1.251	-2.320	1.251	-3.439
	P_{gas}	2.264	6.808	2.264	8.233
H5	P_{el}	2.920	2.920	2.920	2.920
	Q_{el}	1.615	1.615	1.615	1.615
	P_{th}	3.337	3.337	3.337	3.337
	P_{gas}	0.000	0.000	0.000	0.000
H7	P_{el}	-0.599	-0.254	-0.599	0.280
	Q_{el}	0.306	0.309	0.307	0.318
	P_{th}	-1.428	-0.433	-1.428	0.253
	P_{gas}	3.953	0.830	3.953	2.355
P_{el}. SL bus		-1.105	-1.385	-13.029	-13.248
Q_{el}. SL bus		7.026	2.120	5.700	-0.001
P_{th}. SL bus		-1.500	0.218	2.120	-0.339
Obj [€/h]		1178.0	979.0	1178.0	927.0

as an ancillary service. The above prices apply for both purchase and selling electrical and thermal power, whereas natural gas may only be purchased.

Aim of the optimisation is to minimize the hubs operational costs, while respecting all the system constraints and enabling their participation to the electric network voltage regulation.

4.2.2 Results and discussion

A selection of the results is reported in figs. 4.2 and 4.3 (electric network voltage profiles) and table 4.1 (energy hubs operational data, power data in pu with $P_{base} = 1MW$). Without any voltage control provision (OLTC transformer set to tap=0 and bus voltage allowed to vary in the range 0.96-1.04 pu) the two distributed generation scenarios lead to the opposite voltage profiles represented by the red dashed lines in figs. 4a and 5a.

Scenario I

In this case of low DG production bus voltages are generally depleted (N8 reaching the minimum allowed limit of 0.96) and the OLTC is considered to intervene by lowering 1 tap thus increasing the network bus voltage levels (blue solid line in fig.

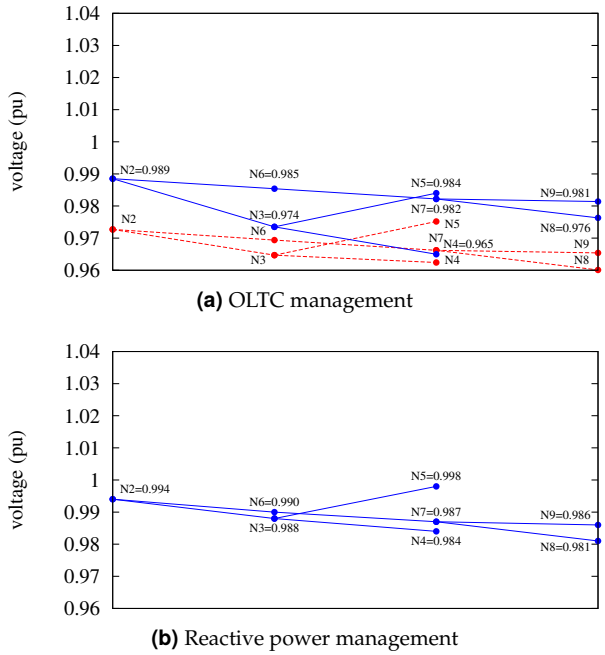

(a) OLTC management

(b) Reactive power management

Figure 4.2: Voltage profiles - scenario I: 4.2a OLTC transformer with tap = 0 (red dashed line) and with tap = -1 (blue solid line) without voltage control; 4.3a OLTC transformer with tap = -1 and voltage control.

4.2a). In the hypothesis of CHPs of the energy hubs instructed to produce active power only ($cos\varphi = 1$), the optimisation results in the hubs import/export power conditions shown in column (1.a) of table 4.1, characterized by a total operational cost of 1178 [€/h].

In order to further improve the network voltage profile, the DSM is supposed to set a minimum bus voltage level equal to 0.98 and the CHPs of the energy hubs are enabled to generate reactive power ($cos\varphi < 1$) within their capability curves. Considering these new constrains, the optimisation procedure is run again resulting in the hubs import/export power conditions shown in column (1.b) of table 4.1 and the network voltage profiles of fig. 4.2b. It can be noticed that the overall better voltage distribution is achieved with a general increase of the levels of feeder L1 bus voltages. This is attained by the optimised re-distribution of the import/export power of the energy hubs, in particular H4 which is the element connected to the most depleted electric bus (N4).

It is of interest to highlight that the overall operational costs of the 4 hubs participating to the voltage regulation is reduced by 17% with respect to the previous case. Such cost reduction is due to the higher exploitation of the CHPs, enabled by the presence of the thermal network which allows CHPs to modulate their heat production and supply also remote loads (although total gas consumption is increased by 20%, the heat power import through slack bus TH5 is almost zeroed and the CHPs increase their reactive power production of more than 1.2 MVAR).

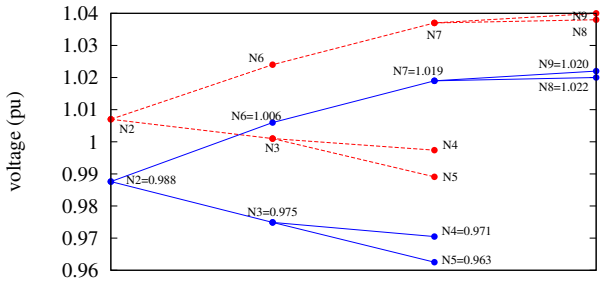

(a) OLTC management

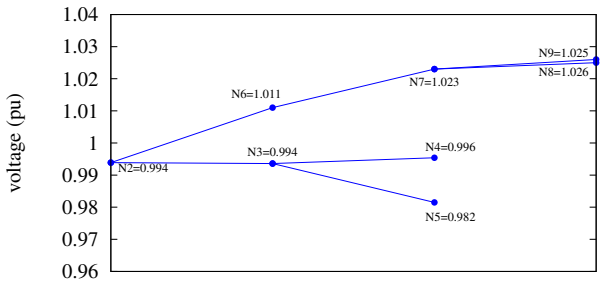

(b) Reactive power management

Figure 4.3: Voltage profiles - scenario II: 4.3a OLTC transformer with tap = 0 (red dashed line) and with tap = 1 (blue solid line) without voltage control; 4.3b OLTC transformer with tap = 1 and voltage control.

Scenario II

In this case of peak distributed generation, mainly concentrated on feeder L4, without any regulation action the voltage distribution would be as shown by the red dashed line in fig. 4.3a, from which it is noticeable that the two feeders have opposite voltage behavior. In such condition the OLTC would react by increasing 1 tap, thus lowering the network bus voltages and leading to the profile given by the blue solid line in fig. 4.3a. As a result, feeder L1 bus voltage levels are considerably lowered with N5 almost reaching the minimum allowed level. With the CHPs of the energy hubs forced to produce active power only, i.e. no participation to voltage regulation, the optimisation procedure leadsd, as it could be expected, to the same hubs import/export power conditions as in the previous scenario (see column (2.a) of table 4.1).

Similarly as before, the DSM is now supposed to set a minimum bus voltage level equal to 0.98 and the CHPs of the energy hubs are enabled to generate reactive power ($cos\varphi < 1$). The optimisation procedure is run again resulting in the hubs import/export power conditions shown in column (2.b) of table 4.1 and the network voltage profiles of fig. 4.3b.

Once again, the optimised re-distribution of the import/export power of the energy hubs leads to an overall better voltage distribution (in particular the levels of feeder L1 bus voltages) and this is accomplished with almost a 20% reduction of overall operational costs of the 4 hubs.

4.3 Optimal co-ordinated operation

In the overall system optimisation problem there are two main issues when considering storage elements and both electrical and thermal loads. Firstly, a multi-period optimisation should be done on the entire system in order to take into account the peculiar characteristics of energy storage elements and the benefits they could provide to the network if suitably managed, like asset deferral and peak lopping. Unfortunately, this is hardly feasible due to the high number of variables which need to be considered. In addition, the presence of thermal loads and their interactions with the electrical system means that extra variables and relationships must be introduced thus increasing further the problem complexity.

The problem has been here approached by applying an iterative procedure where network and energy hubs are separately optimised and suitable information between them is suitably exchanged [45]. Incentiving price signals to each producer/consumer, the network optimisation requires knowledge of generation costs and constraints able to hint the correct behavior to active devices in order to try to satisfy the network needing through economic signals [43]. The decoupled procedure has been introduced in chapter 2. In this specific application the algorithm flow chart is pictured in fig. 4.4 to better understand the steps of the procedure.

4.3.1 Reference voltage and power levels

Considering a multi-period optimisation with n_T time steps, n_T optimal power flows are executed. In the electrical network model each energy hub is represented by an equivalent generator/load. The goal of optimisation is to reach the maximum revenue for all generators participating to regulation. The system operator has to send price information such that the maximum revenue of generators is verified when voltage profile is equal to a desired voltage profile. The system operator has been supposed to know the best voltage profile for the network knowing network characteristics and historical data about loads and generation. This best voltage profile is the desired, or reference, profile. It could be nominal voltage values for all nodes or different values. In this case, for each bus i-th, for each considered time step, the reference voltage $V_{ref,i}$ is supposed equal to the value obtained by a preliminary minimum losses optimisation of the electrical network. Together with those reference values, suitable price signals are elaborated to hint distributed active devices to operate trying to achieve the reference voltage profile.

Similarly to electrical network optimisation, the MPO of each energy hub is performed assuming suitable price signals sent by the system operator. Again, these price signals are proportional to the reference active and reactive power profiles such that the maximum revenue of the energy hub is verified when electrical powers at input side are equal to reference profiles.

The power balance at the corresponding bus of each energy hub is assumed as the reference active and reactive power at input side of each one of them, which match with the optimal behavior of energy hubs from electrical network point of view.

If storage devices are correctly sized, energy hub is able to follow the desired power profiles at input side and increase its revenue. Otherwise, results of energy hubs could negatively affect the optimal network set.

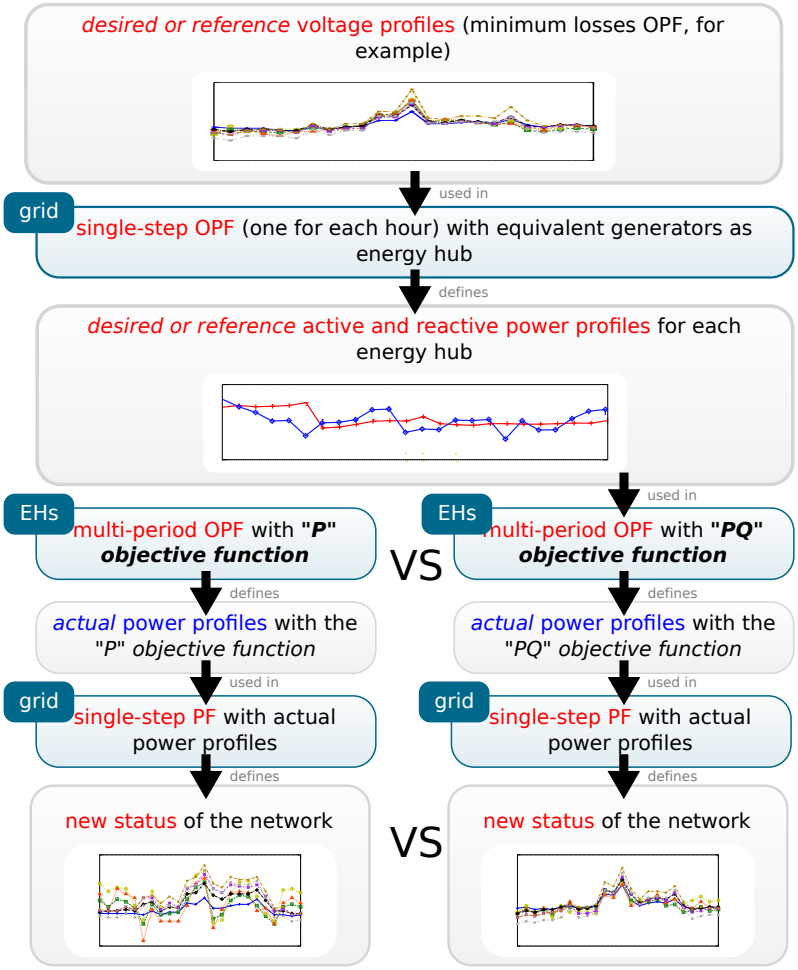

Figure 4.4: Decoupled procedure conceptual algorithm scheme for the management of electrical networks with energy hubs and electrical storage devices.

In this latter case, these results will modulate price signals for a new network optimisation and so on, until a balance between system operator and producer/consumer goals is reached. The final results would be the global optimum.

4.4 Network optimisation

Network optimisation is performed using a standard optimal power flow procedure with the objective function described below.

4.4.1 The objective function of network optimisation

For each considered time step t, the objective function of the optimal power flow is:

$$f_t = \sum_{i=1}^{n_g} (RE_{P,i} + RE_{Q,i} - C_{V,i} - C_{Q,i}) \tag{4.7}$$

where n_g is the number of generators participating to regulation. Revenue $RE_{P,i}$ of active generation (P_i) is given by (4.8). The price coefficient is the difference between the purchase price p_t and the generation cost c_i of i-th generator.

$$RE_{P,i} = (p_t - c_i)P_i \tag{4.8}$$

For the slack generator, sign of (4.8) is reversed, because its generations means import from up stream network.

The second addend $RE_{Q,i}$ is given by (4.9) and represents purchase of reactive energy which is proportional to voltage mismatch between the value V_i and the reference voltage $V_{ref,i}$ at i-th bus:

$$RE_{Q,i} = swc_{V,i}Q_i \tag{4.9}$$

where s is the sign of voltage mismatch used to indicate inductive or capacitive reactive power needs; w is a weight coefficient ($p_t/100$) proportional to variable purchase price of active power and used to modulate the weight of reactive power generation; $c_{V,i}$ represents a linear proportional relation given by (4.10) and provides a bus remote power requirement coefficienct proportional to the voltage mismatch: the purchase price of reactive generation is posed equal to the active one if $V_i = \pm V_{max}$ (with $V_{max} = -V_{min}$).

$$c_{V,i} = \frac{(V_{max,i} - V_{min,i})/2 + |1 - V_i/V_{ref,i}|p_t}{V_{max,i} - V_{min,i}} \tag{4.10}$$

The third addend of (4.7) has been introduced to account for null generations of reactive power. If no reactive power is generated, no price signal is given to generator i-th because (4.9) is zero. Then cost $C_{V,i}$ is directly proportional to voltage mismatch at i-th bus.

$$C_{V,i} = 100wc_{V,i}|1 - V_i/V_{ref,i}| \tag{4.11}$$

Finally, reactive generation cost has been added in the network objective function (4.7). Reactive power is always a cost and it has been supposed equal to active generation cost for each generator.

$$C_{Q,i} = c_i|Q_i| \tag{4.12}$$

4.5 Energy hub optimisation

Referring to constraints needed to correctly modeling energy hubs with storage devices (chapter 2), in this application two MPO have been compared to demonstrate that only suitable price signals could be used by system operator if a virtuous behavior is the main purpose. Obviously, as in network optimisation, this means that the system operator needs to invest in devices participation to ancillary services for the grid support. In particular, in reactive power regulation.

4.5.1 The objective function of energy hub optimisation

Maximum revenue is the objective function of each energy hub. Two objective functions have been considered, here referred to as "P" and "PQ" objective function respectively, as pictorially represented in fig. 4.4. The "P" one considers only optimisation of electrical active input, whereas the "PQ" generates price signals constructed according to the electrical network manager point of view. In this latter case, the goal is to obtain the expected active power P_i and more important reactive power Q_i values at the input side of energy hub in order to maintain the previous optimal power flow results. This is accomplished by assuming suitable electric tariffs including reactive power selling/purchase prices.

The "P" objective function f_P shown in (4.13) maximizes the revenue of energy hub and it is a function of E_t, $E_{gas,t}$, $E_{th,t}$, active, natural gas and thermal energies respectively at input side of the energy hub at time step t.

$$f_P = \sum_{t=1}^{n_T} (R^P_{E,t} + R_{CHP,t} - C_{th,t}) - C_{gas,t} \tag{4.13}$$

The first term $R^P_{E,t}$ is equal to the product between active electrical purchase price p_t and the active electrical energy E_t at time step t. The sign of the product is changed because import energy is a cost and export is a revenue.

A payment for active electrical generation of CHP ($E_{CHP,t}$) is introduced (4.14) to give a price signal to the optimisator.

$$R_{CHP,t} = 0.4 p_t E_{CHP,t} \tag{4.14}$$

Import thermal energy is a cost, export thermal energy is a revenue, both of them referring to the costant coefficient c_{th} (4.15) [33].

$$C_{th,t} = c_{th} E_{th,t} \tag{4.15}$$

The cost of natural gas imports (4.16) is the sum of a fix term $c_{gas,fix}$, a peak-flow term $c_{gas,p}$ and a constant term c_{gas} proportional to gas volume $q_{gas,t}$ [43].

$$C_{gas,t} = \sum_{t=1}^{n_T} (c_{gas} q_{gas,t}) + c_{gas,p} max(q_{gas,t}) + c_{gas,fix} \tag{4.16}$$

The "PQ" objective function f_{PQ} shown in (4.17) is similar to (4.13) but terms proportional to reactive energy $E_{Q,t}$ is introduced and both active and reactive revenues are changed accordingly.

$$f_{PQ} = \sum_{t=1}^{n_T} (R^{PQ}_{E,t} + R_{E_Q,t} + R_{CHP,t} - C_{th,t}) - C_{gas,t} \tag{4.17}$$

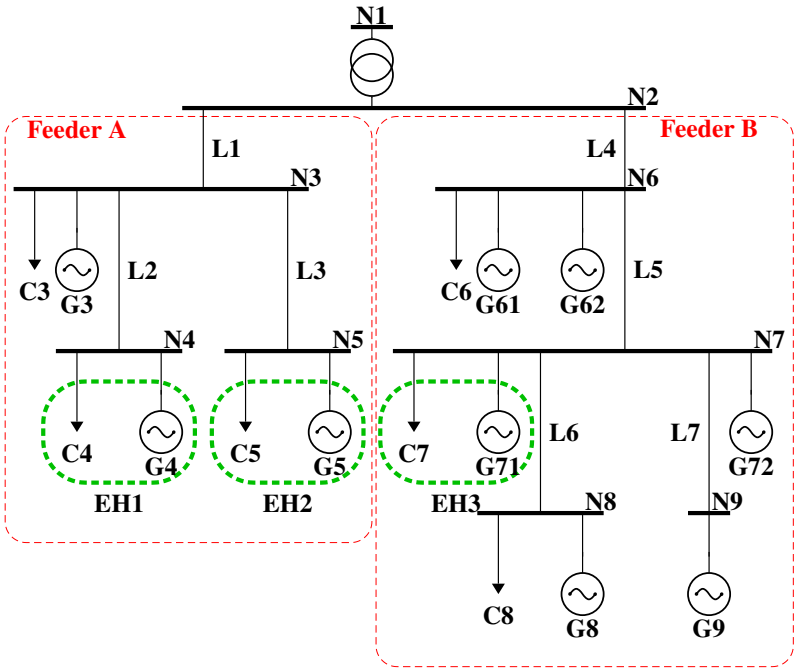

Figure 4.5: Electrical network with energy hubs (EH).

Addends $R_{E,t}$ and $R_{E_Q,t}$ are respectively revenues of active (4.18) and reactive (4.19) energies. Purchase price p_t is equivalent to remuneration if the mismatch between value at time t (E_t and $E_{Q,t}$) and reference ($E_{ref,t}$ and $E_{Q,ref,t}$) values is zero, otherwise penalty costs ($c_{P,t}$, $c_{Q,t}$) are added.

$$R_{E,t}^{PQ} = (p_t - c_{P,t} - c_{Q,t})|E_t| - c_{P,t}|E_{ref,t} - E_t| \tag{4.18}$$

$$R_{E_Q,t} = (p_t - c_{Q,t})|E_{Q,t}| - c_{Q,t}|E_{Q,ref,t} - E_{Q,t}| \tag{4.19}$$

$c_{P,t}$ (4.20) and $c_{Q,t}$ (4.21) are cost coefficients that reduce price at time t proportionately to active and reactive mismatch. $c_{Q,t}$ appears also in (4.18) to give an higher weight to reactive power balance.

$$c_{P,t} = 1.1 p_t |E_{ref,t} - E_t| \tag{4.20}$$

$$c_{Q,t} = 1.1 p_t |E_{Q,ref,t} - E_{Q,t}| \tag{4.21}$$

Other terms in (4.17) are thermal and natural gas input energy costs and payment for active electrical generation of CHP and they have been descrived previously.

4.6 Optimal co-ordinated operation application

The electric network is a 20 kV 9-bus radial network, connected to the bulk grid (slack bus N1) through a on-load tap-changer (OLTC) transformer (which, for the sake of clarity, is not been considered in regulation in this study). The electrical network one-line diagram is reported in Fig. 4.5, whereas Fig. 4.6 shows the total daily active and reactive power produced by generators and absorbed by loads.

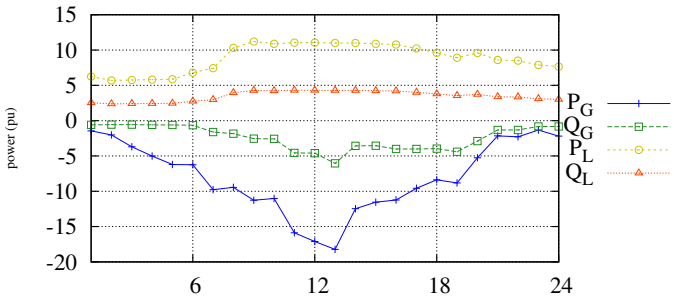

Figure 4.6: Daily total active and reactive power of generators (P_G and Q_G) and loads (P_L and Q_L) for each considered time step.

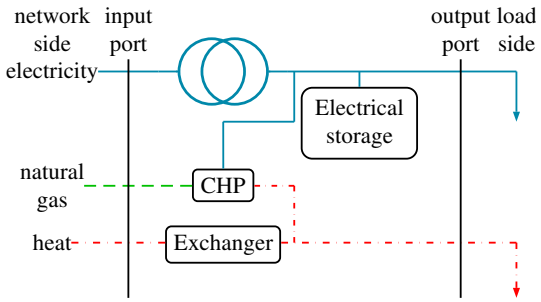

Figure 4.7: Energy hub layout.

G4, G5 and G71 generators with C4, C5 and C7 electrical loads represent the electrical equivalent of the energy hubs for the electrical network simulation.

Energy hubs layout is shown in Fig. 4.7 and data is available in table 4.2. Both CHPs and storage devices participate in voltage regulation.

In this study the assumed gas cost coefficients c_{gas}, $c_{gas,p}$, $c_{gas,fix}$ (4.16) are respectively 0.358 €$/m^3$, 2.96 €$/year/(m^3/day)$ and 1850 €$/year$ [43]. Thermal cost (4.489 €$/kWh$) has been supposed 20% higher than natural gas power cost to account for efficiencies and other thermal generation costs [33]. Electrical generation cost match with fuel costs: 0 c€$/kWh$ for renewables generators, 13 c€$/kWh$ for biomass generator and 16 c€$/kWh$ for equivalent CHPs [46]. Purchase prices p_t has been assumed in accordance with italian day before market and taking into account generation costs (24 c€$/kWh$ is the average).

All electrical generators take part in voltage regulation. The energy hub equivalent generators could generate active and reactive power within $\pm 3MW$ and $\pm 3MVAR$ limits, whereas other generators could vary their active and reactive production within $95 \div 100\%$ of their active and reactive generation at time t.

4.6.1 Results and discussion

Considering a base case where the CHP units are disconnected, the initial power flow provides the bus voltage profile reported in Fig. 4.8. It clearly apperars that the electrical network feeders are characterized by opposite voltage profiles, i.e. feeder A (N3, N4, N5) has depleted voltage levels (which can be lower than 0.95 pu), whereas

Table 4.2: Energy hubs data (pu) ($P_{base} = 1MW, dt = 1h$).

Efficiencies		
transformer efficiency	0.98	
CHP electrical efficiency	0.35	
CHP thermal efficiency	0.45	
exchanger efficiency	0.78	
storage charge efficiency	0.90	
storage discharge efficiency	0.90	
CHP and electrical storages data		
CHP electrical generation	3.5	
starting energy in electrical storage	2.5	
standby losses in electrical storage	0	
CHP and electrical storages constraints		
	max	min
$cos\varphi$ of CHP	0.8	-0.8
stored energy in electrical storage	5	1
power of electrical storage	2	-2
$cos\varphi$ of electrical storage	0	2π
Input power constraints		
input electrical active power	4	-4
input electrical reactive power	4	-4
input thermal power	4	-4

feeder B (N6, N7, N8, N9) busses may even exceed 1.05 pu. In this case the OLTC operation must be inhibited and can not contribute to voltage regulation.

Starting from this base case, the proposed optimisation procedure including the energy hubs has been applied: a selection of the results of the preliminary minimum losses network are reported in Fig. 4.9a (reference bus voltage), whereas the corresponding reference input active P_{ref} and reactive Q_{ref} power for the three energy hubs are shown in Fig. 4.10.

Fig. 4.9b shows the network bus voltage profile resulting from the energy hub optimisation considering the "P" objective function. From electrical point of view, every energy hub aims to export active power and absorb the reactive power from its loads. This behaviour is evidenced in Figs. 4.10a, 4.10b and 4.10c and it is independent from load curves (EH1 and EH2 are characterized by different industrial curves and EH3 by a residential load curve, both electrical and thermal). As a consequence, network bus voltage can be quite different from the desidered reference voltages. From Fig. 4.9b it appears that the "P" objective function gives rise to an acceptable voltage distribution since bus voltage levels remains within the allowable limits; however, within each time step the spread of the voltages does not allow the OLTC to operate correctly.

Conversely, assuming reference voltage profiles as goal, the "PQ" objective function with suitable prices signals is able to satisfy network needings through a redistribution of the import/export power as can be seen by the network voltage dis-

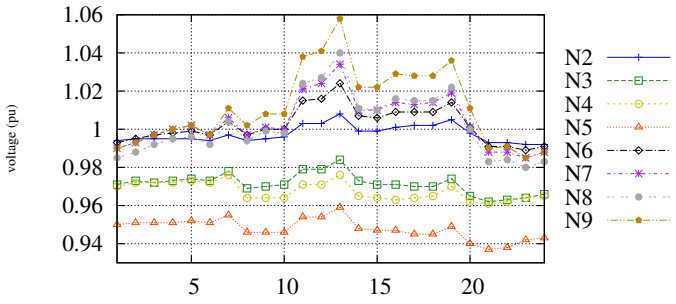

Figure 4.8: Base case voltage profiles.

tribution of Fig. (4.9c). It should be noted that in this case network voltage profiles could be further improved by the OLTC operation since within each time step the bus voltage spread is quite narrow. Input active and reactive power follow reference values quite well (Figs. 4.10a, 4.10b and 4.10c) thanks to electrical storage availability and thermal input that could free electrical and thermal generation of CHPs.

Energy hubs respond in a different manner to price signals, as regards to load curves and input reference power curve. As shown in Fig. 4.10c, for instance, input active power of EH3 is quite different from the reference value due to requested high import set against the relatively low load demand.

It should be emphasized that, in order to satisfy network needings, energy hubs miss out their maximum revenue because purchase prices are proportional to power values. Thus, with the more incentivating "PQ" objective function, a term should be added for compensating for input powers which are constrained to reference values. At the same time, system operator should consider some incentives for investments in electrical storage that may play a key role in network regulation. In fact, energy storages could allow reaching reference power values and maximum gains with asset deferral. The behaviour of storage devices is influenced by size parameters like stand-by losses, maximum and minimum power and energy. Moreover "P" objective function is more susceptible to changes of these parameters and voltage profiles could negatively be influenced, because of the re-distribution of active power export without any control by system operator.

4.7 Conclusion

The developed optimal power flow simulation tool for multi-vector energy systems has been applied to a case study system, formed by a an integrated electric and thermal network system, coupled at nodes with energy hubs, local generation, storage and conversion center among different energy carriers. In particular, CHP units have demonstrated their ability to enable their active active participation to network voltage regulation while reducing their overall operational costs. The optimisation is based on cost functions and even better results could be expected by introducing suitably modulated price signals and different tariff scenarios.

In fact, considering the strong impact of energy prices in present energy policies, energy markets system will be improved in the next future. In particular, innovative price list system and a plurality of energy markets are necessary to provide suitable

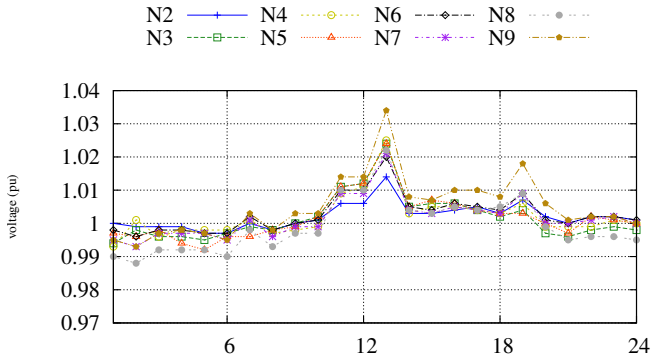

(a) Reference voltage profiles (pu)

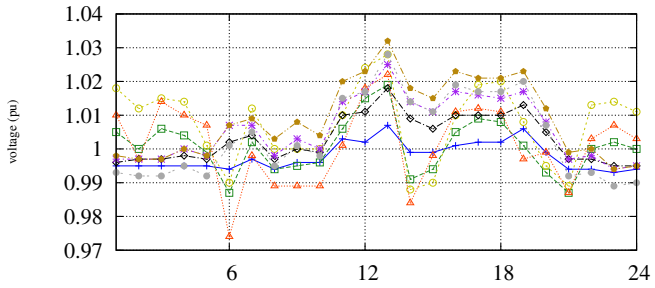

(b) Voltage profiles with "P" objective function (pu)

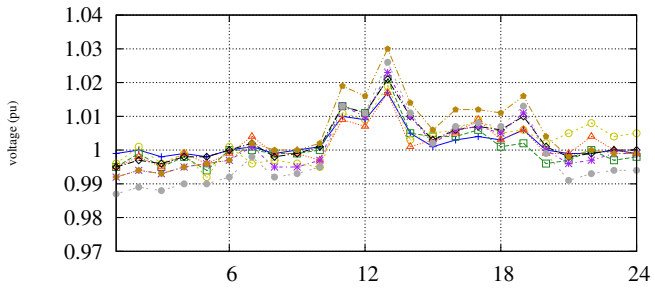

(c) Voltage profiles with "PQ" objective function (pu)

Figure 4.9: Optimised daily voltage profiles of electrical network $V_{base} = 20kV$ (refer to legend at the top).

signals to each active element of the network as in an internet-like model. Furthermore, it seems interesting to translate technical constraints or network needs in suitable price signals which have to reach each bus. In this way, an optimal behavior should be naturally obtained considering the highest owners' revenue.

This idea has been exploited in a second application, where a distribution network has the availability of storage devices and CHP plants located in some nodes, where different energy vectors at input side of the energy hub interface could provide support to electrical network.

A co-ordinated operation of distributed multi-generation in active distribution networks is presented, with specific focus on electrical networks with distributed storage devices and CHP units. Two different optimisations have been proposed for electrical network and energy hubs, for dealing with a multi-period optimisation

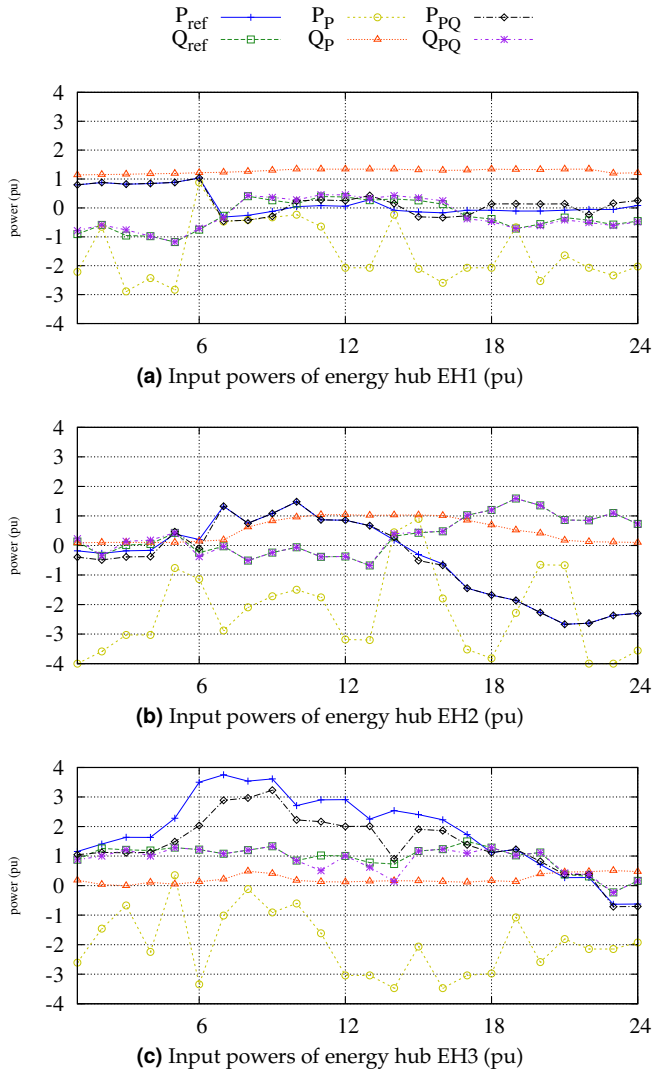

(a) Input powers of energy hub EH1 (pu)

(b) Input powers of energy hub EH2 (pu)

(c) Input powers of energy hub EH3 (pu)

Figure 4.10: Daily input active and reactive power for energy hubs ($P_{base} = 1MW$). For each plot, reference ($_{ref}$), "P" ($_{P}$) and "PQ" functions ($_{PQ}$) values are given. (Refer to legend at the top.)

that is necessary to manage storage devices. Suitable price signals have been introduced to obtain specific voltage profiles, whereas the objectives of each optimisation problem is the maximum overall gain of the distributed generators participating to regulation. A case study has been presented in which it is shown that, by introducing suitably modulated price signals, energy hubs with CHPs and storage devices may enable their active participation to network voltage regulation while reducing their overall operational costs. In particular, storage devices with interface converter devices have a key role adding flexibility to CHP plants, but they are penalized by investment costs (which are not considered in this paper). Consequently, more specific cost terms have to be introduced for incentivating storage installations and a more network compatible behavior of active elements.

5 Electric Vehicles as Distributed Storage Devices

A widespread diffusion of Electric Vehicles (EVs) plugged into distribution networks is strongly dependent on the establishment of a suitable co-ordinated management of all active resources in the grid. Vehicle-to-grid technology, allowing bi-directional power flows of on-board batteries, would enable a responsive behaviour of Plug-in electric vehicles. EVs aggregators, such as swapping stations and car parking, would have the potentiality of providing strategic ancillary services for the grid support. Provided an efficient remuneration scheme is applied, EVs could meet responsively the requirements of the grid, activating their participation also in voltage regulation. In fact, electronic equipments of re-charge infrastructures would enable to exchange reactive power with the grid without practically affecting the downstream flow of batteries. Reactive power management could increase the opportunities for EVs and the benefit for the network. In this chapter, these concept are presented and investigated.

5.1 Introduction

The use of Electric Vehicles (EVs) is expected to increase significantly in the near future due to increasing petrol costs, emission reduction needing, technological improvements particularly for batteries, development of ICT systems for the re-charge system management, the increasing interest in re-charge infrastructures envisaged in a smart grid scenario, the increasing interest of automotive industry in EVs. EVs can be broadly classified as battery vehicles, that store energy on board, hybrid vehicles, with an internal combustion engine and a storage unit, and fuel cell vehicles, with on-board generation using fuels as hydrogen and an optional storage unit [47]. These vehicles can be "plugged in" to the electrical grid (PEVs, Plug-In Electric Vehicles) to re-charge their batteries, having a strong impact on the electrical network [48]. As an example, with new load demand peaks and voltage constraints violations, due to simultaneous re-charge of batteries, and with power quality depletion, due to the electronic equipments of re-charge infrastructure [49], [50], [51].

The out-coming critical situations, in a scenario already stressed by the increasing penetration of Distributed Generation (DG), need to be investigated thoroughly. It clearly appears that, similarly for the DG issues, the connection of a large number

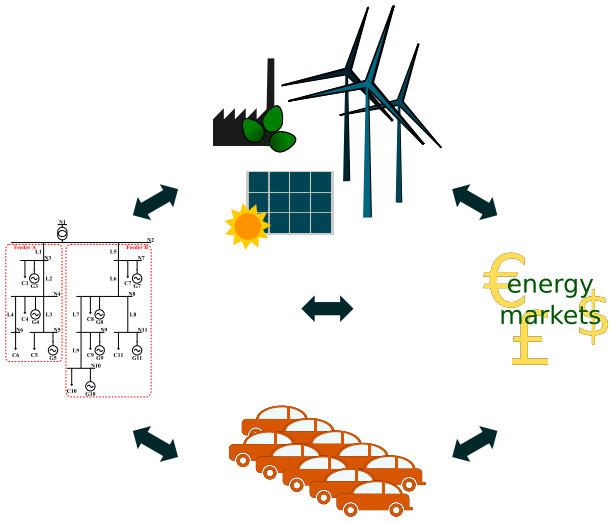

Figure 5.1: Interactions among distributed generation (DG), EVs, electrical networks and energy markets concept.

of EVs into the electrical grid can not avoid the establishment of a suitable network management and a new regulatory framework, in particular when considering the presence of on-board storage elements.

On-board batteries make vehicles interesting for their potential role as distributed Energy Storage Systems (ESSs) thanks to Vehicle-To-Grid (V2G) technology, which enables plugged-in vehicles to reverse the power flow from the vehicle to the grid [52], [53].

The ability to shift the absorption/generation when it is required, gives to storage devices the opportunity to contribute to the grid support (ancillary services), but large electrical storage devices are penalized by actual high investment costs, as demonstrated in chapter 3. In this perspective, a large number of EVs and their re-charging infrastructures represent a remarkable chance for distribution networks.

Transportation network would provide a sort of distributed Energy Storage System (ESS) avoiding starting investment costs by the electrical network, whereas distribution networks could add value to EVs by remunerating their participation in ancillary services for the grid support. In an ideal interactive smart grid scenario, interactions among DGs, EVs, energy markets and energy networks will ensure a greater efficiency in the system management, allowing devices that participate in the grid regulation the freedom to decide whether or not providing the required regulation service depending on price signals. This concept, schematically depicted in fig. 5.1, is consistent with the main thread of this thesis, i.e. to obtain an integrated co-ordinated distribution system management of resources able to obtain optimal results thanks to interactions of different knowledge levels.

In this chapter, large aggregation of EVs[1], like swapping stations and car parkings are considered to analyze both drawbacks and potential benefits associated with a large penetration of EVs if suitably managed and co-ordinated with the network requirements. A co-ordinated procedure for the aggregation of EVs management is

[1]In the following, EVs refers to PEVs with on-board batteries

presented. In particular, participation in voltage regulation of EVs is investigated in a case study electrical network. Their re-charging infrastructure is exploited to provide reactive power without affecting the Status of Charge (SOC) of batteries [54].

5.2 Plug-in Electric Vehicles

Plug-in Electric Vehicles (PEVs) like

- Plug-in Hybrid Electric Vehicles (PHEVs), that run on an internal combustion engine with batteries (e.g., 5-22 kWh) that can be recharged by connecting a plug to an external electric power source;
- Extended Range Electric Vehicles (EREVs), characterized by larger on-board batteries (e.g., 16-27 kWh), able to allow long all-electric ranges (e.g., 40-60 miles);
- and Battery Electric Vehicles (BEVs), pure electric vehicles with no internal combustion engine and recharging needing at the end of their designed driving range, with generally the highest all-electric range (e.g., 60-300 miles) and the largest battery capacity (e.g., 25-35 kWh);

are characterized by on-board battery units [55]. The powering of the vehicle makes PEVs loads that needs to be more or less regularly supplied, impacting into the grid.

However, the key role of storage devices, as batteries, has been already recognized, in order to make electricity grids smarter and to modernize them so that they can accept large amounts of renewable energy resources. In fact, distribution networks is expected to install ESSs making more flexible the system, in order to achieve a clean and secure electric power system, increasing its efficiency and lowering system costs.

As a consequence, the V2G technology has the ambitious purpose to make the transportation network a great opportunity for the electrical system, allowing bi-directional flows between the grid and the on-board battery and providing all control devices for a responsive behaviour of EVs. In this way, the electrical grid may have the availability of batteries and infrastructures without investment needing to make the system more efficient, taking advantages from synergies with the transportation network. EVs with V2G may at this point participate in ancillary services for the grid support, proving power in to the grid when it is needed.

In order to analyze and discuss the potential benefits of EVs, in the following we have assumed a future electric grid scenario with well-established smart grid and V2G technologies. Really, V2G applications are still many years away from practical application, in particular due to the needing to better understand shortening of battery lifetime according to the increasing frequency of charge and discharge cycles to support the grid. Whereas smart grid technology have to be fully developed allowing communication capillarity, real time control and distributed management control [56].

5.2.1 The battery

The battery is the key component for EVs, in particular focusing their availability to participate in grid regulation. On the other hands, it is the most expensive compo-

nent of EV technology (600$ per kWh in [56]) and it is the component most subject to deterioration.

In fact, the expected life of battery, often expressed in terms of number of cycles, is a key parameter in EVs, because it directly influences vehicle costs. Even if degradation aspects are still under investigation, it is clear that all performances degrade lifetime and particularly with change and discharge operations, which define the key potentiality for the electrical network. In lithium-ion batteries, for example, both a deep discharge and a very high state of charge for long periods of time decrease lifetime. For these reasons, many automakers are integrating a reserve portion to avoid fully discharge and overcharging, which limits vehicle range.

Performances of batteries are identified by power, the rate of energy transfer, and energy, that measures the storage capacity. For automakers both high power and high capacity are important to obtain high acceleration and fuel distance values respectively. Lithium-ion batteries are mostly used for automotive purposes, due to improved energy density and power density (from 50 to 175 Wh/kg and 10 to 9000 W/kg), enabling very large batteries with long ranges to be placed in vehicles while minimizing the weight and size burden that nickel metal hydride or lead acid batteries, used at the beginning, would necessitate.

Safety is another important aspect for batteries, which convert chemical in electrical energy through chemical reactions. Safety has to be guaranteed both in typical and critical driving conditions, in particular considering the coupling effect with electrical circuits on-board EVs.

Actual research for new battery generation focuses on the improvement of energy and power density values, taking into account charge and discharge characteristics and the environmental impact of waste disposal of materials. High efficiency is obviously desired, but the main issue is the fast re-charging, required to increase the EVs acceptance of drivers, who prefers the faster petroleum fuel re-charge process at petroleum stations.

5.2.2 Charging infrastructures

A charger for EVs is the device that connects the vehicle to the electrical grid and through batteries are charged, defining the power that could affect the grid.

There are different levels of charging based on the power available. USA are working to define general drawlines whereas Europe is recently involved in EVs demonstrative projects [56].

In USA, level I charging uses the traditional 110 V outlet, usually used for nightly re-charge operations, which may cover most of the owners needing. Many consumers consider fundamental to charge the energy storage unit as quickly as possible so that the vehicle is ready for the next trip in the shortest time. For this reason many drivers may opt for higher-power chargers, Level II, for a faster re-charge (some hours) against a more expensive installation. Level II charging is specified at between 208 and 240 V (the voltage used in many homes by clothes driers, ovens, and well pumps).

Level III chargers are capable of providing a high voltage ($\sim$600 V) “fast charge” that can charge vehicle batteries in minutes rather than hours. This option will be supplied by public chargers, both due to high costs and to safety installation requirements, allowing a fast charge for a driver who forgot to or was unable to charge

(a) A charger **(b)** Charger point

Figure 5.2: Charger of Nissan Leaf and a charger point of Coulomb Technologies.

overnight, or who is traveling beyond the range of the vehicle without the time to stop and wait for a slower charge. Due to high voltage circuits, level III chargers are still under investigation.

In fig. 5.2, two example of chargers are shown [57, 58].

5.3 Impact of EVs in the electrical grid

A large penetration of EVs will have a great impact on power distribution networks, modifying load and voltage profiles, network losses and power quality. Similarly to the distributed generation issues, without a suitable management and a new regulatory framework, the electrical grid could hardly be able to accept the connection of a large number of EVs.

EVs require energy for re-charging their on-board batteries depending on EVs characteristics and paths. This "new" additional load demand will alter the actual network load profiles, which are usually higher during the day rather than night. A high penetration of EVs could create new load demand peaks according to nowadays prices, re-charging habits of drivers and chargers [49]. In the case of massive fast chargers adoption, a hypothetical increase of the peak demand will require new power plants, which should be unnecessary considering both the low increase of vehicles at the beginning and the expected nightly re-charge procedure [48].

On the other hand, the possibility to reverse the flow of power back to the grid with the V2G technology could create different instable situations that electrical grid cannot handle with the actual structure.

V2G could enable, in the future, the participation of EVs in energy markets, enabling them to operate by buying when price is lower and selling when it is higher to maximize the revenue. Accounting driver and technology limitations, it is possible to optimise the behaviour of these economic transactions, but it is foreseen that without a suitable co-ordination the large number of EVs bound to create critical situations.

However, at present and for the near future, the degradation cost of batteries seems not to give sufficient incentives for a market participation [59].

EVs will negatively affect network voltage profiles, which are already stressed by distributed generations, both considering EVs as loads during charge and as generators during discharge [60], [61]. Depending on different conditions of the networks (minimum or maximum and seasonal load profiles) and level of EVs penetration, voltage constraints could be violated, the stability of the system altered and technical efficiency reduced.

Due to their electronic equipments, power quality and phase imbalance could be affected by a high penetration of EVs. Harmonics introduced by battery chargers could cause voltage distortion, in particular considering the likely simultaneity of battery re-charging during the low price hours. Current changes will affect transformers, cables, circuit breakers and fuses [62].

5.4 Role of EVs in the electrical grid

A high penetration of EVs strongly depends on the establishment of a suitable coordinated management of all resources in the electrical network and their active participation on this management. To avoid critical situations and incentiving a virtuous behavior of elements, EVs shouldn't be considered as passive loads, i.e. just batteries to be re-charged according to driver needs. Considering that cars are parked on average more than 90% of the time, EVs should take advantages from their potential as distributed ESS, participating in DSM and network regulation, benefiting from the remuneration provided by the grid for these services.

By enabling bi-directional flows to and from vehicles, power can be released to the grid, likewise ESSs, which are characterized by high investment costs. V2G vision comes just from the idea to inject power to the grid while vehicles are parked [53]. In this way, distribution networks could take advantage of batteries and re-charging infrastructures provided by transmission system, avoiding the investment cost and having to pay only for the service provided.

This scenario is ideally included in a Smart Grid environment, where smart meters and communication technologies would be well developed. In fact, transmission of technical and economical information among active elements, operator system and energy markets is a key factor for smart grids. The exchange of information would enable the elaboration of real time price signals or variable tariffs able to trigger a suitable responsive behavior of the customers aimed at optimising distribution network operation. On the other hand, information as the position of the vehicle and the state of charge of the energy storage unit of the vehicles at all times are expected to be available for the management control system to predict of the next place at which the vehicle will be plugged in and their future power demand and to provide a suitable power management for the grid support.

5.4.1 EVs for the ancillary services

Services identified by the U.K. National Grid for EVs are balancing services like frequency response, to maintain the frequency at its nominal value, and fast reserve, to increase or to reduce the active power; fast start and Short Term Operating Re-

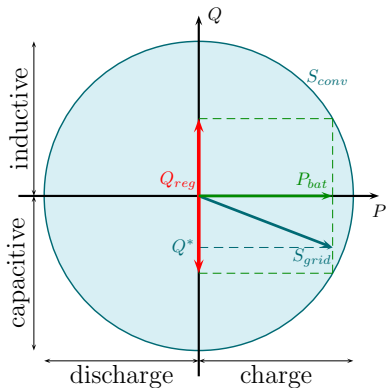

Figure 5.3: Converter (S_{conv} apparent power size) operating scheme.

serve (STOR) in order to deal with unforeseen demand increase and generation unavailability [14]. These services seem to be the most appropriate for four reasons. Firstly, EVs are more suited for supplying large amounts of power in a short time rather than providing long term services. Secondly, since the revenue is proportional to both availability and actual operation, EVs could be remunerated just for being plugged-in. Thirdly, they are compatible with degradation aspects of batteries and with EVs primary application as transport vehicles. Finally, these services are actually remunerated.

Similarly, spinning reserve is considered to be remunerative for EVs applications because payments are both for available capacity and provided energy during operations. Unlike from frequency services, spinning reserve is less frequent, thus preserving lifetime of batteries, although the yearly revenue could be lower.

Another feasible application for battery and fuel cell vehicles could be storage and backup support for intermittent renewable generators like photovoltaic and wind generators [63].

Some other services that could be reasonably provided are the control of power factor for some applications/loads and local voltage regulation. The presence of the converter interface makes it possible to provide reactive power without affecting the active power management of the batteries. The inverter interface of battery chargers, equipped with a 4-quadrant converter, can easily be enabled to exchange reactive power with the grid without affecting the downstream batteries [54]. As depicted in Fig. 5.3 the active power affecting SOC (P_{batt}) determines the available reactive power (reactive power bounds, Q_{reg}), which could be exchanged with the grid. Within these bounds the reactive power Q^* provided to the grid could be modulated, defining the complex power S_{grid} [64, 34].

However, remuneration is fundamental to enable the participation of customers like EVs in regulation services, particularly in voltage regulation [55]. Considering the higher penetration of DGs and the evolution towards a Smart Grid scenario, energy markets are expected to evolve in the next future. New remuneration systems will be created and economical opportunities for EVs are expected to increase. Of particular interest, among others are the reactive power management and voltage regulation services, at present not remunerated.

5.5 EVs aggregators

For either passively supplying a high number of EVs or actively use them for grid support services, a co-ordinated management of the resources is fundamental. Smart meter applications will allow capillarity and differentiation of price signals in a Smart Grid environment and transmission of information regarding plug-in vehicles, such as State of Charge (SOC) and driver requirements (mainly when a fully charged battery is needed). A centralized control will have to co-ordinate the presence of EVs, SOCs and time constraints in order to match active and reactive power requirements.

Even so, the co-ordination of single EV owners and their participation in energy markets appear a hard goal, whereas it appears more likely that aggregation of EVs, such as car parking and swapping stations, will actively participate in the network management [65], [66]. Firstly, they have the critical mass for providing suitable infrastructures for these services [55], [67]. Secondly, a co-ordinated management of resources and participation in ancillary services cannot be dependent only on the availability of vehicles connected to the grid relying on driver needing. Driver needing is a priority, but it is possible to motivate a desired behavior trying to change trends with suitable price signals or variable tariffs, that represent a key factor to modify the unpredictability of EVs which move from/to different locations, referring in particular to ancillary services that are remunerated depending on a contracted available capacity. Consequently, the availability of different price signals for ancillary services would be more feasible with aggregation of vehicles, even if smart meter applications will allow capillarity and differentiation of price signals in a smart grid vision. Finally, the co-ordination of a large number of available batteries would allow a better control of important aspects as degradation of batteries and transportation objectives [34].

In case of battery swap systems, which substitute the depleted battery with a fresh one (swapping station, fig. 5.4 [65, 68]), the electric vehicle's owner could reasonably contract the service, leasing the battery from the swapping station. In this way, the swapping station's owner could supply more effectively the transportation service, ensuring the fully-charged battery to drivers, and the support services for the grid at the same time, negotiating with the distributed system operator its participation to network management.

Car parking of supermarket, industry, office and residential areas have a standard behavior, even if the a random factor depending on people's actions is unpredictable and less estimable. In particular, car parking availability for ancillary services depends on EVs presence, defining capacity and SOC of aggregators. On the other hand, large car parking could have more flexibility in offering different parking/charging prices to incentive the presence of private EVs owners. In this way, the car parking's owner would reduce the pay-back time for the re-charging infrastructures, and be remunerated by the grid for ancillary services.

From the network management point of view, swapping stations and car parking behavior and capacity could be estimated in advance according to historical data, traffic patterns and working hours, plus a random factor depending on driver's decisions (e.g. leaving time, level of charge needed etc.). Swapping stations providing the services to coaches or busses stations are very close to traditional ESS. The number of batteries is always available but the SOC varies according to the service demand [34].

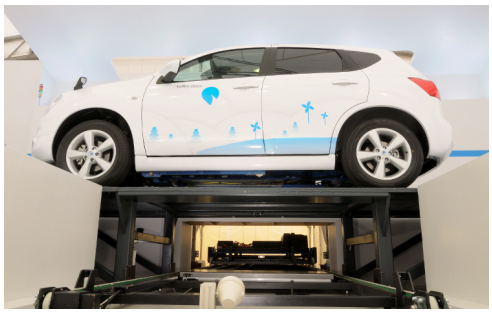

(a) EV loading

(b) The battery swap

(c) The battery

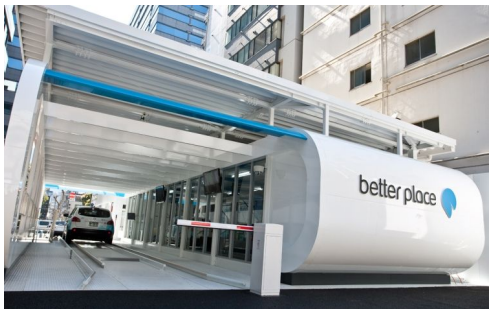

(d) The swapping station

Figure 5.4: The battery swapping station.

The operational characteristics of swapping stations make them particularly suitable for providing grid services as ESS, besides satisfying their main duty of vehicle batteries re-charging.

5.6 Co-ordinated optimal management of EVs aggregators

The management of EVs car parking or swapping stations in a power distribution network can be formulated as a multi-period optimisation problem, which caters for the constraints arising from both the electrical grid and the storage system characteristics. The decoupled procedure introduced in chapter 2 has been adopted, to manage the active power, whereas the reactive power management has been considered in a further step [34]. Fig. 5.5 and 5.6 schematically represents the algorithm scheme used for this specific application.

5.6.1 Multi-period optimisation of EVs aggregators

As shown in fig. 5.5, a multi-period economical optimisation for each EVs aggregator connected to the grid is preliminarily performed, aimed at identifying the active power profiles during the simulated time period.

Since this optimisation does not consider any network constraint, this profile

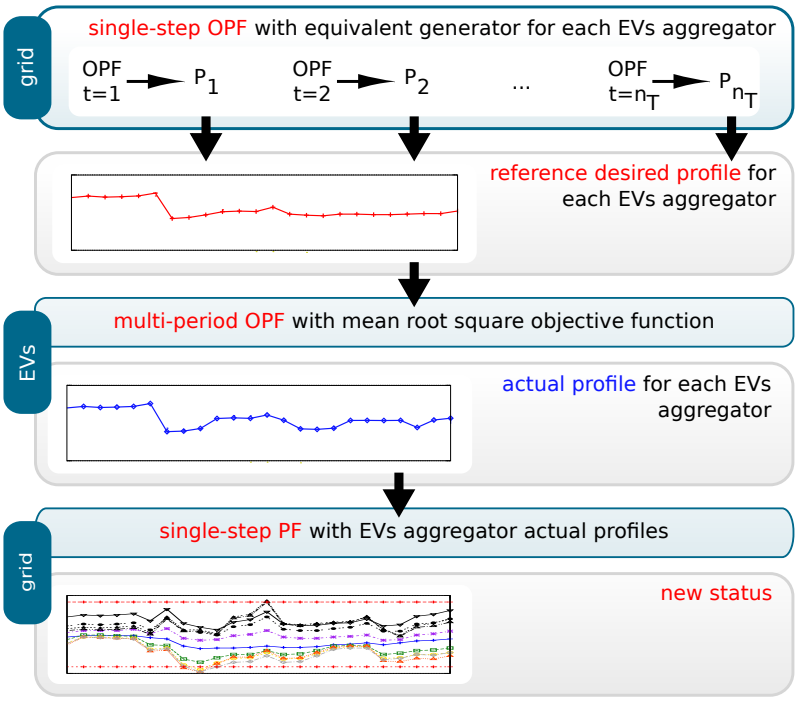

Figure 5.5: Conceptual algorithm scheme for the co-ordinated optimal managament of EVs aggregators (part I).

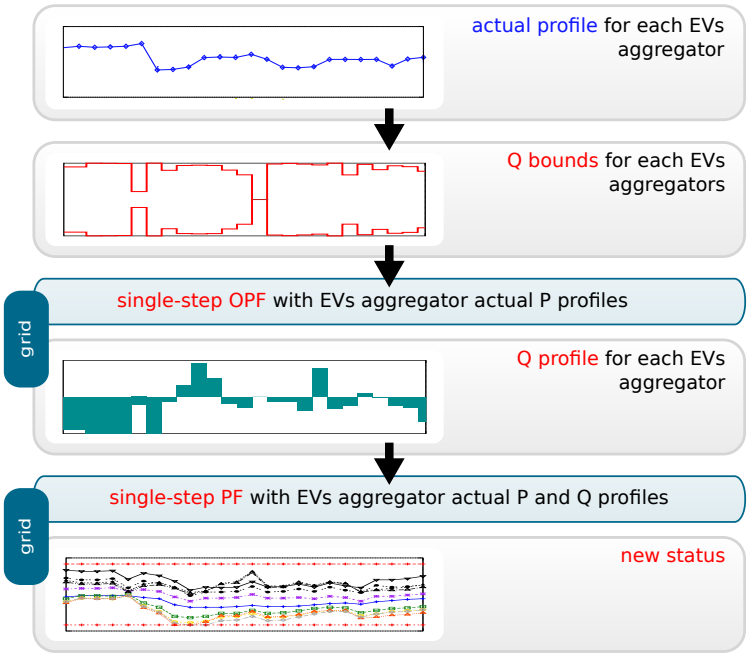

Figure 5.6: Conceptual algorithm scheme for the co-ordinated optimal managament of EVs aggregators (part II).

could either positively or negatively affect the network status. In case of constraints violation, it is possible to suitably modulate the so determined active power profiles on the basis of technical and/or economical information exchanged between network and the aggregators. This is done by means of single-step Optimal Power Flows (OPFs) with a root mean square power deviation minimization from a reference profile multi-period optimisation as objective function, a reference active power profile from the grid point of view is obtained (this profile is the closest one to the profile previously obtained from EVs aggregators optimisation, which complies with the networks constraints). In the same way, a new multi-period optimisation could be run with objective function a root mean square power deviation minimization from the reference profile provided by the OPFs. A suitable compromise between economic consideration of aggregators and technical objectives of the grid is thus achieved iteratively.

5.6.2 Single-step reactive optimisation

As shown in fig. 5.6, the actual active power profiles define the available hourly reactive power of the converters as previously explained (refer to fig. 5.3).

These constraints are used in a single-step OPF, with a root mean square voltage deviation as objective function, assuming reactive power values as unknown variables. In fact, the reactive power is provided by the electronic equipments of re-charge infrastructures, without affecting SOC of batteries. Consequently, the reactive power management to achieve a voltage regulation service can be performed by means of single-step OPFs.

5.7 A case study electrical network with swapping stations

Swapping stations (SSs) dedicated to coaches requires the total amount of batteries fully-charged once in the morning and once in the evening, when coaches leaves and comes back the coach main station. Due to this particular battery service that makes SSs very close to standard ESSs, as large batteries, particular focus on active power management is given. To each SS in the grid is required to provide an active power service. Suitable price signals are supposed to be available but their mechanism of creation will not be investigated in this chapter. Finally, the reactive power regulation to provide voltage regulation is considered.

Case study system

The case study is focused on the investigation of potential benefits of two suitably managed swapping stations connected to the electric network (see fig. 5.7). This network is already operating near critical conditions, mainly determined by the presence of several DGs. The electric network is a 20 kV 11-bus radial network, connected to the bulk grid (slack bus N1) through an on-load tap-changer (OLTC) transformer (data in appendix D). Due to the high spread of bus voltage amplitudes during the day, the tap-changer regulation is inhibited.

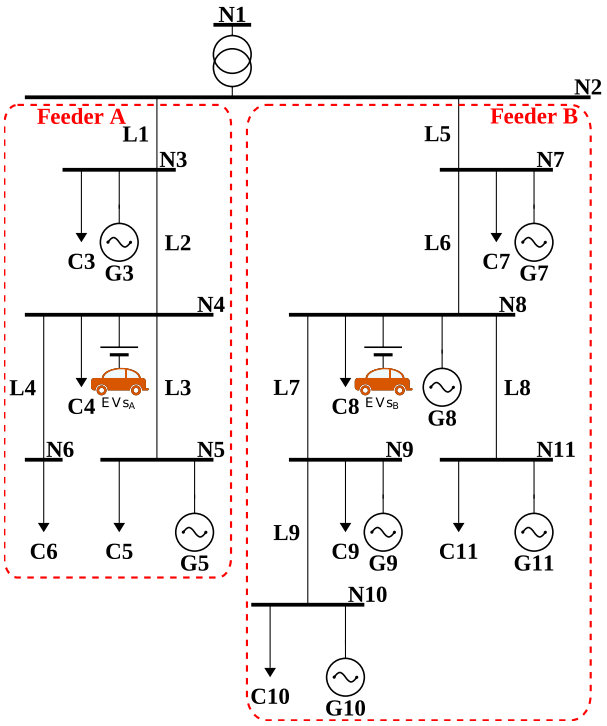

Figure 5.7: Electrical network one-line diagram.

Two identical aggregators of EVs (swapping stations with 200 batteries, 35 kWh each one) are connected to busbars N4 (EVs_A) and N8 (EVs_B) respectively. Charge and discharge efficiencies are both equal to 0.87. DOD has been supposed to be 80%, for both parked (E_{min} profile is thus defined) and incoming batteries [69, 70]. 20 chargers of 120 kW has been assumed [71]. 100% of batteries are swapped at 6am and 40% of batteries at 7pm, this behaviour representing a typical operation of a swapping station for coaches.

Fig. 5.8a reports the daily profiles of the busbar voltages without the swapping stations. It can be seen that the two feeders are characterised by the opposite voltage profiles, i.e. Feeder A (busbars N2 through N5) has depleted voltage levels, N5 even lower than 0.95 pu at 10am, whereas Feeder B busbars (N6 through N11) have voltages always higher than unity, with N11 even exceed 1.05 pu at 1pm. In addition, at 1pm lines L5 and L6 result overloaded.

These critical grid characteristics represent a good testbed for assessing the performance of the proposed ESSs optimisation procedure. In the following, only the two EVs aggregators have been considered to participate in the network regulation. In a smart grid scenario, their participation will be co-ordinated with other active elements present in the network and better results could be achieved.

Tariffs are assumed to be 152€/MWh for peak hours (8am-7pm), 126€/MWh for shoulder hours (7am-8am, 7pm-11pm) and 90€/MWh for off-peak hours (0am-7am, 11pm-12pm), both for imports and exports [43].

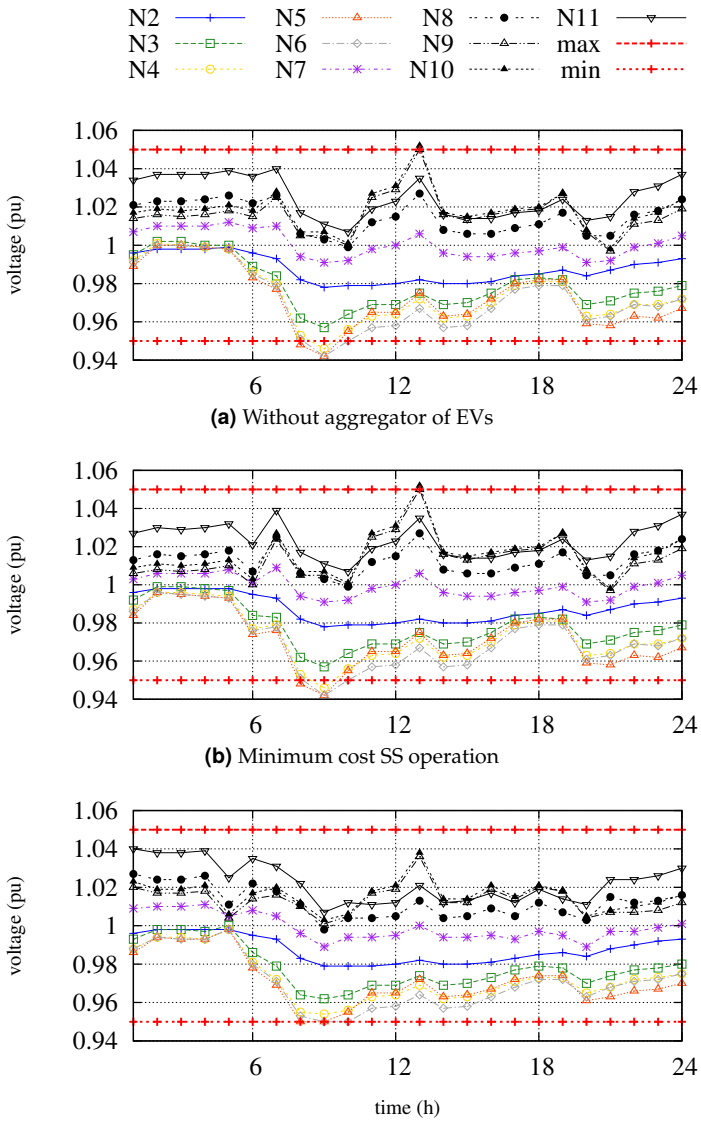

(a) Without aggregator of EVs

(b) Minimum cost SS operation

(c) Multi-period SS technical optimisation

Figure 5.8: Daily voltage profiles ($V_{base} = 20kV$). Refer to the legend on the top.

5.7.1 Results and discussion

Active power management

With the above tariffs, without considering network requirements, the two swapping stations are pushed to re-charge their batteries during early morning (off-peaks hours) to be ready for the swapping actions. The dark-yellow bars in figs. 5.9a-5.10a and 5.9b-5.10b show respectively SOC and charge/discharge profiles for both EVs aggregators resulting from applying the minimum cost swapping station optimisation (as expected EVs aggregators have identical daily energy/power profiles).

The resulting network bus voltages are reported in fig. 5.8b, showing that the

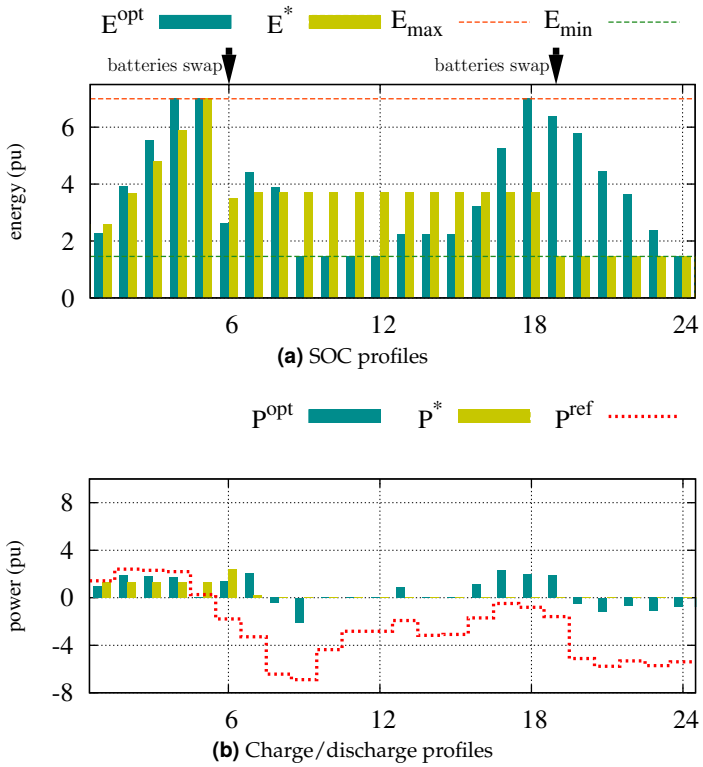

Figure 5.9: SOC (above) and charge/discharge (below) profiles of aggregator EVs_A ($P_{base} = 1MW, dt = 1h$). Arrows (above) identify "swapping actions".

swapping stations operation does not substantially alter the original voltage profiles. However it should be noted that this is due to the fact that swapping stations are not absorbing/injecting power during the critical peak hours. Different results would occur if different tariff scenarios are considered. For example, assuming hourly prices where active power exports are incentivised during peak hours, the probability of line congestions as well as higher voltages of Feeder B busbars will increase further, in which case the grid would encounter serious operation problems.

By applying the grid co-ordinated management procedure described above, the swapping station active power daily profiles would be modified trying to follow the reference profiles P_w^{ref} obtained by single-step OPFs, thus better satisfying network requirements. It is interesting to observe that the computed reference profiles shown with red-dashed lines in figs. 5.9b and 5.10a have opposite profiles. These are consistent with the opposite voltage requirements of the two feeders. A SS installed in N8 should adsorb, whereas an SS installed in N4 should export, for most of the time. In figs. 5.9b and 5.10b, dark-cyan bars represent import (>0) and export (<0) contributions of aggregators respectively EVs_A and EVs_B, resulting from the grid co-ordinated management applying the iterative procedure described in 2.7.1. The corresponding voltage profile is reported in fig. 5.8c. It can be observed that the above mentioned congestions, which occur at 1pm in lines L5 and L6, are solved and network losses are reduced during the day. Voltage profiles are only marginally

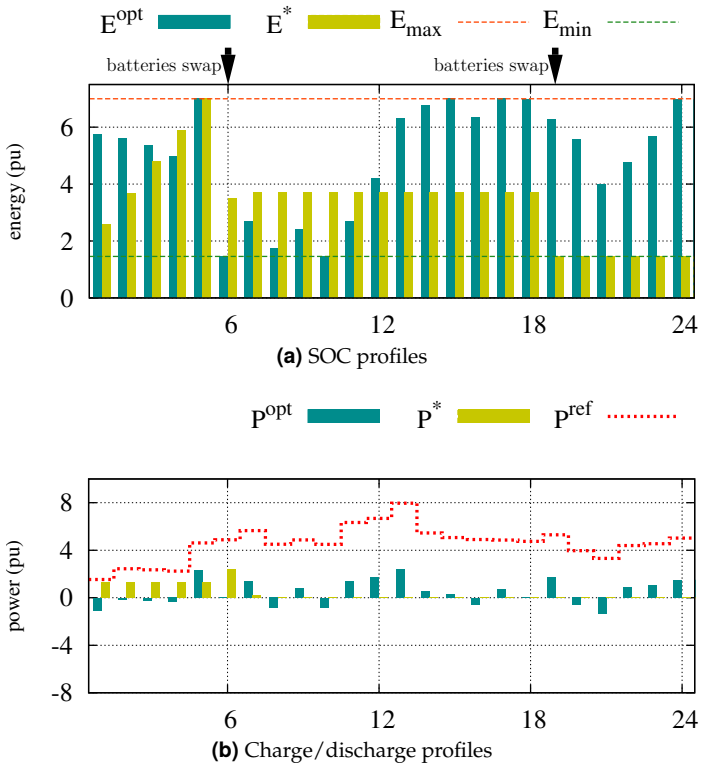

Figure 5.10: SOC (above) and charge/discharge (below) profiles of aggregator EVs_B ($P_{base} = 1MW$, $dt = 1h$). Arrows (above) identify "swapping actions".

improved, but maintained within the allowed band.

Referring to tariffs above, swapping stations spend 1277€ (EVs_A) and 1443€ (EVs_B) respectively to provide P_w^{opt}, whereas P_w^* profile costs 892€. The reason for the high costs of technical optimisation is twofold. Firstly, the swapping stations are importing when the price is higher, for example EVs_B (fig. 5.10b) is always importing between 11am and 3pm. This means that electrical network requirements are not consistent with the tariff scenario assumed. Secondly, as a consequence of the above, battery losses are more costly thus increasing the overall daily cost.

Reactive power management

Network voltage regulation is better performed by reactive, rather than active, power management. In this section the two SSs are considered to provide a reactive power grid voltage regulation. Once the SS active power optimisations, namely minimum cost and multi-period technical, have been performed, the available hourly reactive power bounds of the converters are defined.

The corresponding reactive power bounds for minimum cost SS operation and multi-period SS technical optimisation respectively are shown with red lines in figs. 5.11 and 5.12. As expected, both SSs have the same minimum cost SS operation reactive power bounds, having identical daily power profiles. But multi-period SS technical optimisation reactive power bounds vary according to their different active

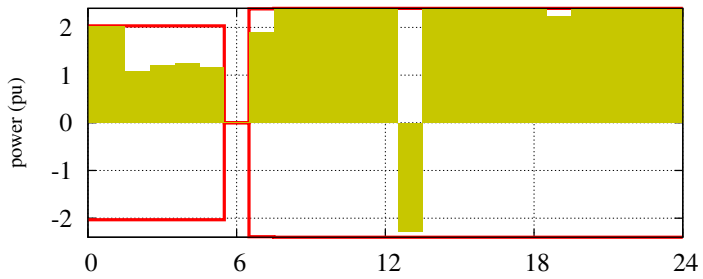

(a) Reactive bounds and profile of EVs_A

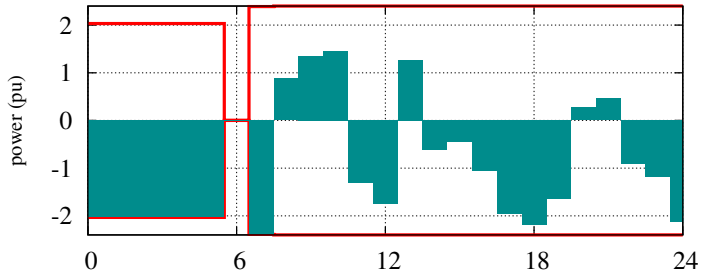

(b) Reactive bounds and profile of EVs_B

Figure 5.11: Minimum cost SS operation available hourly reactive power (within red lines) and reactive power profile (colored bars) for both SSs ($P_{base} = 1MW$).

power profiles.

The results from single-step OPFs with the SS active power profiles determined previously, and reactive power regulated to minimize the root mean square network bus voltage deviation are shown in figs. 5.11 and 5.12. It can be observed that in both cases the two SSs have opposite profiles, consistently with the opposite voltage requirements of the two feeders. Differences in minimum cost SS operation and multi-period SS technical optimisation reactive management are determined by the different available reactive power bounds.

Voltage profiles are improved as shown in figs. 5.13a and 5.13b. In particular, minimum cost SS operation voltage profiles are within voltage constraints (compare figs. 5.8b and 5.13a), whereas multi-period SS technical optimisation reactive management further improves its voltage profiles (compare figs. 5.8c and 5.13b), in particular the feeder with depleted voltage levels.

Considering the operational costs, it appears that the minimum cost SS operation combined with the reactive optimisation is the most convenient with good technical performances.

5.8 A case study electrical network with car parking

In this application, no active power management of EVs aggregators, namely car parking is considered. Due to their daily requirements of fully-charged battery, presence of EVs etc., car parking improves or worsens the network status depending on their location, network status before EVs penetration and their active power profile. With only the reactive power management, co-ordinated with the OLTC, EVs aggre-

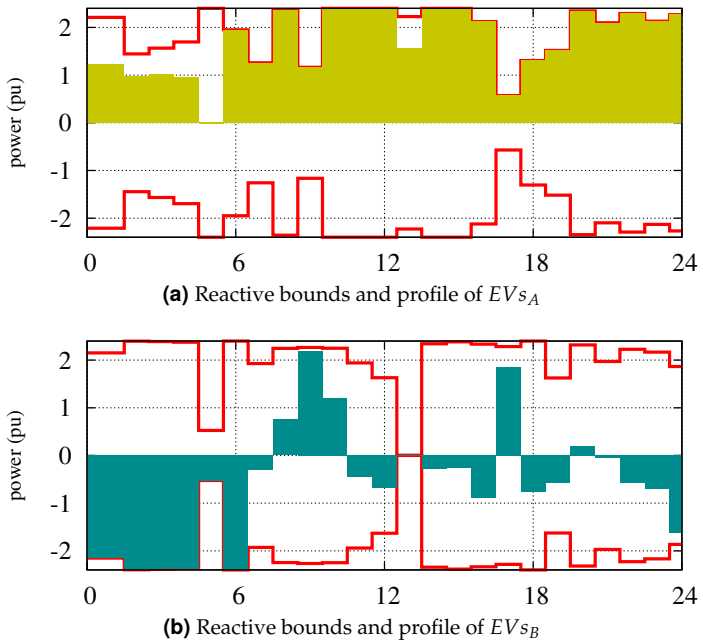

(a) Reactive bounds and profile of EVs_A

(b) Reactive bounds and profile of EVs_B

Figure 5.12: Multi-period SS technical optimisation available hourly reactive power (within red lines) and reactive power profile (colored bars) for both SSs ($P_{base} = 1MW$).

gators could performe services for the grid support, without affecting SOC of EVs batteries, which would make shorter their expected lifetime.

5.8.1 Case study system

The case study is focused on the investigation of potential benefits of car parking connected to the electric network (see Fig. 5.14). This network is already operating near critical conditions, mainly caused by the presence of several DGs. The electric network is a 20 kV 17-bus radial network, connected to the bulk grid (slack bus N1, 132 kV) through an on-load tap-changer (OLTC) transformer.

Loads vary during the day according to residential, commercial, tertiary and industry load profiles, whereas generators vary with wind, photovoltaic, hydro and co-generation production profiles. Feeder FC (busbars N13 through N17, 8.65 km) is passive, with loads summing up to a rated power of 4.88 MW and 3.16 MVAR. Feeder FA (busbars N8 through N12, total length 22.02 km) has loads and generators summing up to rated power of 9.29 MW/3.97 MVAR and 13.4 MW/0 MVAR respectively, whereas feeder FB (busbars N2 thought N7, 26.17 km) has loads for a rated power of 6.16 MW/3.28 Mvar and DGs for 8 MW/0 MVAR (additional data in appendix E). EVs aggregators have been considered at busbar N6, N10 and N16, depending on scenario: aggregator at N6 for scenario A; at N10 for scenario B; at N16 for scenario C; at N6, N10 and N16 for scenario D.

Fig. 5.15 reports the daily profiles of the busbar voltages without car parking: these profiles are used as reference situation (scenario 0) to evaluate the impact of EVs aggregators in the grid. It can be seen that the three feeders are characterised by different voltage profiles, depending on distribution of loads and generators and

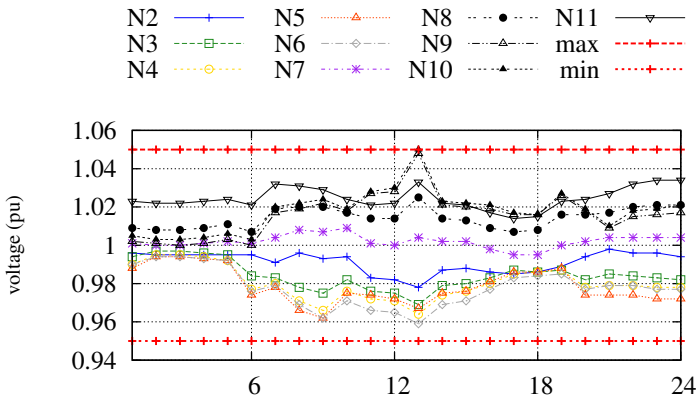

(a) Minimum cost SS operation + reactive

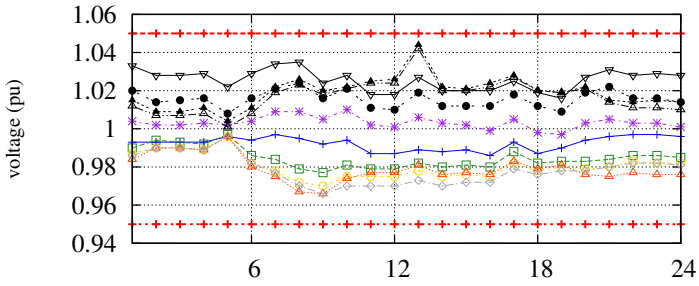

(b) Multi-period SS tehcnical optimisation + reactive

Figure 5.13: Daily voltage profiles with reactive management ($V_{base} = 20kV$). Refer to the legend on the top.

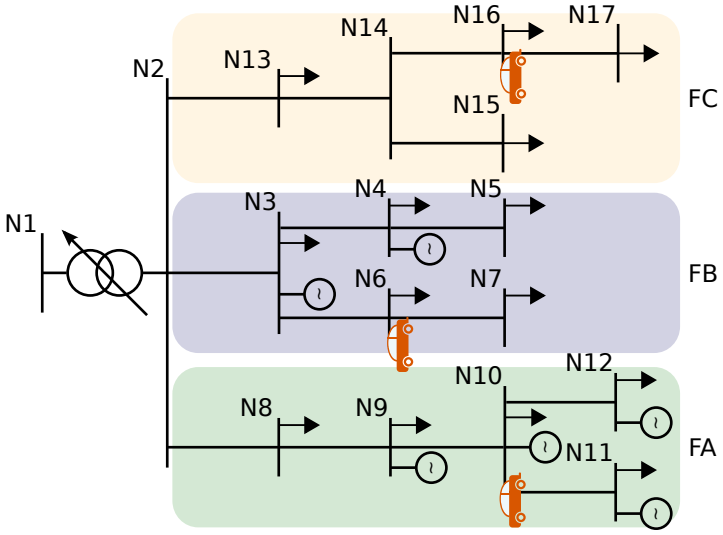

Figure 5.14: Electrical network one-line diagram. Car icons represent EVs aggregators, namely car parking.

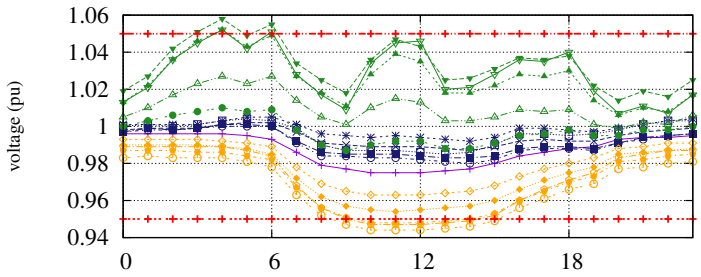

Figure 5.15: Daily voltage profiles ($V_{base} = 20kV$) of scenario 0 (without EVs). Color legend: green for busbars of FA; blue for busbars of FB; orange for busbars of FC, violet for N2, red for voltage constraints (1.05 pu and 0.95 pu).

on power profiles. Feeder FC has depleted voltage levels, even lower than 0.95 pu during peak hours of the day. Feeder FA busbars have voltages higher than unity, with nodes even exceeding 1.05 pu at 4am and 6am, due to high DG penetration. Feeder FB is characterized by voltage levels close to unity. In such situation, without any other voltage regulation means, substation OLTC operations are necessarily inhibited, in particular during peak hours.

For the sake of clarity, in the following only the car parking (EVs aggregators) have been considered to participate in the network regulation, co-ordinated with the OLTC ($\Delta tap = 0.75\%$), whose tap position is an additional unknown of the optimisation problem. In a fully implemented Smart Grid scenario, their participation would be co-ordinated with other active elements present in the network (e.g. distributed generation and storages) and better results could be achieved.

5.8.2 Car parking assumptions

In figs. 5.16a and 5.16b typical scenarios of "residential" and "office" car parking respectively are reported. These scenarios have been estimated on the basis of profiles provided in Ref. [67], considering average italian habits (tertiary work: 8/9am $\div$ 5/6pm, lunchtime: 12am $\div$ 2pm). Outgoing EVs are supposed to move with an average SOC of 90%, assuming some drivers would leave before the scheduled living time. A 40% SOC has been supposed for incoming EVs, whereas the minimum SOC for parked EVs is assumed 20%.

Using forecasting curves as in figs. 5.16a and 5.16b, it is possible to apply a hourly tariff and estimate a possible optimal management of these car parking to provide a re-charging service at minimum cost (objective function $C = \sum_{t=1}^{n_T} c_t P_t^*$ where c_t are hourly cost coefficients and P_t^* are hourly active power values).

Figs. 5.17a and 5.17b show the "residential" and "office" car parking load curve necessary to provide the re-charging service. Car parking size has been assumed of 500 EVs, with batteries of 35 kWh (efficiency 0.87) [**?**]. 3.3 kW charger for each EV has been supposed for the "residential" car parking (a charger for each house), whereas 100 chargers of 19.2 kW for "office" car parking assuming faster charging operations requirements and a first stage of investment for charger infrastructures [72]. Cost coefficients are assumed to be 152€/MWh for peak hours (8am-7pm), 126€/MWh for shoulder hours (7am-8am, 7pm-11pm) and 90€/MWh for off-peak hours (0am-7am, 11pm-12pm) [43].

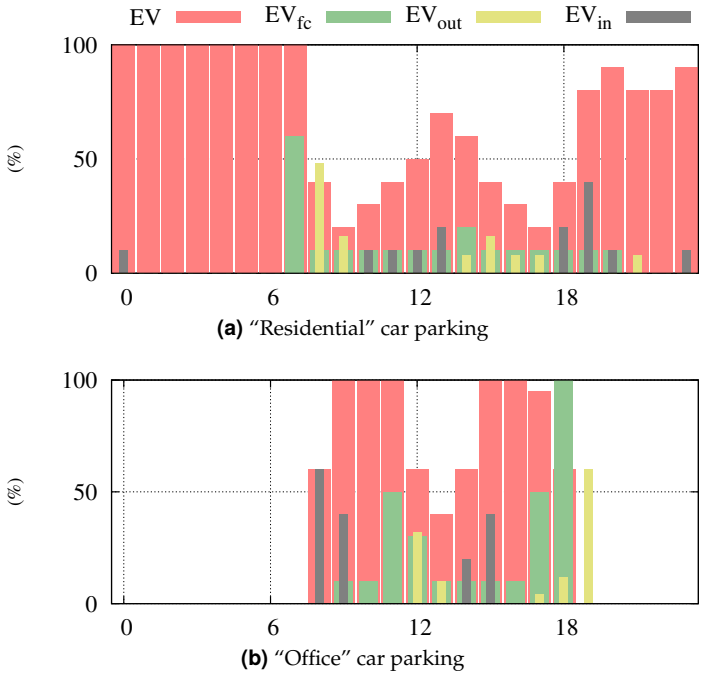

(a) "Residential" car parking

(b) "Office" car parking

Figure 5.16: "Residential" and "office" car parking daily profiles: hourly availability of EVs (EV), required fully-charged batteries (E_{fc}), outgoing EVs (EV_{out}) and incoming EVs (EV_{in}) supposed percentages. (Refer to the legend on the top; $P_{base} = 1MW$, $dt = 1h$.)

As shown in fig. 5.16b, the "office" car parking has not availability of EVs during the cheaper charging hours of the day. Consequently, the re-charging of batteries occurs during peak hours and the cost of the service is 1651€, whereas the "residential" car parking pays only 1083€ (fig. 5.17a, starting energy of 5.18 pu is a result of the multi-period optimisation).

As shown in figs. 5.17a and 5.17b both car parking has availability of EVs to modify their load profile. In fact $E_{max} > SOC$ for most of the day, whereas $dE <$ (number of charger $\cdot$ charger size) for this simulation, which considers one-hour time steps and average profiles. In this paper, EVs active power management based on grid requirements has been disabled by purpose, in order to better highlight the reactive power management aspects.

In the following, the car parking connected to the grid is supposed to be an equivalent car parking comprising a "residential" and an "office" car parkings of the same type described above. Active power profiles and reactive power bounds are the sum of each car parking active power profiles and reactive power bounds respectively. Reactive power values resulting by the single-step reactive optimisation are provided for the equivalent car parking.

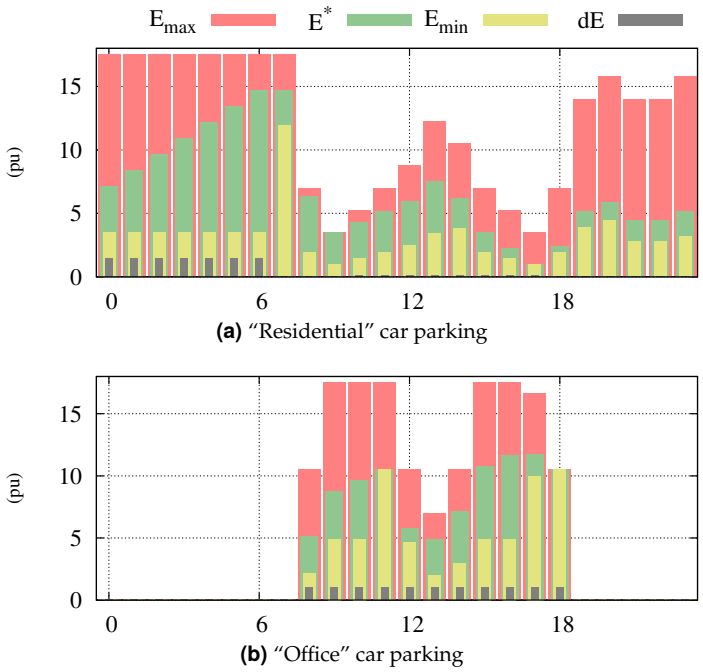

Figure 5.17: "Residential" and "office" car parking daily profiles: hourly availability (E_{max}), required service (E_{min}), SOC (E^*) and power adsorption (dE) profiles. (Refer to the legend on the top; $P_{base} = 1MW$, $dt = 1h$.)

5.8.3 Results and discussion

Active power car parking impact

EVs increasing penetration could affect positively or negatively the electrical network status depending on its operating conditions.

The grid shown in fig. 5.14 is composed by three feeders characterized by opposite voltage behaviour (refer to fig. 5.15).

Voltages in feeder FA are improved if EVs aggregator is connected to that feeder (see fig. 5.18a), characterised by high DG penetration. The adsorption of this extra load compensates the local power generation, particularly in the early morning (4am-6am) when the wind plant is generating and during the peak hours (11am-12am) when photovoltaic plants have their maximum generation.

Connecting the EVs aggregators to the feeder FB no substantial change occurs in terms of voltage profiles (fig. 5.19a).

Since feeder FC is already characterised by severely depleted voltages, the additional car parking adsorption further decreases FC busbar voltages, resulting in a wider network busbar voltage spread during peak hours, which causes the inhibition of the OLTC operation at 11am-12am (see fig. 5.20a).

It is envisaged that EVs aggregators impact will depend on their location within and, on the operational state of, the electrical network. Assuming car parking being evenly distributed in the network, the global effect would be different, as shown in fig. 5.21a reporting the more uniform decrease of voltages in case of considering one

Table 5.1: Maximum and minimum voltage (pu, $V_{base} = 20kV$) and tap changer values at 4am and 11am for each scenario. On the left side, values refer to network status before any regulation ("pre Q-t"). On the right side, values refer to network status after reactive power - OLTC regulation ("post Q-t").

t=4							
scenario	EVs	pre Q-t			post Q-t		
name	at node	max	min	tap	max	min	tap
0	-	1.058	0.983	0	-	-	-
A	N10	1.048	0.983	0	1.030	0.972	0
B	N6	1.058	0.983	0	1.049	0.973	1
C	N16	1.058	0.975	0	1.045	0.962	2
D	all	1.047	0.975	0	1.030	0.976	1
t=11							
scenario	EVs	pre Q-t			post Q-t		
name	at node	max	min	tap	max	min	tap
0	-	1.047	0.944	0	-	-	-
A	N10	1.037	0.950	0	1.030	0.953	-3
B	N6	1.047	0.944	0	-	-	-
C	N16	1.047	0.937	0	1.050	0.950	1
D	all	1.038	0.938	0	1.049	0.969	-4

aggregator for each feeder.

Reactive power management

The active power absorption of EVs aggregators of fig. 5.17 determines the reactive power bounds drawn with red bars in both plots of fig. 5.22.

As explained above in section 5.6.2, these bounds are applied in the single-step OPFs. In order to improve the network voltage profile by minimizing the spread, a modified root mean square voltage deviation objective function was adopted in this work, setting the reference voltage to 1 pu with a $\pm$ 0.025 pu tolerance.

The resulting reactive power exchange with the grid for each scenario are depicted in figs. 5.22a (scenarios A, B, C) and 5.22b (scenario D). The much greater reactive power amounts required during peak hours in order to improve voltage profiles can easily be observed.

Table 5.1 reports maximum and minimum voltage values at 4am and 11am, respectively before ("pre Q-t") and after reactive power and OLTC co-ordinated regulation ("post Q-t") for each scenario.

In scenario A voltage profiles are improved by the car parking (compare figs. 5.18a and 5.18b), which provides inductive reactive power to reduce the high voltage values for most of the day (fig. 5.22a).

As it could be expected, the car parking presence on FB doesn't significantly modify voltage profiles (scenario B, compare figs. 5.19a and 5.19b). For this reason, at 11am and 12am it would not be possible to solve the critical situation without involving other generators in voltage regulation.

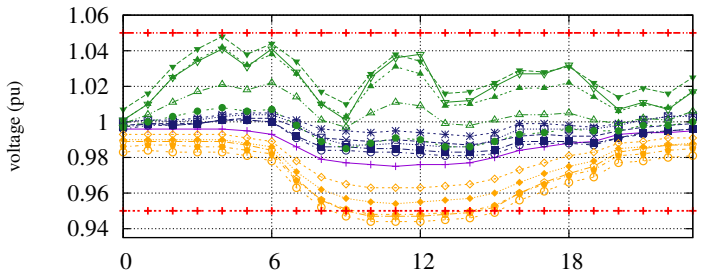

(a) Scenario A (EVs in N10)

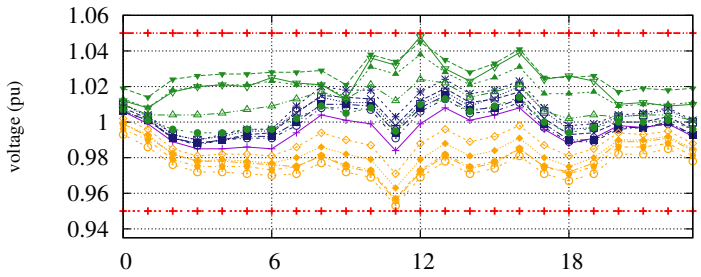

(b) Scenario A (EVs in N10) with Q-t management

Figure 5.18: Scenario A - daily voltage profiles ($V_{base} = 20kV$). On the top, network status with car parking as loads. On the bottom, network status with reactive power - OLTC management. Color legend: green for busbars of FA; blue for busbars of FB; orange for busbars of FC, violet for N2, red for voltage constraints (1.05 pu, 0.95 pu).

In scenario C, capacitive reactive power injection is required to increase the generally depleted FC voltage profiles (compare figs. 5.20a and 5.20b).

EVs aggregator represents an additional load for the feeder, but its effect could be either detrimental or beneficial depending on the voltage characteristics of the feeder itself. From the above comparative analysis, for instance, it appears that the most efficient alternative is to connect the EVs aggregator (car parking) to feeder FA (scenario A) since it better compensates the high generation connected at the same feeder by both active power absorption and reactive power regulation.

Even better results would be obtained if the car parking could be evenly distributed in the different areas considering a distributed management, as in Scenario D with three EVs aggregators (one for each feeder) and a co-ordinated reactive power and OLTC management (compare figs. 5.21a and 5.21b). In this case the goal of the OPF (voltage values within tolerance bounds of $\pm$ 0.025 pu) can be achieved. Reactive power profiles provided by EVs aggregators optimally co-ordinated differ from results obtained during scenarios A, B, C where car parking act separately (compare figs. 5.22a and 5.22b). In particular, in scenario D the total amount of reactive power provided at each time step is higher due to the possibility to obtain better results using all car parking.

From the economical point of view, until any reactive power remuneration is provided for voltage regulation service, consideration would be done on active power costs. Voltage regulation is provided by “residential” and “office” car parking at different costs, due to economical optimisation of active power described in subsection

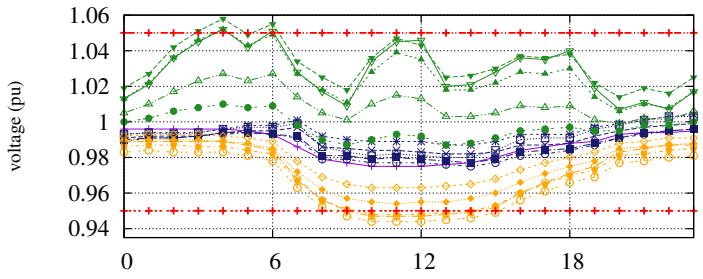

(a) Scenario B (EVs in N6)

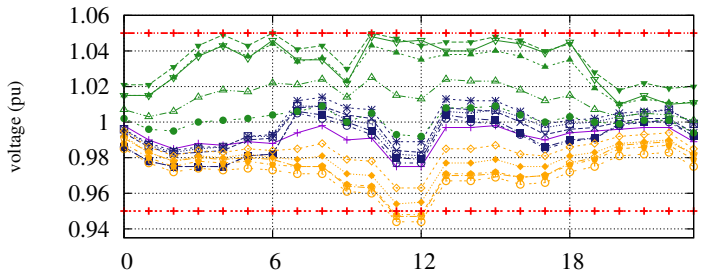

(b) Scenario B (EVs in N6) with Q-t management

Figure 5.19: Scenario B - daily voltage profiles ($V_{base} = 20kV$). On the top, network status with car parking as loads. On the bottom, network status with reactive power - OLTC management. Color legend: green for busbars of FA; blue for busbars of FB; orange for busbars of FC, violet for N2, red for voltage constraints (1.05 pu, 0.95 pu).

5.8.2.

5.9 Conclusion

EVs aggregators such as car parkings and swapping stations might have a great potentiality for voltage regulation services in distribution networks.

The possibility given by 4-quadrant charger converters to exchange reactive power with the grid without affecting the SOC of batteries could be efficiently exploited in a Smart Grid scenario. EVs and their re-charge infrastructures will ensure to distribution networks flexible storage systems. In this perspective, new distributed resources will be provided to the grid at service costs as well as new opportunities for EVs will be created (i.e. reduction of investment costs).

EVs aggregators have demonstrated to have the potential capability to participate in voltage regulation. However, the creation of a regulation scheme and incentives for the reactive power management are required to enable such EVs participation in grid support services, allowing investments in infrastructures (i.e. larger converters).

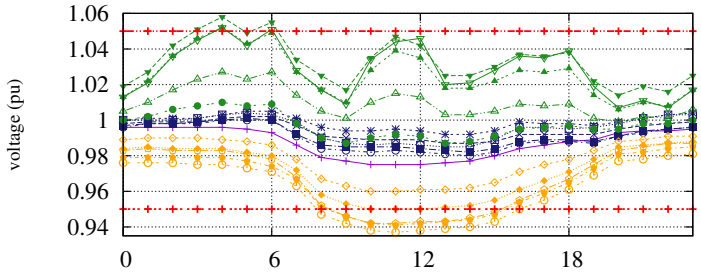

(a) Scenario C (EVs in N16)

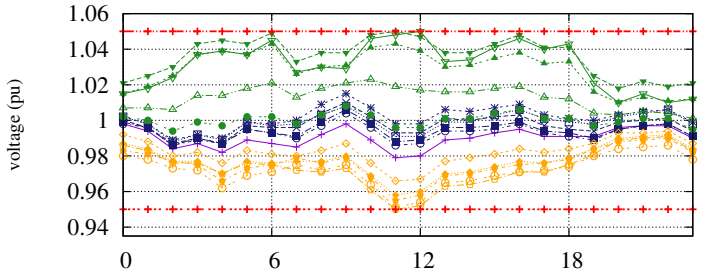

(b) Scenario C (EVs in N16) with Q-t management

Figure 5.20: Scenario C - daily voltage profiles ($V_{base} = 20kV$). On the top, network status with car parking as loads. On the bottom, network status with reactive power - OLTC management. Color legend: green for busbars of FA; blue for busbars of FB; orange for busbars of FC, violet for N2, red for voltage constraints (1.05 pu, 0.95 pu).

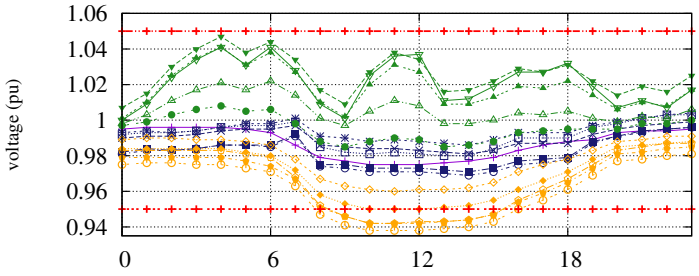

(a) Scenario D (EVs in N6, N10, N16)

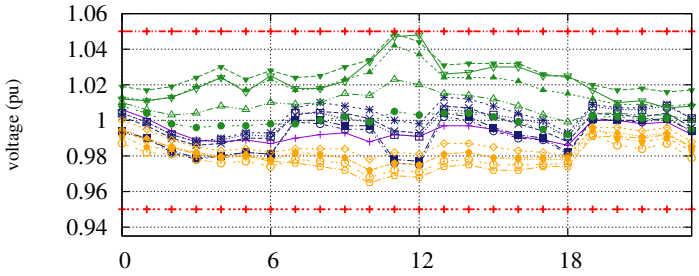

(b) Scenario D (EVs in N6, N10, N16) with Q-t management

Figure 5.21: Scenario D - daily voltage profiles ($V_{base} = 20kV$). On the top, network status with car parking as loads. On the bottom, network status with reactive power - OLTC management. Color legend: green for busbars of FA; blue for busbars of FB; orange for busbars of FC, violet for N2, red for voltage constraints (1.05 pu, 0.95 pu).

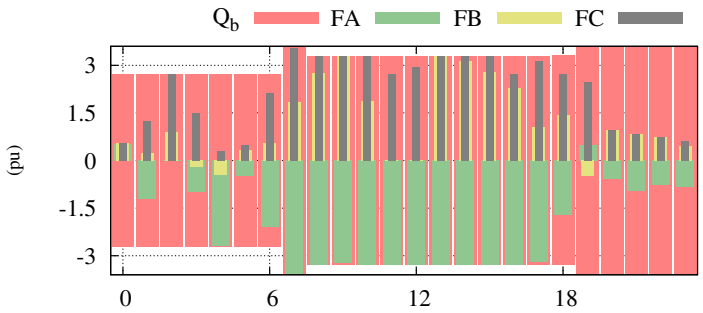

(a) Scenarios A, B and C reactive power results

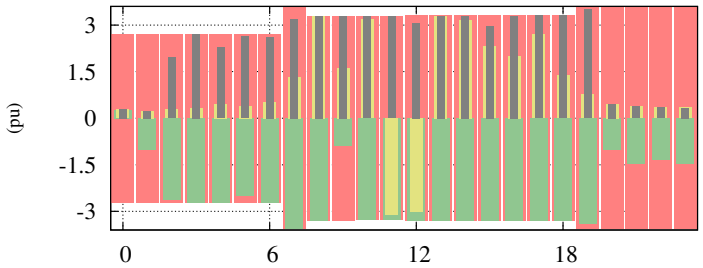

(b) Scenario D reactive power results

Figure 5.22: Reactive power bounds (Q_b) and results ($P_{base} = 1MW$). Scenario A, B, C results are depicted above, whereas scenario D results are shown in the bottom plot. Refer to the legend on the top. (Positive sign injected capacitive power.)

6 A Token Ring Like Management Procedure for Smart Grids

In this chapter, an internet-like procedure for power management of distribution electrical networks with responsive nodes is presented. This procedure is based on the "token ring" internet protocol and considers a multi-level co-ordination of all active customers. It aims at reducing the complexity of distributed networks management while ensuring free customer participation in services for the grid support on the basis of power-price signals. This procedure grounds on a smart grids scenario, where smart meters and communication technologies allow connectivity and interactivity among distributed customers, whereas information are exchanged enabling a flexible and price-smart behaviour of each node.

6.1 Introduction

Connectivity and interactivity among different distributed resources will be a challenge in a future smart grids scenario. The electrical network management is envisaged to evolve towards an internet-like model, where every node can exchange information with other grid elements thanks to smart meters and communication technologies. One of the more concerning goals is to make nodes responsive to every signals, flexible and price-smart, enabling free participation of all customers in grid regulation. Quality/price options according to needs for both active and reactive power should be provided to activate a responsive behavior of all controllable generators and loads in the grid, enabling local energy markets. However, these characteristics will increase the complexity of the system and its management.

In this chapter two concepts are investigated and developed. Firstly, if the power grid management is to become more similar to internet, internet based procedures to manage controllable devices are required. Active elements are thus activated sequentially like in the token ring technology, in which data is transmitted sequentially from one ring station to the next with a control token circulating around the ring controlling access. Secondly, every complex process can be decomposed into single simpler processes, from a lower (micro) to a higher (macro) system level.

Besides, a key feature to be ensured is the free choice of any active element to

participate or not in network regulation, i.e. each costumer will freely decide, at any time, its contribution according to power availability, offered remuneration for the regulation service, regulation priority level required and allowed maximum active and reactive power variation set by the system operator.

All active elements will operate sequentially and autonomously. In order to ensure a correct co-ordination among controllable devices, a multi-level management of active elements is implemented which reduces the complexity of control decisions and operations in a grid.

A main network controller should monitor the grid in order to identify critical situations or situations which need to be improved in some specific areas or nodes, for example where voltages exceed allowed limits or line ampacities are violated. By providing suitable signals to the active elements of these areas, for example prices, the network controller can trigger a virtuous behavior of these elements. Each area should then act on the basis of such signals, by means of its active elements according to their power availability and willingness to participate. The multi-level management ensures an overall objective to be achieved, by decomposing the complexity of the management of system into micro-area levels.

In this chapter, the proposed procedure is presented with two case study electrical networks to demonstrate its applicability.

It should be emphasized that in this work only the feasibility of the token ring approach for network distributed regulation is investigated, whereas no considerations to transmission communication issues have been made assuming as working hypothesis, a well-established communication environment as expected in a smart grid scenario.

For the sake of clarity, in this chapter no investigations and considerations on communication framework have been provided. It has been assumed well-established communication technologies which are expected in a smart grid scenario. All transmission issues (failure of transmission system, for example) have not been considered, as information network issues, which have been supposed to be solved in a smart grid scenario. In particular, referring to token ring technology, token ring has not been supposed to be the transmission internet protocol of future network.

6.2 Towards internet-like electrical networks management

By optimising the contribution of single customers, the system operator is expected to obtain the maximum technical result at minimum cost. Network costs are remuneration for customers, which could receive economical incentives to assume a correct behaviour from the network point of view, if suitable price signals are provided.

Optimisation techniques may more or less easily be applied to solve the problem considering all constraints (both network and customer constraints). On the other hands, optimisation requires all data to solve a problem, which means the knowledge of status and regulation possibilities for all customers. This approach also gives to the system operator the task of identifying the active and reactive power settings for all active devices participating in the regulation.

Another option is the management without solving a single optimisation problem, but rather a set of simpler sub-problems in order to obtain sub-optimal results

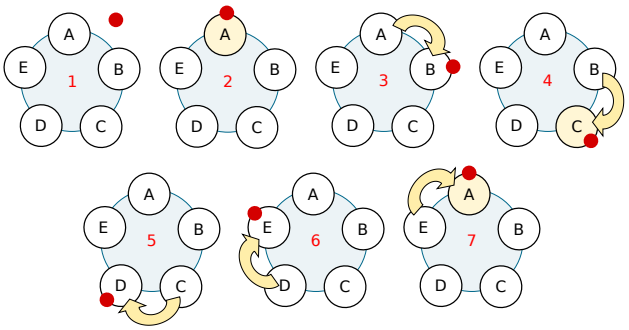

Figure 6.1: Token ring concept in internet network. Capital letters identify computers. Red dot is the token sent from A to C and from C back to A (yellow filled circles identify sender and recipient when they own the token). Token goes around the ring in clockwise order (red numbers identify the procedure steps).

very close to the optimal one. In this perspective, every node could act independently from the others and from the network operator, searching for a local optimum, on the basis of signals received from the network and considering its own constrains. If the signals are suitably constructed, the local decisions of each node would positively contribute towards an optimal status of the network. This approach seems to be more consistent with an electrical internet-like network which smart grids scenario aims to. In smart grids, every node is responsive and independent, whereas customers are able to freely interact with the network and energy markets.

6.2.1 The token ring concept

For developing novel management systems in a smart grids scenario it seems advisable to try to exploit the know-how of well-established internet network technologies.

Token ring technology is a protocol for local area network in internet network. Data is sent from one machine to the next and so on around the ring until it ends up back where it started [73]. Assume there are computers A, B, C, D and E sequentially connected in a ring and computer A needs to send data to computer C. In fig. 6.1 the five computers are represented by the capital letters in white circle, which becomes yellow when the computer owns the right to send data. This right is represented by the red dot.

If no computer is yet sending something to others (step 1 of fig. 6.1, no yellow computers, the token is waiting), computer A takes the token and sends its data. Data starts to go around the ring (step 2). The following computer B isn't the recipient (step 3), then it doesn't accept the data. Then data reaches computer C, which accepts the data (step 4, C becomes yellow) and returns to computer A, passing through computers D and E, the acknowledgment to say the data is received. The signal with data is called token.

This procedure seems to be ideally suited for the goals stated above. It would let the participation of single nodes in a co-ordinated distributed management, where every customer receives signals and provides a reply action to the system operator.

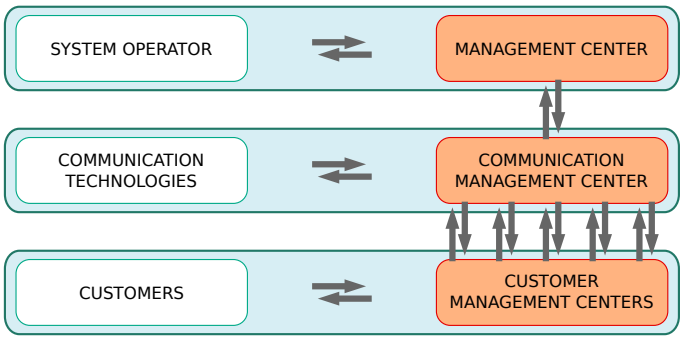

Figure 6.2: System operator, communication and customers levels in a co-ordinated management system based on exchange of information: communication infrastructures exchange signals among the system operator and customers. Management systems co-ordinate operations among different levels and within levels.

The token could be a request to provide an active or reactive power variation (ΔP or ΔQ with sign) against a certain remuneration (p_P or p_Q).

The customer-recipient decides to provide only part of the required power variation, the total amount or nothing, depending on attractiveness of the remuneration, plant status or whatever reason. The system operator receives the answer and evaluates whether or not the objective has been reached or a new token is needed to be sent to the successive customer.

This conceptual idea of distribution networks management is well-suited in a smart grid scenario, where an information network will allow capillary interconnections among distributed resources in the networks. Nodes will receives signals depending on network needing and they are not supposed to be physically connected in a ring. As schematically pictured in fig. 6.2, the token ring-like procedure is a co-ordinated management control scheme that manages interactions between the system operator and devices available to vary their generation/adsorption (customers), through the interface created by communication infrastructures, which co-ordinate the signals exchange between system operator and customers. System operator, communication technologies and customers operates at different levels, where management systems co-ordinate operations among levels and within each level.

6.2.2 Problem decomposition

Several customers can be available for a concurrent participation in system regulation and it is thus necessary to co-ordinate them with grid requirements (for example voltage and line loading constrains violation). Moreover, loadings of a specific branch is likely influenced only by a limited number of active devices, whereas some active devices affect voltage levels of specific nodes more than others. In order to solve congestion or voltage violation problems at specific branches or busses, the network needs the participation in regulation of such elements trying to avoid the use of less influencing elements whose intervention would be practically useless and expensive. Consequently, grid decomposition into regulation areas would enable a more efficient management of different resources. When a line congestion or bus voltage violation occurs, restoring operations would involve only customers in the

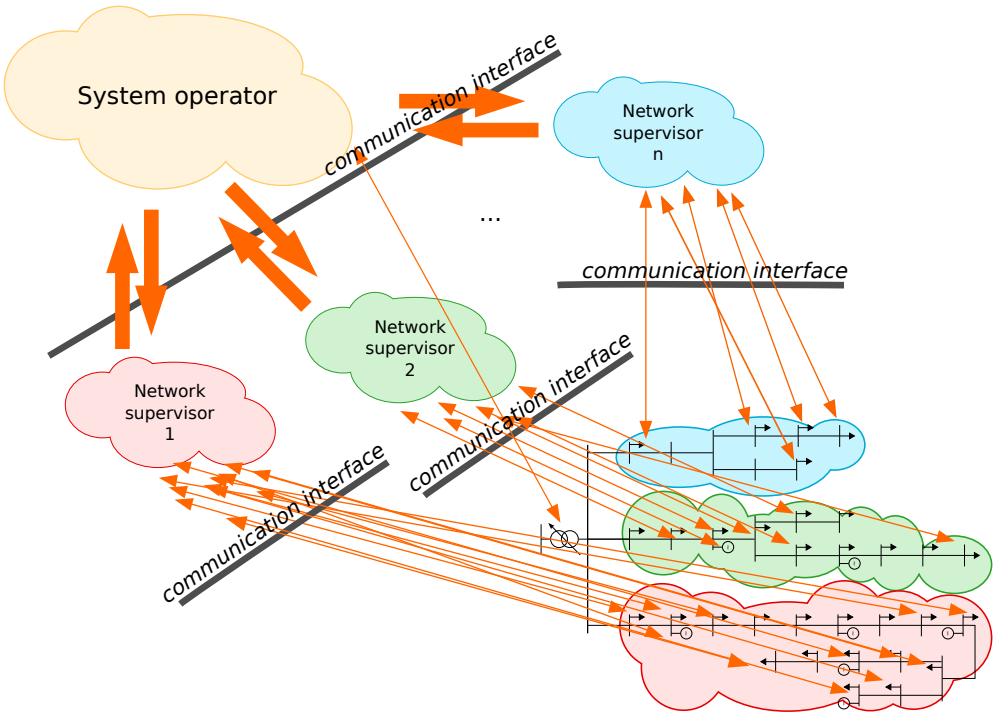

Figure 6.3: Multi-level structure conceptual scheme: the system operator interacts with customers through medium co-ordination entities (network supervisors) that supervise control areas. The management system of the control areas co-ordinates customers.

concerned area.

Areas are well-suited to a multi-level structure. Decomposition at different knowledge levels will improve allocation of tasks. Additionally, levels could act disregarding aspects which do not concern themselves.

For example, fig. 6.3 represents a three-levels structure. The higher level (system operator) knows all of the grid it is supervising, whereas customers involved in the grid regulation are the lower level which operates on the basis of system operator requirements. Between customer level and system operator level, more network supervisors are pictured. The system operator communicates to each network supervisor specific issues and network supervisors interact with customers within their correspondent control area. The communication interface provides infrastructures to exchange and co-ordinate communications, whereas control areas are managed by customer management systems, as shown in fig. 6.2. Clouds are these management control centers, logical entities, which co-ordinate incoming and outgoing tokens.

6.3 Distributed co-ordinated power management

Fig. 6.4 represents the distributed co-ordinated management in distributed networks. The network supervisor is the higher level which co-ordinates areas at the lower level.

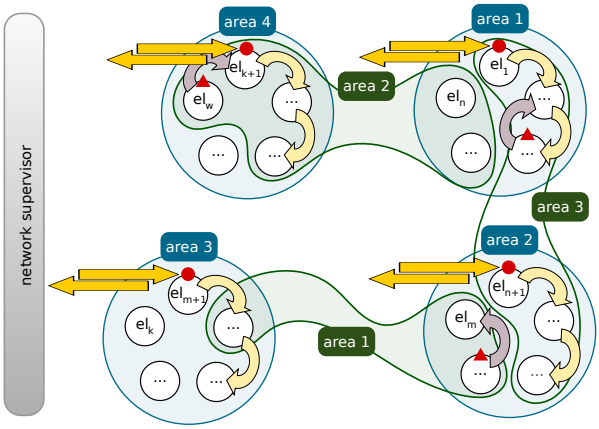

Figure 6.4: Distributed co-ordinated power management scheme. Active elements (el) are rounded in blue and green curves. Each color represents an area for bus voltage and current regulation respectively. Red dot and triangle represent voltage and current tokens respectively, which move following yellow and violet arrows. Dark yellow arrows represent exchange of information with the network supervisor.

Depending on type and location of violations, customers can be organized in areas. In fig. 6.4, active elements (el) are rounded in blue and green curves. Each color represents an area for bus voltage and line congestion violations respectively.

Referring to fig. 6.4, the token ring procedure introduced above can be schematically summarized by the following steps:

1. some violations occur and the relevant regulating areas are identified;
2. tokens are simultaneously sent by the network supervisor to the concerned areas (tokens are pictured as red circles and triangles for voltage and current regulation respectively);
3. tokens go to the first customer of each area;
4. each customer receives its own token and replies to the network supervisor, as described in fig. 6.1;
5. the network supervisor receives the answer back from each customer-recipient and checks the network status;
6. if violation still exists, another token is sent to the subsequent customer of the area, otherwise the goal has been achieved and the procedure stops;
7. when the last customer of each area replies to its token, if violations still exist remuneration is step increased and the procedure from step 2 to 7 is repeated;
8. if new violations occur, new token are created and sent to the relevant areas concurrently with the other tokens (step from 1 to 8).

The procedure stops when all goals are achieved.

Algorithm 1 shows the pseudo-code used for the token ring-like procedure implementation.

Algorithm 1 Token algorithm pseudo-code

Data: : electrical distance matrix, TCDF matrix, voltage and current control areas information

Results: : voltage and current violations are solved

$counter \leftarrow 0$
$p_P \leftarrow p_{P,init}$
$p_Q \leftarrow p_{Q,init}$
while there are voltage or current violations in some areas **do**
  $ng \leftarrow 1$
  while $ng \leq ngMax$ **and** there are voltage or current violations in some areas **do**
    $nc \leftarrow 1$
    exit condition variables updating
    while $nc \leq$ voltage and current areas number **and** there are voltage or current violations in some areas **do**
      if $ng \leq$ generators number in voltage control nc-area **and** the goal in voltage control nc-area has not been achieved **then**
        dQ at ng-generator bus in nc-area to solve voltage violation estimation
      end if
      if $ng \leq$ generators number in current control nc-areas **and** the goal in current control nc-area has not been achieved **then**
        ng-generator in nc-area lower and upper bounds $\leftarrow$ updated
      end if
      if $ng \leq$ generators number in voltage and current control nc-areas **and** the goal in current control nc-area has not been achieved **and** ng-generator in voltage control nc-area = ng-generator in current control nc-are **then**
        P and Q $\leftarrow$ optimal value calculation {considering both voltage and current token}
      end if
      if $ng \leq$ generators number in voltage control nc-area **and** the goal in voltage control nc-area has not been achieved **then**
        P and Q $\leftarrow$ optimal value calculation {considering voltage token}
      end if
      if $ng \leq$ generators number in current control nc-areas **and** the goal in current control nc-area has not been achieved **then**
        P and Q $\leftarrow$ optimal value calculation {considering current token}
      end if
      $nc \leftarrow nc + 1$
      exit condition variables updating
    end while
    θ, V updating and tap control {new PF and tap position regulation}
    exit condition and other variables updating
    $ng \leftarrow ng + 1$
  end while
  $counter \leftarrow counter + 1$
  $p_P \leftarrow p_P + \Delta p_P$
  $p_Q \leftarrow p_Q + \Delta p_Q$
end while

6.3.1 Voltage regulation areas

A voltage regulation area is formed by a group of electrically coherent busses, which may be co-ordinated to improve area voltage profiles. It can be identified by inspection by the network supervisor on the basis of network electrical characteristics and historical analysis. Alternatively, a sensitivity analysis is necessary to implement an automatic procedure for area definition.

For the scope, useful information can be drawn from the Jacobian matrix, as defined in the Newton-Raphson method applied to power flow problems, in particular, the inverse of $\partial Q/\partial V$ sub-matrix, also called sensitivity matrix, whose coefficients represent the relationships between bus reactive power and voltage variations.

From the sensitivity matrix, the attenuation of voltage variations between all system nodes can easily be determined in the form [74]:

$$\Delta V_i = \alpha_{ij}\Delta V_j = \left[\frac{\partial V_i}{\partial Q_j} / \frac{\partial V_j}{\partial Q_j}\right] \Delta V_j \tag{6.1}$$

allowing the electrical distance between these two busses to be expressed as:

$$ed_{ij} = -ed_{ji} = -log(\alpha_{ij}\alpha_{ji}) \tag{6.2}$$

The electrical distance matrix, formed by ed_{ij} elements for each pair of busses in the grid, lets to define voltage areas and corresponding pilot bus, the reference node for each area.

The electrical distance matrix is normalized with the maximum ed_{ij} value and its coefficients vary between 0 ($= ed_{ii} \quad \forall i$ in the grid) and 1. Closer busses are thus aggregated with different criteria, until all busses are assigned to a specific area, within a specified radius ($0 \leq r_d \leq 1$). Closest busses could be aggregated, otherwise closer busses to busses with generators could be considered (hierarchical criteria) [75, 76]. The electrical distance between bus k and aggregators of i and j is evaluated as

$$max(ed_{ik}, ed_{jk}) \quad \forall k \in \{1, \ldots, n\} \tag{6.3}$$

for each bus (n is the total number of busses in the grid). In the following the pilot bus is defined as the electrically closest bus to the others in the same area. Different criteria could be identified for the pilot bus definition.

Further details are available in Ref. [74].

6.3.2 Current regulation areas

Current regulation areas are identified by the network supervisor depending on overloaded branches, flow direction and active customers location. A sensitivity analysis could support network supervisor decision and automatize the selection of customers whose operation could alleviate congestion problems. For the scope, a procedure originally developed for transmission networks presented in [77] has been exploited and applied to distributed networks.

The transmission congestion distribution factor (TCDF) matrix coefficients in eq. 6.4 represents the active power flow variation in line k between bus-i and bus-j (ΔP_{ij}) due to active power injection variation at bus i (ΔP_i).

$$TCDF_i^k = \frac{\Delta P_{ij}}{\Delta P_i} \tag{6.4}$$

Using Taylor's series approximation and ignoring higher order terms, ΔP_{ij} is express by eq. 6.5.

$$\Delta P_{ij} = \frac{\partial P_{ij}}{\partial \theta_i}\Delta\theta_i + \frac{\partial P_{ij}}{\partial \theta_j}\Delta\theta_j + \frac{\partial P_{ij}}{\partial V_i}\Delta V_i + \frac{\partial P_{ij}}{\partial V_j}\Delta V_j \tag{6.5}$$

Substituting eq. 6.6 in 6.5, the $TCDF_i^k$ coefficient is expressed by eq. 6.7 if coupling terms between active power and voltage amplitude variation in eq. 6.5 are neglected.

$$\Delta\theta = \frac{\partial\theta}{\partial P}\Delta P = \left(\frac{\partial P}{\partial\theta}\right)^{-1}\Delta P \tag{6.6}$$

$$TCDF_i^k = \frac{\partial P_{ij}}{\partial\theta_i}\frac{\partial\theta_i}{\partial P_i} + \frac{\partial P_{ij}}{\partial\theta_j}\frac{\partial\theta_j}{\partial P_i} \tag{6.7}$$

Eq. 6.6 defines the voltage phase variation $\Delta\theta$ at busses through Newton-Raphson Jabobian relationship between voltage phases and active power.

The TCDF matrix sets a criterion for identifying coherent busses groups. In particular, for each branch $k \in \{1,\ldots,n_b\}$ (with n_b number of branches in the grid) it is possible to identify which active elements influence the line loading in branch-k, depending on network characteristics and line flow direction.

6.3.3 The token

The token is a request to provide an active or reactive power variation against a given remuneration.

When voltage or current limits are violated, the ΔP and ΔQ amounts required from the regulation area concerned in order to restore the system to an acceptable condition are estimated by the network supervisor, knowing network status and characteristics. As an example, let us consider that k-th branch becomes overloaded and the i-th bus voltage is outside the allowed limits. The overloading in branch k is estimated to be solved with an active power variation ΔP_m at bus m, where m indicates the first consumer-recipient listed in the current regulation area for branch k. Similarly, the voltage violation at bus i is solved with a reactive power contribution at bus-n ΔQ_n, where n indicates the first consumer-recipient listed in the voltage regulation area for bus i.

The network supervisor could decide to limit the token to a portion of the estimated ΔP_m and ΔQ_n. In this way, the first customer in the regulation area list can't solve the contingency and other customers are called to participate in regulation action.

The customer-recipient has the freedom to fully or partially providing the required ΔP or ΔQ on the basis of remuneration (p_P and p_Q) proposed in the token, since each customer needs to maximize its own revenue, while respecting its constraints such us capability curve, thermal limits etc.

Eq. 6.8 represents the economic balance for a generator called for a current regulation action by the network supervisor through a token. The active power generated before the token request, P^*, is remunerated at p_P^s price, whereas the regulating active power decrement ΔP is remunerated at p_P. After responding to the token request, the generator active power is $P^* + \Delta P$.

$$p_P|\Delta P| + p_P^s(P^* - |\Delta P|) + c_P|P^* + \Delta P| \tag{6.8}$$

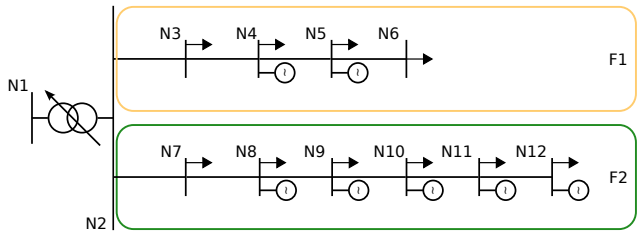

Figure 6.5: Electrical network one-line diagram.

Eq. 6.9 represents the economic balance for a generator called for a voltage regulation action by the network supervisor through a token, remunerated at p_Q to provide the required reactive power ΔQ. Active and reactive power costs are c_P and c_Q respectively, whereas reactive power Q^* is not remunerated. In case the generator needs to reduce the active power production due to capability curve limits, the active power decrement is indicated as ΔP_Q.

$$(p_P^s - c_P)(P^* + \Delta P_Q) + p_Q|\Delta Q| + c_Q|Q^* + \Delta Q| \tag{6.9}$$

When all customers for each area have replied to their token, the network supervisor decides whether or not a new token is required. If this is the case, required ΔP and ΔQ amounts are updated for the subsequent token rounds, whereas p_P and p_Q are increased of specified Δp_P and Δp_Q amounts. The procedure is repeated until either normal system conditions are restored or number of token iterations or the remunerations overcome the specified limits set by the network supervisor.

6.4 A 12-bus 2-feeder test case

6.4.1 Case study system

Applicability of the proposed token ring control procedure has been verified on the case study system depicted in fig. 6.5 (distribution network, rated voltage 20 kV, base power 1 MW).

For the sake of simplicity, lossless inverter interfaced generators are here assumed to participate in the regulation, all supposed to vary their generation within a circular capability curve.

An active power remuneration of 100 mu/pu (mu = monetary unit, pu = per unit) is taken as reference for all other costs; the initial token for line loading (current) regulation is assumed $p_P^s + \Delta p_P = 110$ mu/pu. The initial reactive power (voltage) regulation token is assumed equal to $p_Q = 60$ mu/pu with $\Delta p_Q = 10$ mu/pu. To be noted that the mu prices above are arbitrary assumptions taken for the sake of assessing the applicability of the distributed token regulation approach, the issue of investigating on realistic monetary values being outside the scopes of this work.

The electric network of fig. 6.5 is a 20 kV 12-bus radial network, connected to the bulk grid (slack bus N1) through an on-load tap-changer (OLTC) transformer. The total load and generation data of the two feeders are summarized on table 6.4. Refer to appendix F for additional data.

Table 6.1: Load and generation data.

Feeder	length, km	load, pu		generation, pu	
		active	reactive	active	reactive
F1	15.3	6.3	3.9	7.2	0
F2	24.0	9.6	4.8	20.2	0

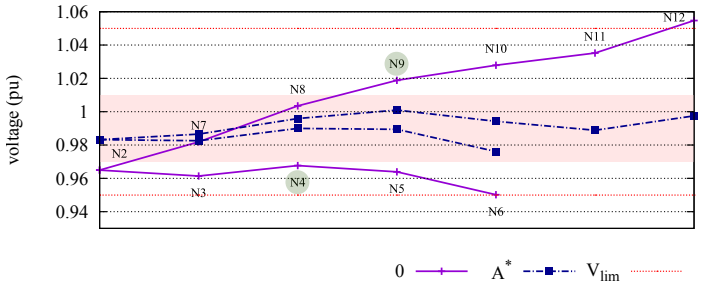

(a) Scenario A*: voltage profile

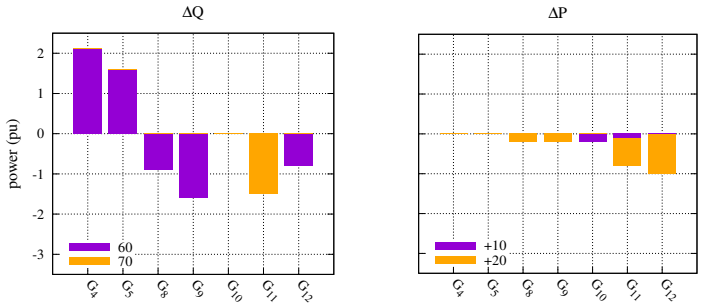

(b) Scenario A*: ΔQ and ΔP

Figure 6.6: Left hand side: voltage profiles for scenario A* depicted with blue dashed curves are compared with the initial scenario 0 (violet). Right hand side: the supplied ΔQ for voltage regulation and ΔP for current regulation are pictured, highlighting each token turn (legends show p_Q and Δp_P for voltage and current token respectively).

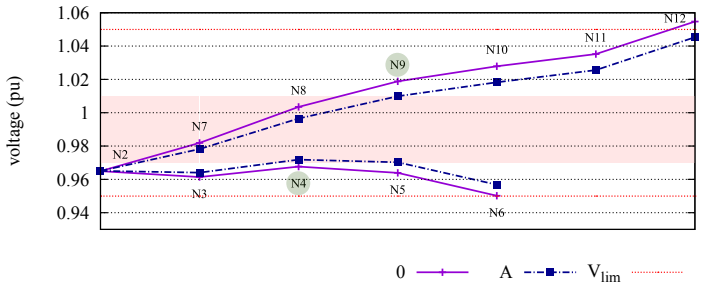

(a) Scenario A: voltage profile

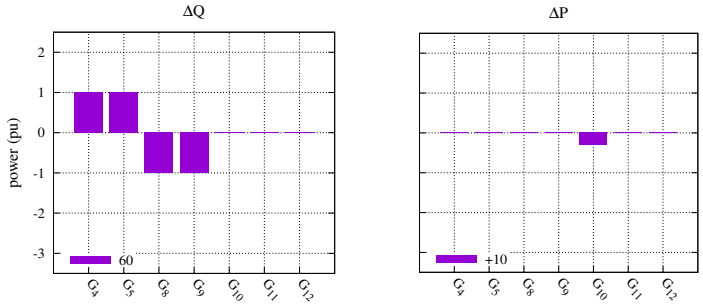

(b) Scenario A: ΔQ and ΔP

Figure 6.7: Left hand side: voltage profiles for scenario A depicted with blue dashed curves are compared with the initial scenario 0 (violet). Right hand side: the supplied ΔQ for voltage regulation and ΔP for current regulation are pictured, highlighting each token turn (legends show p_Q and Δp_P for voltage and current token respectively).

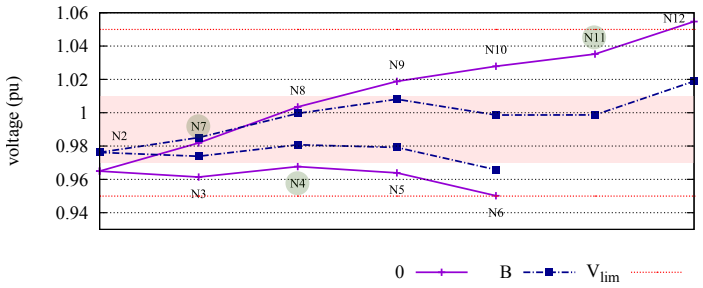

(a) Scenario B: voltage profile

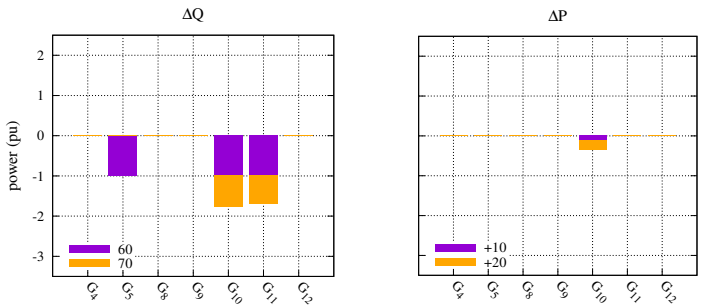

(b) Scenario B: ΔQ and ΔP

Figure 6.8: Left hand side: voltage profiles for scenario B depicted with blue dashed curves are compared with the initial scenario 0 (violet). Right hand side: the supplied ΔQ for voltage regulation and ΔP for current regulation are pictured, highlighting each token turn (legends show p_Q and Δp_P for voltage and current token respectively).

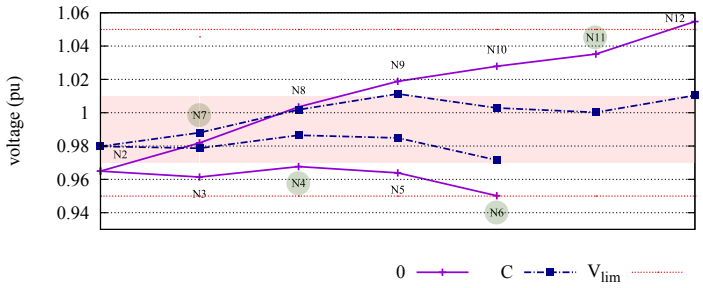

(a) Scenario C: voltage profile

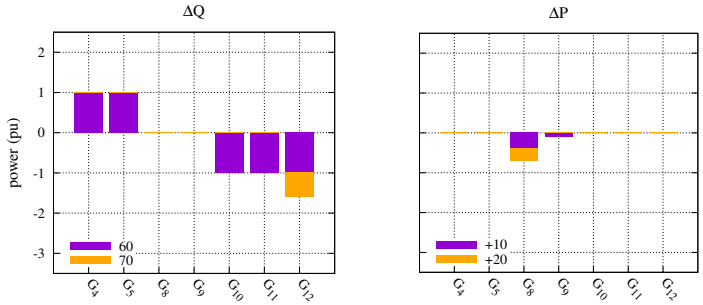

(b) Scenario C: ΔQ and ΔP

Figure 6.9: Left hand side: voltage profiles for scenario C depicted with blue dashed curves are compared with the initial scenario 0 (violet). Right hand side: the supplied ΔQ for voltage regulation and ΔP for current regulation are pictured, highlighting each token turn (legends show p_Q and Δp_P for voltage and current token respectively).

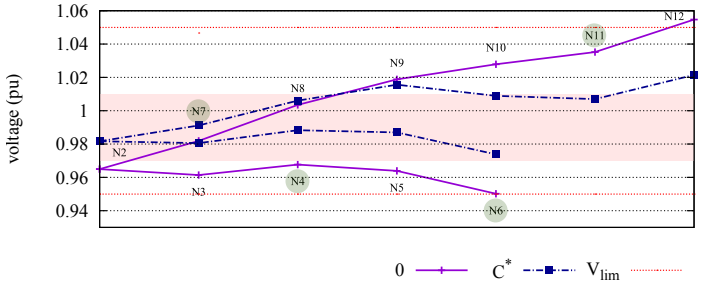

(a) Scenario C*: voltage profile

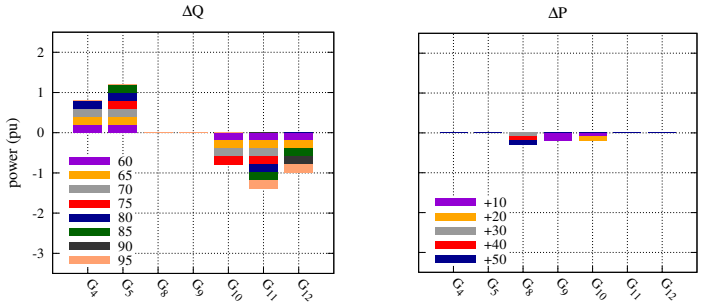

(b) Scenario C*: ΔQ and ΔP

Figure 6.10: Left hand side: voltage profiles for scenario C* depicted with blue dashed curves are compared with the initial scenario 0 (violet). Right hand side: the supplied ΔQ for voltage regulation and ΔP for current regulation are pictured, highlighting each token turn (legends show p_Q and Δp_P for voltage and current token respectively).

Table 6.2: Voltage regulation scenarios (for each scenario radius, areas, pilot bus, in bold, and allowed ΔQ are reported).

scenario	r_d	areas	ΔQ
A*	0.75	A_1: N3,**N4**,N5,N6 A_2: N2,N7,N8,**N9**,N10,N11,N12	∞
A	0.75	A_1: N3,**N4**,N5,N6 A_2: N2,N7,N8,**N9**,N10,N11,N12	± 1
B	0.50	A_1: N3,**N4**,N5,N6 A_2: N2,**N7**,N8,N9 A_3: N10,**N11**,N12	± 1
C	0.25	A_1: N3,**N4** A_2: N5,**N6** A_3: N2,**N7**,N8,N9 A_4: N10,**N11**,N12	± 1
C*	0.25	A_1: N3,**N4** A_2: N5,**N6** A_3: N2,**N7**,N8,N9 A_4: N10,**N11**,N12	± 0.2

6.4.2 Results and discussion

This system is characterized by a high not evenly distributed DG penetration, resulting in the wide busbar voltage spread depicted in figs. from 6.6 to 6.10 (b subplots), which show the busbar voltage profile obtainable applying different management criteria. In particular, violet profiles in each sub-figures refers to starting unregulated network conditions (scenario 0). It can be seen that the two feeders are characterised by the opposite voltage profiles (violet profile), i.e. Feeder F1 has depleted voltage levels, whereas Feeder F2 busbars exceed 1.05 pu with busbar N12. In this wide voltage spread conditions, the OLTC operation ($\Delta tap = 0.75\%$) is necessarily inhibited.

The token ring approach has been assessed by comparing the results of different regulation scenarios, obtained varying the size of the regulation areas and the max ΔP, ΔQ assigned to the token each turn. In the following the discussion is limited, for the sake of clarity, to the 5 regulation scenarios described in table 6.2 (labeled A*, A, B, C, C* respectively) and the results are reported in figs. from 6.6 to 6.10 and table 6.3 for a direct comparison.

For all scenarios the same closest busses aggregation criteria has been applied and the size of the voltage areas depends on the assumed radius ($0 \leq r_d \leq 1$). By reducing r_d from 0.75 to 0.25 the number of areas (and pilot busses) increases, as shown in table 6.2.

On the basis of the starting voltage conditions (scenario 0) of the pilot busses with respect to the busses with the highest (N12) and the lowest (N6) voltages, the allowed bounds for the pilot busses to be achieved through the voltage regulation action are set to 1.01 and 0.97 pu for all the scenarios.

In scenario 0 there are no line congestions. However, during the voltage reg-

Table 6.3: Main results for each scenario: voltage spread for each feeder and the grid; active and reactive power variation for each feeder, due to regulation; total remuneration for active and reactive regulation; total increase of remuneration for generators participating in regulation, final OLTC position.

Scenario	ΔV_{F1}	ΔV_{F2}	ΔV	ΔQ_{F1}	ΔQ_{F2}	$C_{\Delta Q}$
0	0.073	0.011	0.105	-	-	-
A*	0.015	0.007	0.021	3.72	-4.79	421
A	0.067	0.007	0.088	2.00	-2.00	240
B	0.034	0.015	0.053	1.00	-3.48	283
C	0.023	0.015	0.040	2.00	-3.60	342
C*	0.030	0.015	0.045	2.00	-3.20	367
Scenario	l_{cong}	ΔP_{F1}	ΔP_{F2}	$C_{\Delta P}$	R%	t
0	-	-		-	-	0
A*	N7-N8	-	2.40	296	17.73	-3
A	N7-N8	-	0.30	33	6.94	0
B	N7-N8	-	0.40	47	6.46	-3
C	N7-N8	-	0.80	91	9.44	-3
C*	N7-N8	-	0.70	89	11.04	-3

ulation action, congestion conditions may arise, that are identified by the network controller which promptly initiates a current regulation action by circulating the appropriate token within the current regulation areas.

For each regulation scenario a pictorial overview of the results is reported in figs. from 6.6 to 6.10 (b subplots: starting and final bus voltage distribution - c subplots: active and reactive regulating power provided by the active customers participating in the regulation in response to circulating tokens), whereas the numerical values of the most significant quantities are summarized in table 6.3.

As expected, increasing the number of areas and pilot busses (compare scenarios A, B and C, characterized by r_d equal to 0.75, 0.50, 0.25 respectively), the control is more accurate leading to a lower voltage spread ΔV. This is accomplished because as the number of areas (and pilot busses) increases, the participation of the different active customers is intrinsically better co-ordinated, as can be observed in figs. 6.7, 6.8 and 6.9, center subplots. However, this also leads to higher costs for the network operator ($C_{\Delta Q}$ and $C_{\Delta P}$ in table 6.3) which should thus find the best compromise between costs and quality level: in this case Scenario B represents the best solution.

Scenario A* represents a variant of Scenario A where no limitations are enforced on the maximum amount of reactive power required by the token per generator. In this way, voltage violations could be solved by the first generators recipient of tokens, if they decide to provide the whole amount of regulating power required (as assessed by the network controller).

This criterion could thus be useful in case of particularly critical situations, where the system operator needs a fast response. However, care must be taken to avoid possible unstable conditions which could arise due to high power step changes injected by the single generators. The final voltage profile obtained in Scenario A* is much better than in Scenario A. However, it may easily be drawn from figs. 6.6 and

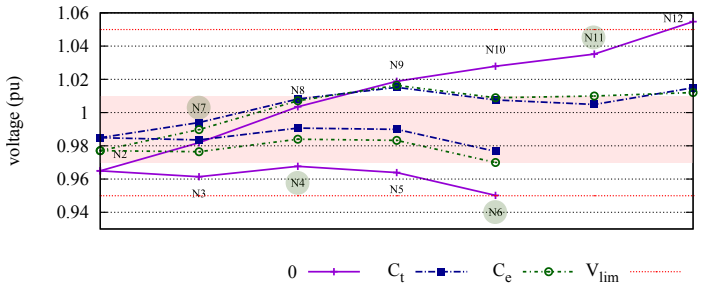

(a) Voltage profiles

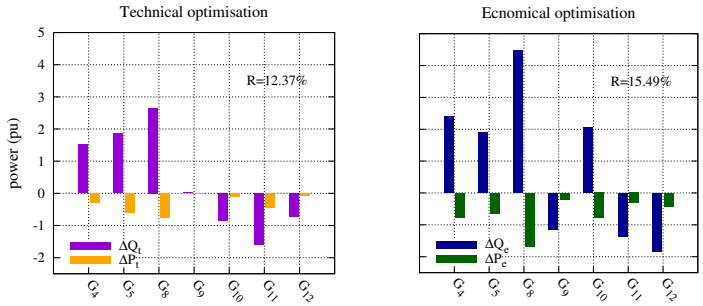

(b) Power variations

Figure 6.11: Voltage profiles of technical and economical optimisations on the left, corresponding power variations on the right.

6.7 and table 6.3 that such improvement is achieved with a higher (and expensive) regulating power injection of the generators in both areas. In addition the reactive regulation action gives rise to a severe congestion in the line N7-N8 which requires a substantial active power reduction to be solved. The total increase of remuneration (which is a cost for the network) for the generators participating to the regulation is 17.73%, calculated as

$$\frac{R_{new} - R_{old}}{R_{old}} 100 \tag{6.10}$$

(R_{new} = new total remuneration, R_{old} = old total remuneration). For each generator this value oscillates between 0.75% at N10 and 38% at N12, due to different participation of the single generators in regulation.

In scenarios A, B and C, the maximum active and reactive power variation per token is set to ± 1 pu. The smaller this value the greater the number of tokens which may be circulated in each regulation area to solve voltage violations and line congestions. Smaller ΔQ, ΔP tokens circulated several times allows a finer co-ordination of the regulating power provided by the different generators, although at higher costs since the remuneration is increased each time the token is re-circulated.

For the sake of comparison, Scenario C* represents a variant of Scenario C with ΔP, ΔQ set to 0.2 pu and the cost step increase $\Delta p_Q = 5$ mu/pu. As can be seen in figs. 6.9 and 6.10, the two scenarios voltage profiles are quite similar, but obtained with a different contribution of the generators participating in the regulation. In Scenario C* the overall regulating power (both active and reactive) is lower than in Scenario C, but the generators remuneration (and thus the costs for the network) is

almost 10% higher, due to the cost increments of the tokens which circulate in each area 7 times, rather than 2, in order to solve the contingencies.

The performances of the token ring procedure are finally compared with the results of a classical Optimal Power Flow (OPF), set to perform both an economical and a technical optimisation. In the economical OPF (C_e) the boundary constraints for pilot bus voltages are set to 0.97 and 1.01 pu and the objective is to maximize the generators remuneration through the function

$$\sum_{i=1}^{n_g}(p_P^S - c_{i_P})P_i + (p_Q - c_{i_Q})|Q_i| \tag{6.11}$$

where n_g is the total number of generators which participates in regulation. It is interesting to note that the voltage profiles obtainable with the economical OPF (fig. 6.11, Scenario C_e) and token ring procedure (fig. 6.9, Scenario C) are quite similar, although achieved with a different contribution of regulating power from the participating generators. Eq. 6.11 represents the maximum gain for all generators participating in voltage regulation. In this way, all generators find their feasible active and reactive power combination maximizing their gain, according to network requirements and constraints. The resulting increased remuneration for the generators is 15.49%, considerably higher than the 9.44% corresponding to Scenario C (table 6.3). The technical OPF (Scenario C_t) aims at minimizing the mean root square deviation of voltages, with a 0.02 tolerance and respecting 1.01-0.97 pu constraints for pilot busses, as in Scenario C. As appears from Fig. 6.11, the results are similar to those achieved with the economical OPF. In this case the required regulating reactive power is 8.72 pu, and the corresponding generators increased remuneration is equal to 12.37%. In both cases, the system operator would thus pay an higher price for reactive power, without a corresponding remarkable improvement in voltage regulation performances.

6.5 A 38-bus 3-feeder test case

6.5.1 Case study system

Further investigation has been performed with the 20 kV 38-bus radial network depicted in figs. 6.12, 6.13 and 6.14, connected to the bulk grid through an on-load tap-changer (OLTC) transformer (distribution network, rated voltage 20 kV, base power 1 MW). The total load and generation data of the three feeders are summarized on Table 6.4. Refer to appendix G for additional data.

As in previous application, only generators are allowed to participate in regulation, co-ordinated with the OLTC, whose operation is supervised by the System Operator, whereas the OLTC is allowed to operate provided that the network bus voltage spread is sufficiently contained so as OLTC operation does not cause any bus voltage violation. Again, the initial active and reactive power remuneration are 100 mu/pu and $p_Q = 60$ mu/pu, with $\Delta p_P = \Delta p_Q = 10$ mu/pu.

6.5.2 Results and discussion

The token ring approach has been assessed by comparing the results of different regulation scenarios, obtained by varying the number and size of the voltage regulation areas and the aggregation criteria for busses. The different voltage regulation areas with indication of the corresponding pilot busses for the three scenarios are depicted in figs. 6.12a, 6.13a and 6.14a.

In Scenarios A=3 and A=6 (with 3 and 6 regulation areas respectively) the areas are identified by applying the hierarchical criterion, which ensures at least one active customer per area, with reference to a large, A=3, and a small, A=6, electric distance (radius), whereas the aggregation of closest busses with a large radius has been used in Scenario A=4. Further details on the criteria for regulation areas definition can be found, summarized, in ref. [78].

Figs. 6.12, 6.13 and 6.14 shows the voltage profiles and the share of regulating power provided by the participating generators for the 3 different regulating scenarios. Violet profiles in each sub-figure (on the left hand side) depict the initial voltage conditions of the network (scenario 0), characterized by the different behaviour of each feeder. The high level of distributed generation in Feeder F1 results in high busbar voltages with N17 and N18 even exceeding the upper limit (1.05 pu). Feeder F3 has a generally depleted voltage distribution typical of passive feeders with N38 lower than 0.95 pu, whereas Feeder F2 voltage distribution presents an abnormal maximum value along the feeder. The novel distributed co-ordinated power management procedure is thus tested on a rather disuniform voltage distribution, different from traditional increasing and decreasing profiles. The different concentration of generation and loads in feeders causes a voltage spread of 0.125 pu, thus the OLTC operation ($\Delta tap = 0.75\%$) is inhibited.

In scenario 0, branches N3-N4 in F1 and N20-N21 in F2 are overloaded and thus a current regulation action is performed concurrently to the voltage regulation. The corresponding current regulation areas are formed by the downstream generator nodes, i.e (N4, N8, N11, N14, N18) and (N21, N24) respectively.

Considering the poor initial voltage conditions, in this application the required token ΔQ is not limited. The amount of regulating reactive power provided by each customer-recipient depends on its own convenience, and is determined on the basis of p_Q, p_P^s and constraints. Differently, active power token is limited to ± 1 pu, for a better distribution of customers operations in the congestion regulation.

On the basis of the starting voltage conditions (scenario 0) of the pilot busses with respect to the busses with the highest (N18) and the lowest (N38) levels, the allowed bounds for the pilot busses to be achieved through the voltage regulation action are set to 1.015 and 0.985 pu for all the busbars but N31, whose minimum reference level is set to 0.967 pu.

As can be seen in figs. 6.12b, 6.13b and 6.14b, similar voltage profiles can be achieved by applying the different regulation scenarios (average voltage spread of 0.07 pu against 0.125 pu of scenario 0), although through a quite different contribution, in terms of active and reactive regulating power, of the various participant customers, depending on number of areas and token procedure. To be noticed that, in this case study system, the line congestions influence the starting behaviour of voltage tokens, whose customer-recipient are not allowed to participate in voltage regulation if their operations increase the current flow in already overloaded lines.

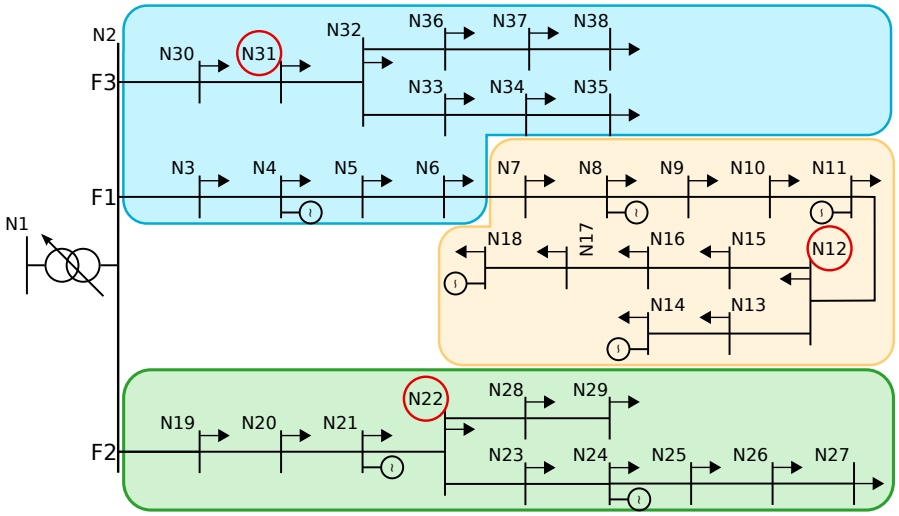

(a) Scenario A=3: voltage control areas

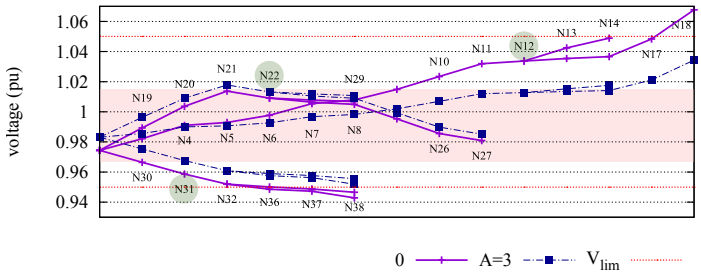

(b) Scenario A=3: voltage profile

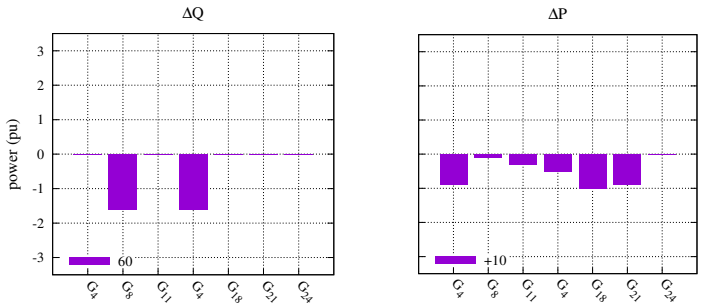

(c) Scenario A=3: ΔQ and ΔP

Figure 6.12: Scenario A=3: 3 voltage control areas are defined. Voltage profiles depicted with blue dashed curves are compared with the initial scenario 0 (violet), on the top, the supplied ΔQ for voltage regulation and ΔP for current regulation are pictured, highlighting each token reply (legends show p_Q and Δp_P for voltage and current token respectively).

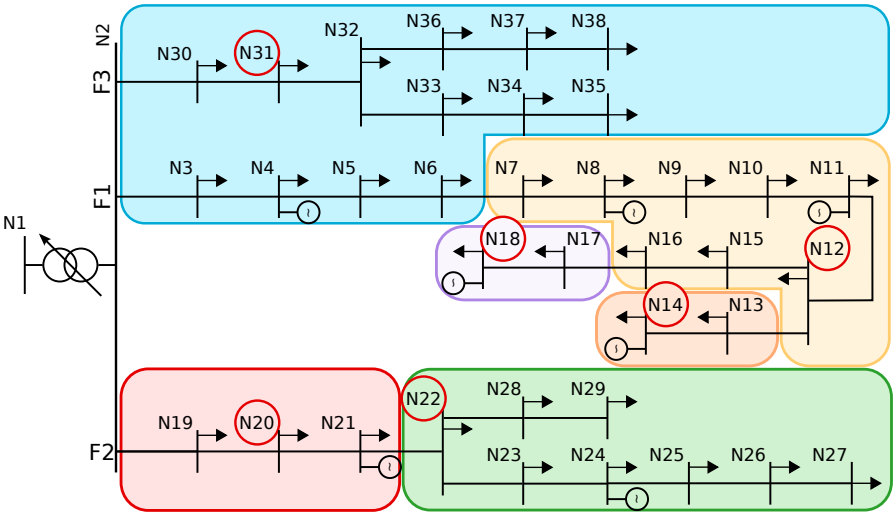

(a) Scenario A=6: voltage control areas

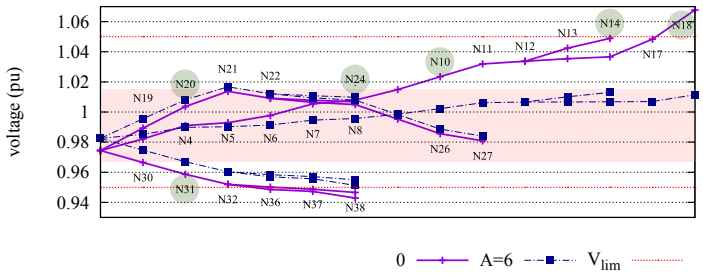

(b) Scenario A=6: voltage profile

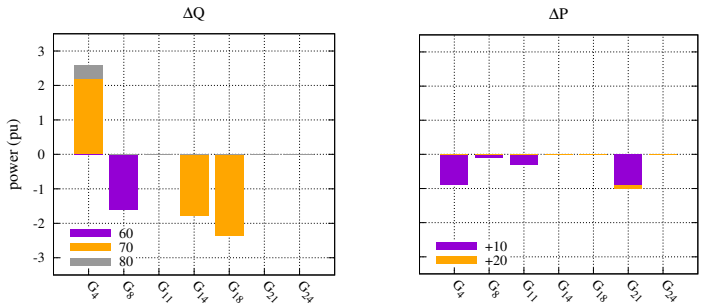

(c) Scenario A=6: ΔQ and ΔP

Figure 6.13: Scenario A=6: 6 voltage control areas are defined. Voltage profiles depicted with blue dashed curves are compared with the initial scenario 0 (violet), on the top, the supplied ΔQ for voltage regulation and ΔP for current regulation are pictured, highlighting each token reply (legends show p_Q and Δp_P for voltage and current token respectively).

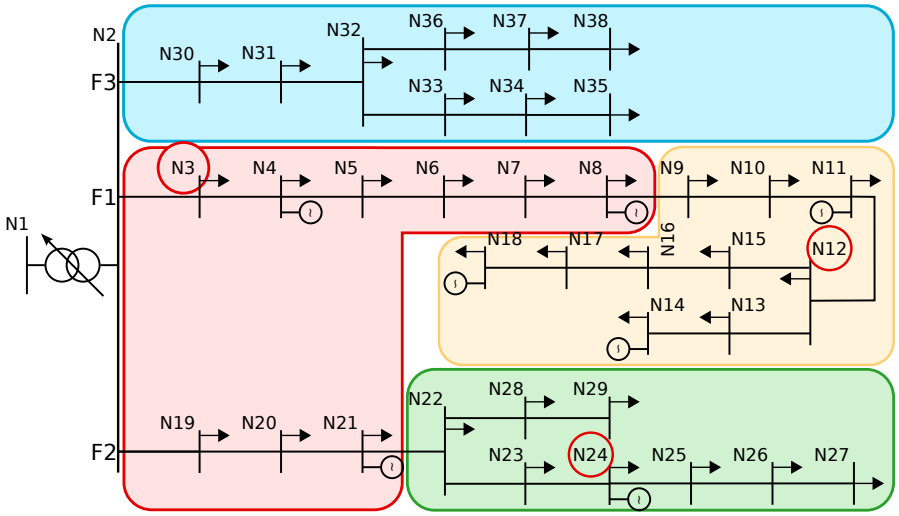

(a) Scenario A=4: voltage control areas

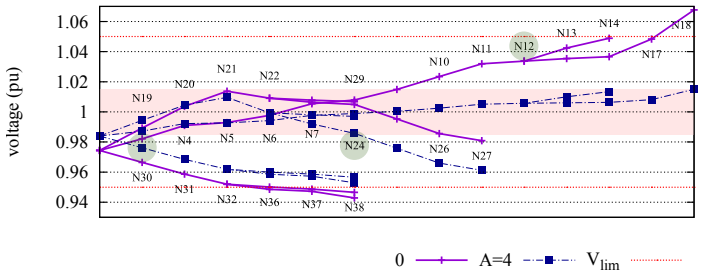

(b) Scenario A=4: voltage profile

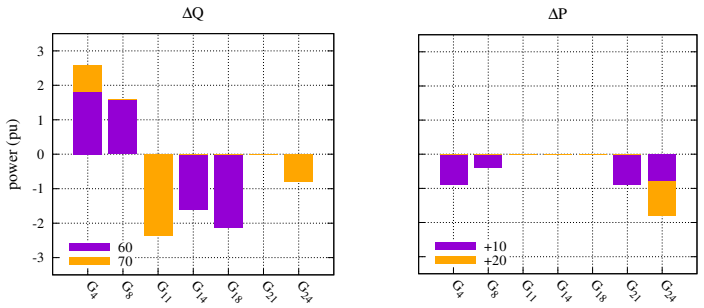

(c) Scenario A=4: ΔQ and ΔP

Figure 6.14: Scenario A=4: 4 voltage control areas are defined. Voltage profiles depicted with blue dashed curves are compared with the initial scenario 0 (violet), on the top, the supplied ΔQ for voltage regulation and ΔP for current regulation are pictured, highlighting each token reply (legends show p_Q and Δp_P for voltage and current token respectively).

Table 6.4: Load and generation data.

Feeder	length, km	load, pu		generation, pu	
		active	reactive	active	reactive
F1	27.0	8.4	4.3	19.6	0
F2	29.2	3.9	2.2	13.0	0
F3	19.8	4.3	3.4	0	0

Both the participation order of customers in each regulation area and the pilot bus location affect the token ring procedure and thus the results achievable.

Table 6.5 reports some main results of the different token ring scenarios. Scenarios A=3 and A=4 are characterized by 3 regulating areas (the forth area defined for Scenario A=4 has not active customers). Although Scenario A=4 seems to have the same, or even slightly better, voltage results than Scenario A=3, this is achieved by a much higher regulating power provided by the active customers (corresponding to an higher revenue for these customers – see R% in Table 6.5, calculated as the percentage difference between the new and old total generators remuneration - and thus an higher cost for the network operator). This is due to a the different area definition and pilot busses location in Scenario A=3, which are better suited for the voltage regulation in the presence of the specific line congestion contingency.

A finer voltage profile is obtained with Scenario A=6. Its six areas allow a more accurate grid control, thanks to corresponding distributed pilot busses, against an increasing number of token turns, which however doesn't lead to the most expensive regulation scenario.

In this case the total increase of remuneration (which is a cost for the network) for the generators participating to the regulation is 12.92% against 16.27% for Scenario A=4 (see Table 6.5).

It may be concluded that all the three scenarios are applicable in this case study, with different technical and economical results for the network. In particular, the token ring procedure could properly manage also feeder with no monotone voltage profiles, such as feeder F2 characterized by a maximum voltage level in N21.

6.6 Conclusion

A distributed co-ordinated power management in MV electrical network where every active customer could freely participate in services for the grid support has been presented.

The grid is divided in areas for voltage and current control. When a violation is recognized by the network controller, a suitable price/power signal (the token) is elaborated and sent sequentially to each customer of the designated regulation area. The token essentially contains an active/reactive power variation request and the remuneration offered for such service. Several tokens could be sent concurrently, depending on the number of simultaneous violations, to the customer-recipients which have complete freedom to satisfy or not such request, depending on the attractiveness of the offer.

Table 6.5: Main results for each scenario: voltage spread for each feeder and the grid; active and reactive power variation for each feeder, due to regulation; total remuneration for active and reactive regulation; total increase of remuneration for generators participating in regulation, final OLTC position.

Scenario	ΔV_{F1}	ΔV_{F2}	ΔV_{F3}	ΔV	$\lvert\Delta Q_{F1}\rvert$	$\lvert\Delta Q_{F2}\rvert$	$\lvert\Delta Q_{F3}\rvert$	$C_{\Delta Q}$	$\lvert\Delta P_{F1}\rvert$	$\lvert\Delta P_{F2}\rvert$	$\lvert\Delta P_{F3}\rvert$	$C_{\Delta P}$	R%	t
0	0.086	0.033	0.024	0.125	-	-	-	-	-	-	-	-	-	0
A=3	0.049	0.033	0.023	0.082	3.19	0	-	191	2.80	0.90	-	407	5.91	-1
A=6	0.028	0.033	0.023	0.065	8.35	0	-	570	2.30	1.30	-	254	12.92	-1
A=4	0.028	0.048	0.023	0.062	10.25	0.80	-	702	4.00	1.30	-	321	16.27	-1

The feasibility of the of the token-ring approach is demonstrated on an electrical network test case and compared also with the results of more classical Optimal Power Flow applications.

These preliminary results are quite promising, although further investigation and development in token management criteria are required.

It is advisable that future work would focus on improving the area and pilot bus definition, in particular a dynamic definition of voltage control area, accounting for actual reactive power availability, to achieve a better distributed regulation and avoid critical instabilities.

7 Conclusion

The first part of this thesis has been focused on multi-energy vector systems.

Electricity is the most versatile and widely used form of energy in the world. Additionally, electricity is the most interchangeable. This means synergy among different energy vector could improve the efficiency of electrical network management, increasing efficiency of the whole system thanks to added degrees of freedom. Particularly, investigation on energy hub management, as generation, conversion and storage center, have demonstrated the possibility to improve electrical network efficiency exploiting the integration of CHP plants with storage devices.

The management of distributed resources in energy networks has been performed solving optimisation problems, in order to achieve the best dispatch of different resources usually to minimize generation costs. In fact, economic aspects have been considered as main thread of important decisions, from both network and customers point of view. The system operator evaluates the total costs necessary to improve quality of electricity services at any system operating conditions and chooses the best compromise, whereas customers have the freedom to modulate their power generation/absorption depending on revenue and costs.

For this reason, price signals have been supposed key for the system operator, which aims to obtain a specific behavior from customers. This means devices are involved to absorb/generate the power that the network desires in order to improve its performance and particularly to avoid any critical situation, providing suitable price signals.

Suitable price signals means price coefficients able to translate technical issues (voltage amplitude at nodes within limits, no overloaded lines etc.) in an understandable language by customers, i.e. in an economical information useful for customers to decide how to behave. In fact, customers have not direct interest in technical quality goals, but only maximize their revenue or minimize their cost.

Constant price coefficients usually used have a limited effectiveness in this translation from technical to economical information because they have not intrinsic information about network requirements. For this reason, the concept of "reference signals" has been investigated: price coefficients proportional to a reference value are able to incentive customer to provide that specific reference value in order to maximize its revenue, whereas any other value would mean reducing its revenue or increasing the costs. The reference signal is an information provided by the system operator, that, knowing characteristics (lines and transformers data, generators and loads capacity) and status (voltages at nodes and flows in lines) of the network, esti-

mates changes it would like obtaining by customers for the critical situation solving or the improvement of the network status.

Even if further investigations are required in order to obtain absolute values useful in actual grids, reference signals have allowed investigation on smart grids scenario where interconnections ensure information exchanges among system operator and customers, that increase interactions and activates participation of customers in network regulation issues, being more aware of possibilities offered by the market and their on-line response.

Additionally, reference signals have demonstrated their feasibility in a co-ordinated procedure used to separately optimise single-step (a single instant) and multi-period (multiple instants linked by integral constraints) problems. In order to easy the computation burden calculations, electrical network with ESS optimisation has been divided in two problems: on one hand, the electrical network, which does not require integral constraints, is optimised in single sequential instants disregarding what happens in other instants, providing the optimal solution that the ESS should provide from the network point of view. On the other hand, ESS replies to the grid optimisation on the basis of the reference profile, considering its integral constraints and economic aspects (remuneration VS costs), that strictly depend on the reference signal.

The usage of reference signals supports a multi-level management structure, that seems to be ideally suited in smart grids scenario, characterized by interconnections and interactions. A multi-level management aims to split the electrical network management problem into a number of easier and smaller problems able to provide a solution very close to the initial problem, distributing the complexity of the management problem in a scenario with a large amount of variables.

Electrical storage devices have demonstrated to have a key role in future electrical grids, but they are penalized by high investment costs. For this reason, aggregators of EVs have been considered. EVs plugged in to the grid to re-charge their batteries could be used by the grid to provide services for the grid support according to requirements of drivers. Analyzing characteristics of EVs and issues linked to EVs penetration, aggregators of EVs have been recognized as important energy storage devices for electrical network, which could support transportation network transition between petrol fuel to "electric fuel". In fact, electric networks could remunerate the transportation network reducing the Pay Back Time of re-charging infrastructures and EVs costs, making feasible leasing opportunities. Aggregators seem to be interesting option to increase EVs acceptance by people, thanks to leasing services or re-charging contract services.

Two main typologies of EVs aggregators have been identified and defined: swapping station, for the depleted battery exchange with fresh ones, and car parking, with public re-charge infrastructures. The operational characteristics of swapping stations make them particularly suitable for providing grid services as ESS, besides satisfying their main duty of vehicle batteries recharging. In particular, swapping stations could be very close to traditional ESS, making really feasible the possibility to provide active power regulation with batteries of EVs, even considering degradation aspects of batteries. On the other hand, car parking is more complex to investigate, due to the higher aleatory behavior of outgoing and incoming vehicles, that defines the availability of batteries. "Residential" and "office" car parking have been designed with

some assumptions: if "residential" car parking does not affect peak hours, considering a traditional three slots tariff for electricity imports, it could be considered of low impact to the grid; "office" car parking service is concentrated during peak hours, thus the peak load demand increases.

However, the four quadrant converter interface between the grid and the EV makes EVs re-charging infrastructures interesting for the reactive power regulation. Flows does not affect SOC of batteries, consequently degradation issues lack. Considering the reactive power market is the most probable energy market that will be subject to changes in the next future due both to importance of reactive power and to lack of standards for remuneration, EVs could take major advantages from reactive power regulation than active power regulation. The importance to use these devices for voltage regulation has been investigated, but further investigation is required, particularly on the mechanism for the remuneration of reactive power.

In the last part of this thesis an innovative co-ordinated distributed management procedure has been investigated. A multi-level multi-area management inspired on token ring has been proposed. Electrical network has been supposed divided into control areas each one dedicated to a specific issue (solve a congestion in a specific branch or reduce/increase voltage at a specific bus), which co-ordinates customers belonging to that area. Each area operates on its issue, managing its customers with a co-ordinated procedure based on the token ring philosophy, where each area customer interact sequentially with the network supervisors. In this way, customers are allowed to freely participate in network regulation, deciding on the basis of network signals, prices, what to do. Each area is supervised by a network supervisors, that performs the co-ordination of customers and interacts with higher level supervisors. In this way, supervisors know only information necessary to solve their own issues and the management problem of the electrical network could be performed without knowing everything about the network. As an example, supervisors of each area knows only data and objective of their control areas. Higher levels know goals of control areas they supervise but they have no access inside areas details (how many customers, how customers behave etc.) The highest level is the system operator, that knows everything, but its role is to co-ordinate sub-levels disregarding what really happens in those sub-levels. This procedure has demonstrated its applicability in two test cases with promising results, even if further investigation on aggregation of customers are required, to improve robustness of this co-ordinated distributed management system.

In this thesis, smart management procedures for co-ordinating different resources in energy networks have been investigated. The importance of price signals as suitable indicators of the network status and its needs has been analyzed, with the aim of demonstrating how the economic aspect may represent a valid tool for the system operator in order to smartly manage responsive customers in a deregulated network. It should be noted, that the mechanism of construction of such price signals, although of fundamental importance, were out of scope of this work and deserve a further, much deeper future analysis.

In this research an effort has been made in trying to re-think the traditional concepts of electrical network management, exploiting the peculiar properties of smart grids (interactivity and connectivity); this has led to the proposal of decentralized methodologies not only because they can better deal with the distributed active ele-

ments but also because they enable to decompose a complex management problem in different layers. This approach seems to be more suited for a smart grid scenario where each actor may participate in the management given the availability of suitable signals but without full knowledge of the network operational status. The feasibility of such "distributed" approach has been demonstrated in this work, although further investigation is needed to verify its reliability in all foreseeable operating conditions.

A Optimal Daily Profiles of Energy Hubs

In this appendix, results (daily profiles) of the optimisation of the energy hub presented in chapter 3 are reported.

A.1 "Residential" load profiles scenario

Figures in next pages are organized as follow: for each tariff scenario, two figures are reported. Each first figure shows daily profiles for energy hub without storage devices and with an electrical storage device. Each second figure shows daily profiles for energy hub with both electrical and thermal storage devices and with a thermal storage device.

Each couple of figures correspond to "Base scenario", A, B and C tariff scenario, shown one after the other. In each figure, sub-figures represent power at input side of the energy hub, stored energies and electrical generation of the CHP and thermal generation of the furnace power profiles.

A.1.1 "Base case" tariff scenario

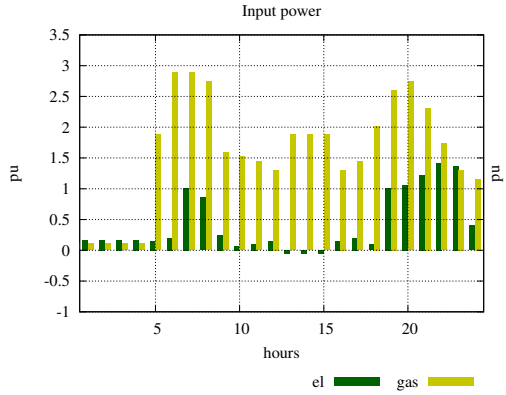

(a) B.c. tariff - without storage - input power

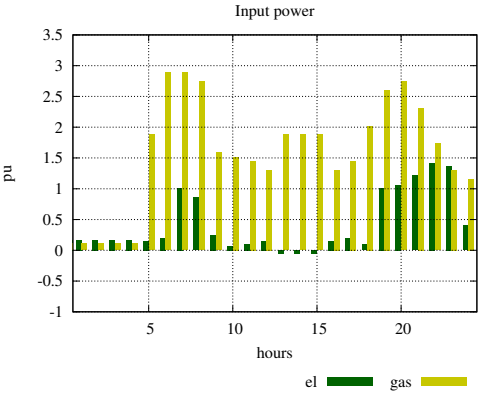

(b) B.c. tariff - electrical storage - input power

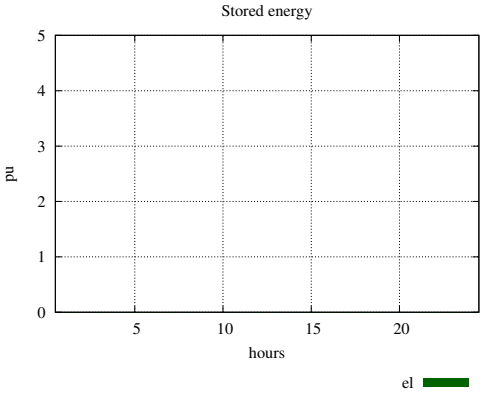

(c) B.c. tariff - without storage - stored energies

(d) B.c. tariff - electrical storage - stored energies

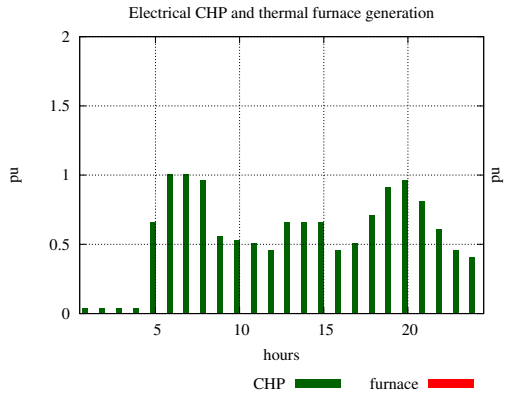

(e) B.c. tariff - without storage - P_{el}^{CHP}, P_{th}^{f}

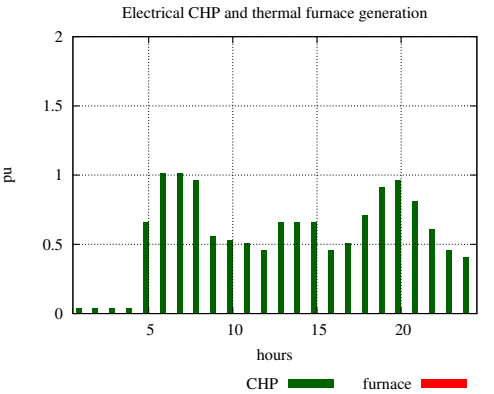

(f) B.c. tariff - electrical storage - P_{el}^{CHP}, P_{th}^{f}

Figure A.1: Left hand side: "Base case" (B.c.) tariff scenario and no storage devices in the energy hub (consequently A.1c is missing). Right hand side: B.c. tariff scenario and electrical storage. From the top to he bottom: input powers, stored energies and CHP electrical and furnace generation profiles.

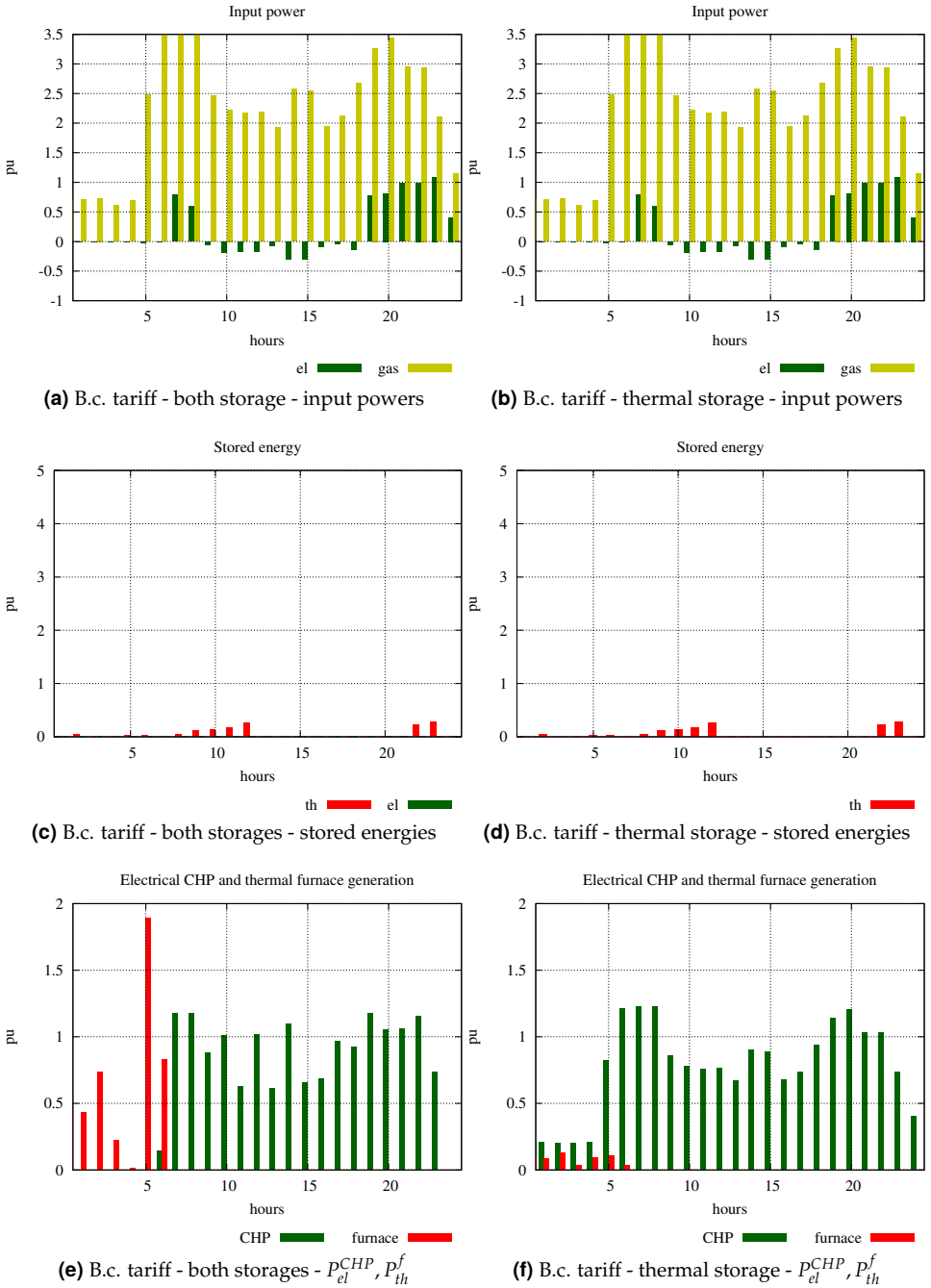

(a) B.c. tariff - both storage - input powers

(b) B.c. tariff - thermal storage - input powers

(c) B.c. tariff - both storages - stored energies

(d) B.c. tariff - thermal storage - stored energies

(e) B.c. tariff - both storages - P_{el}^{CHP}, P_{th}^{f}

(f) B.c. tariff - thermal storage - P_{el}^{CHP}, P_{th}^{f}

Figure A.2: Left hand side: "Base case" (B.c.) tariff scenario and both storage devices in the energy hub. Right hand side: B.c. tariff scenario and thermal storage. From the top to the bottom: input powers, stored energies and CHP electrical and furnace generation profiles.

A.1.2 Tariff A scenario

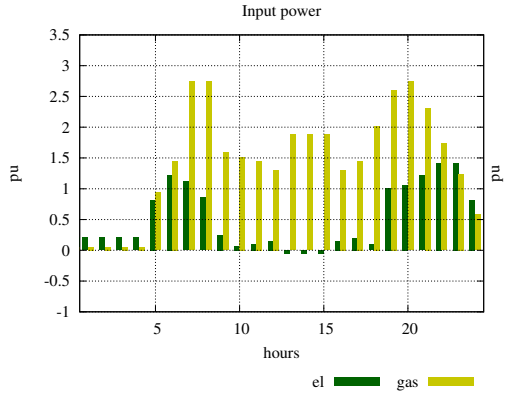

(a) Tariff A - without storage - input power

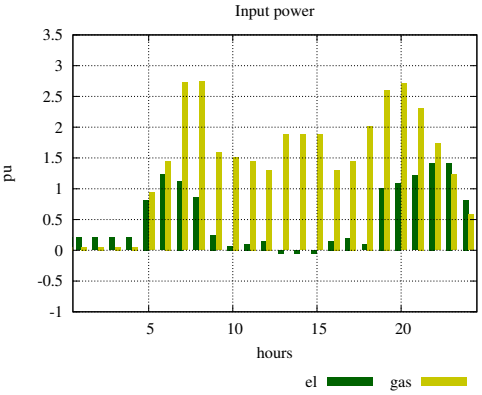

(b) Tariff A - electrical storage - input power

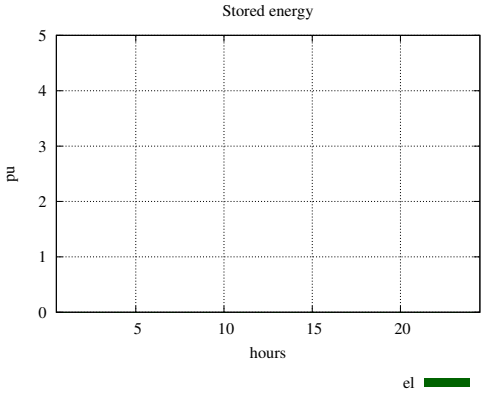

(c) Tariff A - without storage - stored energies

(d) Tariff A - electrical storage - stored energies

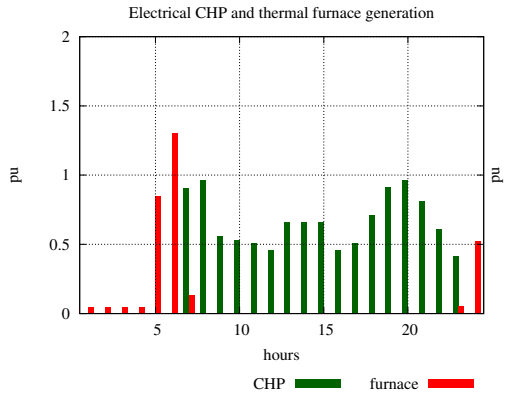

(e) Tariff A - without storage - P_{el}^{CHP}, P_{th}^{f}

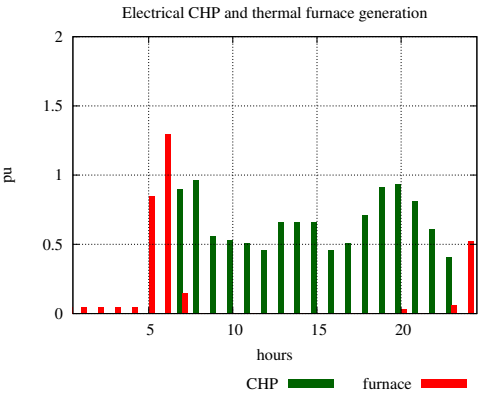

(f) Tariff A - electrical storage - P_{el}^{CHP}, P_{th}^{f}

Figure A.3: Left hand side: tariff A scenario and no storage devices in the energy hub. Right hand side: tariff A scenario and electrical storage. From the top to the bottom: input powers, stored energy and CHP electrical and furnace generation profiles. (Missing picture A.3c is due to absence of the storage devices in the energy hub.)

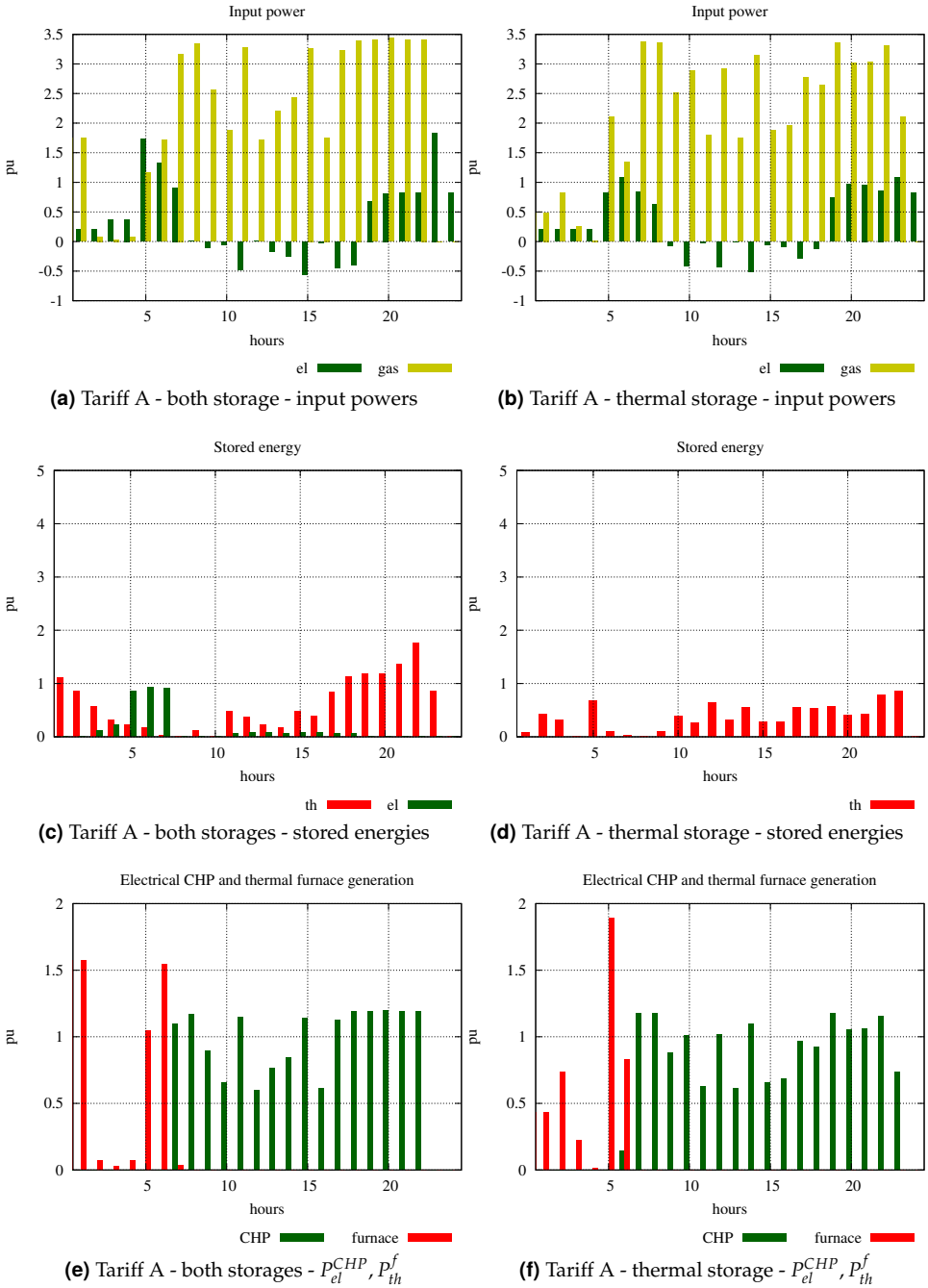

(a) Tariff A - both storage - input powers

(b) Tariff A - thermal storage - input powers

(c) Tariff A - both storages - stored energies

(d) Tariff A - thermal storage - stored energies

(e) Tariff A - both storages - P_{el}^{CHP}, P_{th}^{f}

(f) Tariff A - thermal storage - P_{el}^{CHP}, P_{th}^{f}

Figure A.4: Left hand side: tariff A scenario and both storage devices in the energy hub. Right hand side: tariff A scenario and thermal storage. From the top to the bottom: input powers, stored energies and CHP electrical and furnace generation profiles.

A.1.3 Tariff B scenario

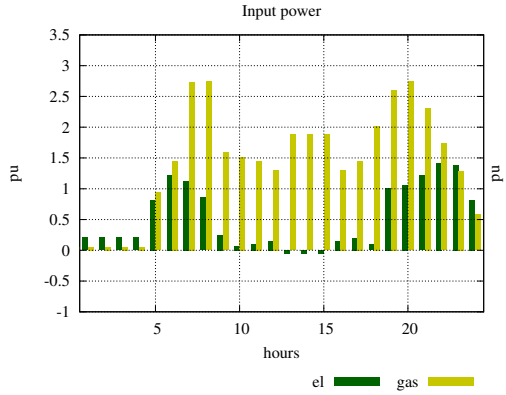

(a) Tariff B - without storage - input power

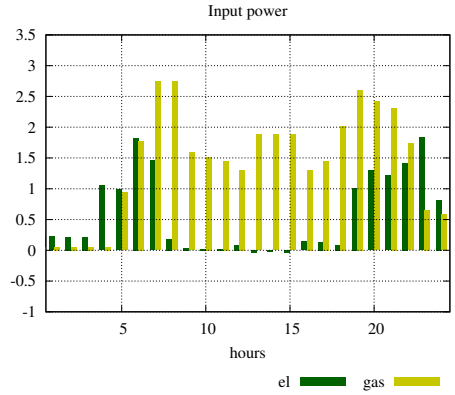

(b) Tariff B - electrical storage - input power

(c) Tariff B - without storage - stored energies

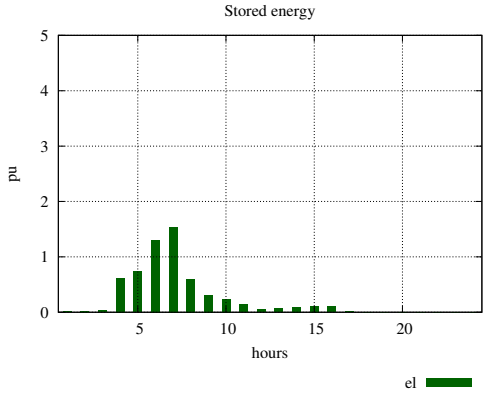

(d) Tariff B - electrical storage - stored energies

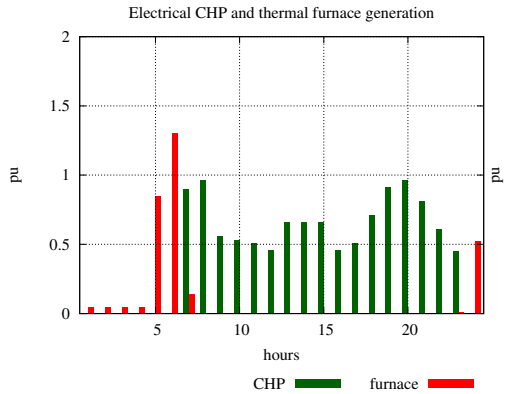

(e) Tariff B - without storage - P_{el}^{CHP}, P_{th}^{f}

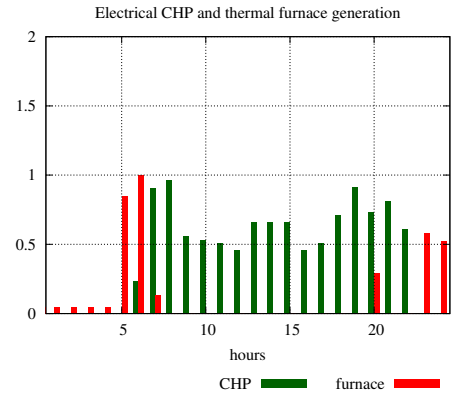

(f) Tariff B - electrical storage - P_{el}^{CHP}, P_{th}^{f}

Figure A.5: Left hand side: tariff B scenario and no storage devices in the energy hub. Right hand side: tariff B scenario and electrical storage. From the top to the bottom: input powers, stored energy and CHP electrical and furnace generation profiles. (Missing picture A.5c is due to absence of the storage devices in the energy hub.)

(a) Tariff B - both storage - input powers

(b) Tariff B - thermal storage - input powers

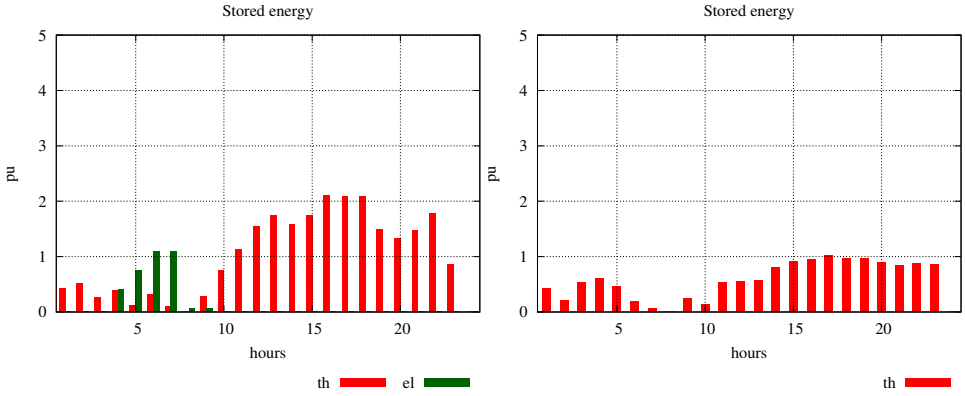

(c) Tariff B - both storages - stored energies

(d) Tariff B - thermal storage - stored energies

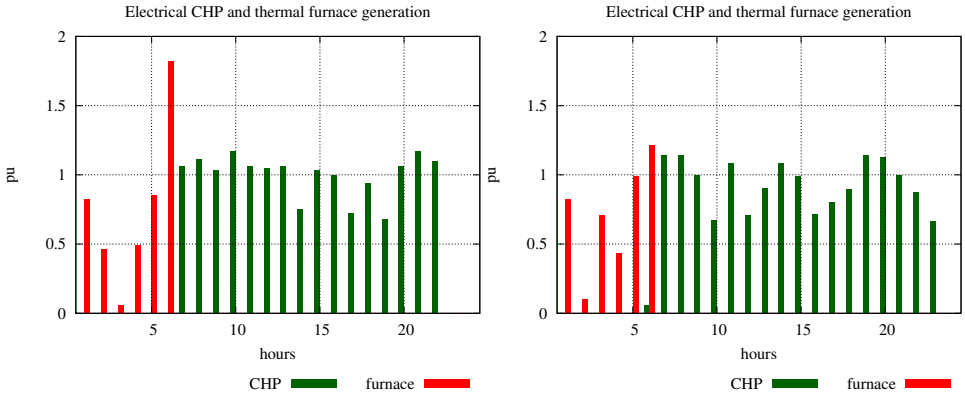

(e) Tariff B - both storages - P_{el}^{CHP}, P_{th}^{f}

(f) Tariff B - thermal storage - P_{el}^{CHP}, P_{th}^{f}

Figure A.6: Left hand side: tariff B scenario and both storage devices in the energy hub. Right hand side: tariff B scenario and thermal storage. From the top to the bottom: input powers, stored energies and CHP electrical and furnace generation profiles.

A.1.4 Tariff C scenario

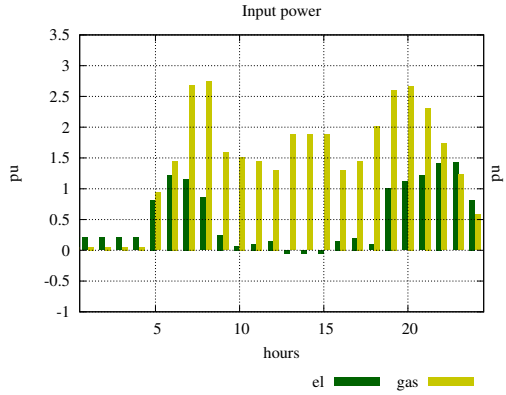

(a) Tariff C - without storage - input power

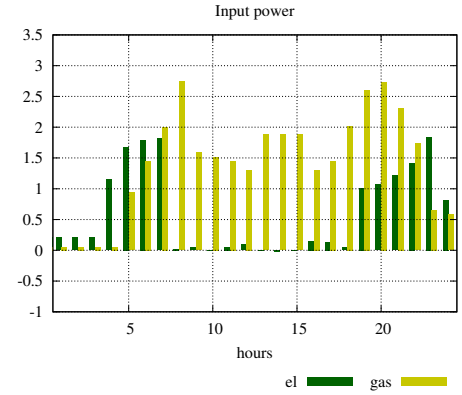

(b) Tariff C - electrical storage - input power

(c) Tariff C - without storage - stored energies

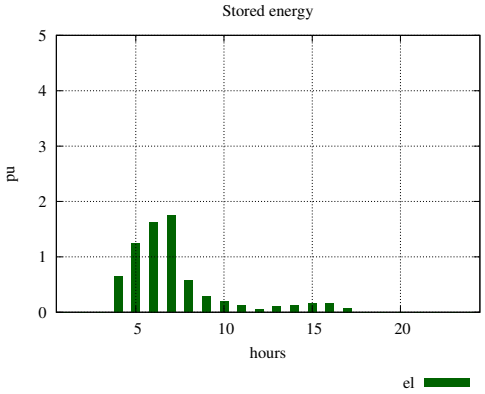

(d) Tariff C - electrical storage - stored energies

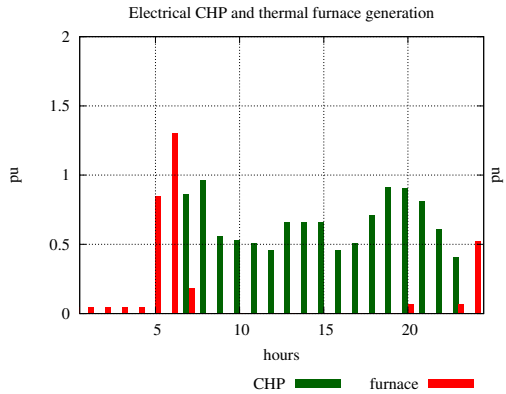

(e) Tariff C - without storage - P_{el}^{CHP}, P_{th}^{f}

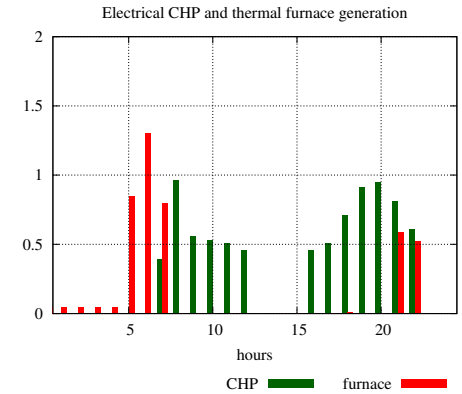

(f) Tariff C - electrical storage - P_{el}^{CHP}, P_{th}^{f}

Figure A.7: Left hand side: tariff C scenario and no storage devices in the energy hub. Right hand side: tariff C scenario and electrical storage. From the top to the bottom: input powers, stored energy and CHP electrical and furnace generation profiles. (Missing picture A.7c is due to absence of the storage devices in the energy hub.)

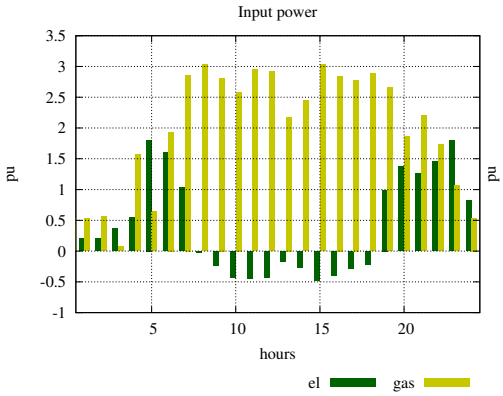

(a) Tariff C - both storage - input powers

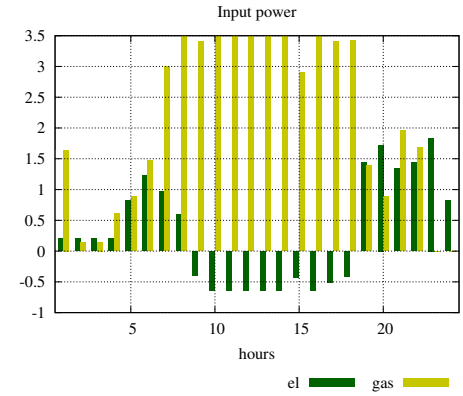

(b) Tariff C - thermal storage - input powers

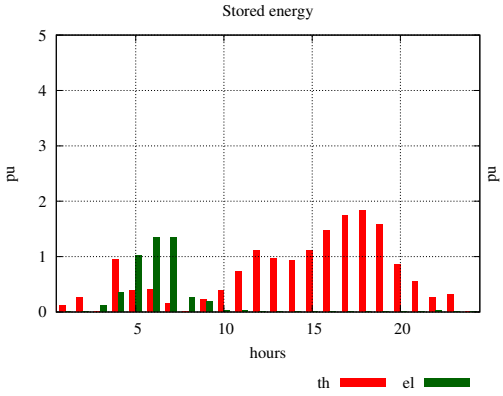

(c) Tariff C - both storages - stored energies

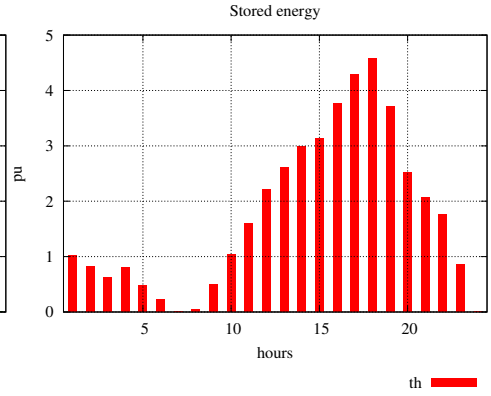

(d) Tariff C - thermal storage - stored energies

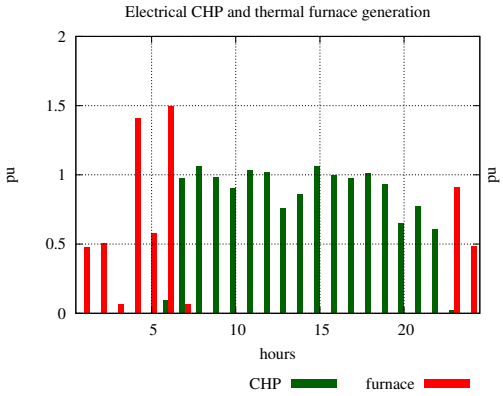

(e) Tariff C - both storages - P_{el}^{CHP}, P_{th}^{f}

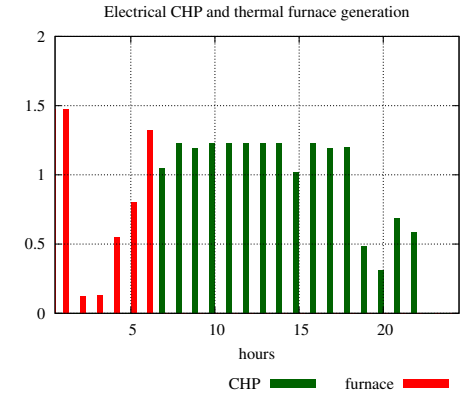

(f) Tariff C - thermal storage - P_{el}^{CHP}, P_{th}^{f}

Figure A.8: Left hand side: tariff C scenario and both storage devices in the energy hub. Right hand side: tariff C scenario and thermal storage. From the top to the bottom: input powers, stored energies and CHP electrical and furnace generation profiles.

A.2 “Industrial” load profiles scenario

In next pages, figures with optimal profiles for the energy hub with “industrial” load profiles are provided.

To be noticed, only energy hub without storage devices for “Base case” and tariff A scenario are reported in fig.A.9, because optimisation does not provide interesting results considering storage devices (as explained in chapter 3.

A.2.1 "Base case" and tariff A scenarios

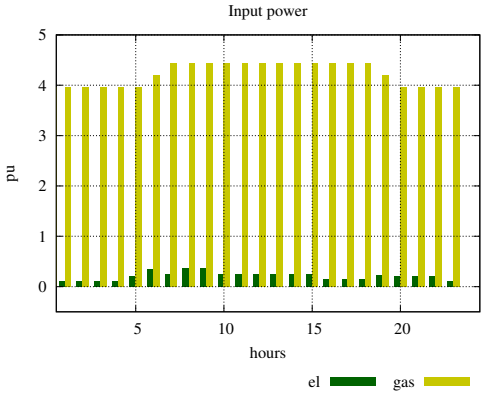

(a) B.c. tariff - without storage - input power

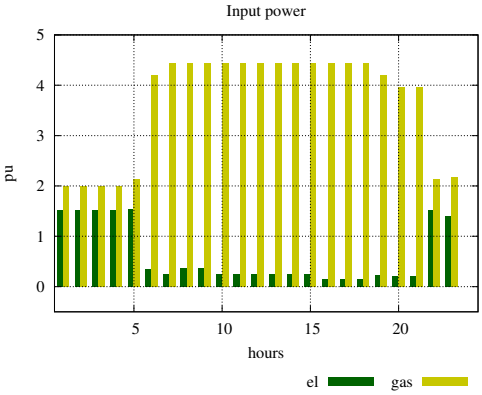

(b) Tariff A - without storage - input power

(c) B.c. tariff - without storage - stored energies

(d) Tariff A - without storage - stored energies

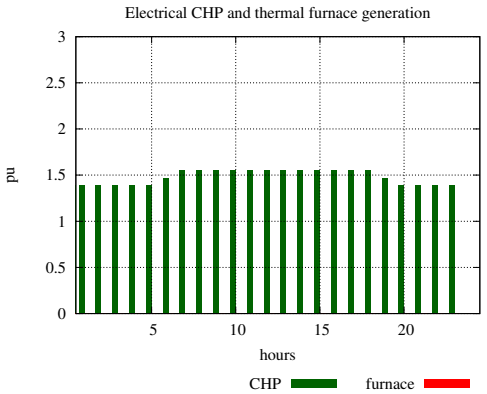

(e) B.c. tariff - without storage - P_{el}^{CHP}, P_{th}^{f}

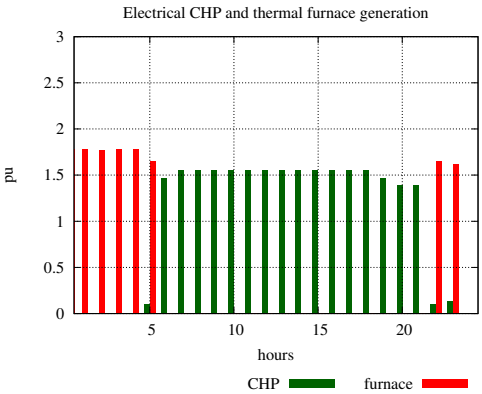

(f) Tariff A - without storage - P_{el}^{CHP}, P_{th}^{f}

Figure A.9: Left hand side: "Base case" (B.c.) tariff scenario and no storage devices in the energy hub. Right hand side: tariff A scenario and no storage devices in the energy hub. (Consequently A.9c and A.9d are missing) From the top to he bottom: input powers, stored energies and CHP electrical and furnace generation profiles.

A.2.2 Tariff B scenario

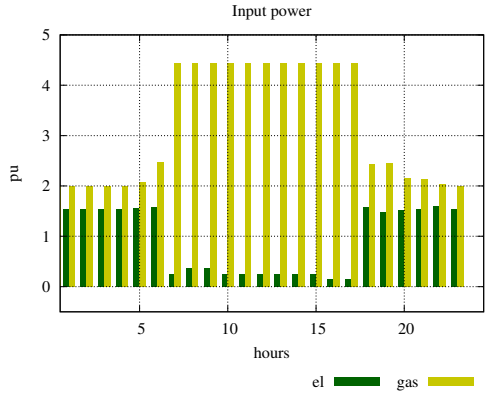

(a) Tariff B - without storage - input power

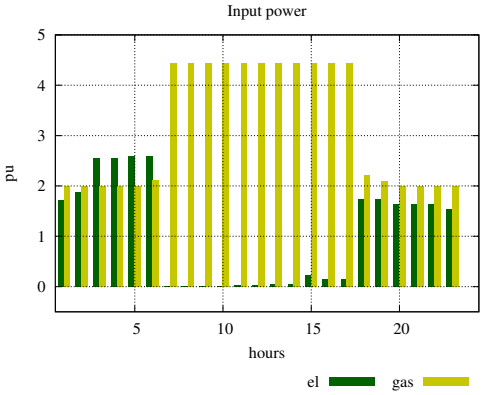

(b) Tariff B - electrical storage - input power

(c) Tariff B - without storage - stored energies

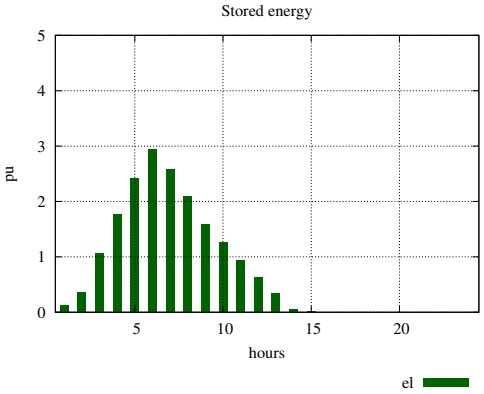

(d) Tariff B - electrical storage - stored energies

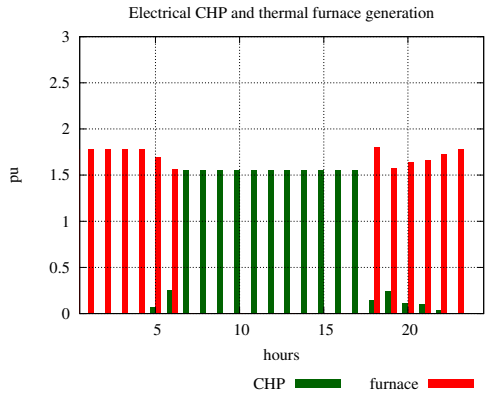

(e) Tariff B - without storage - P_{el}^{CHP}, P_{th}^{f}

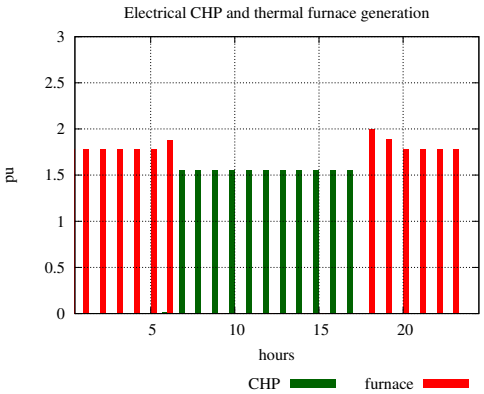

(f) Tariff B - electrical storage - P_{el}^{CHP}, P_{th}^{f}

Figure A.10: Left hand side: tariff B scenario and no storage devices in the energy hub. Right hand side: tariff B scenario and electrical storage. From the top to the bottom: input powers, stored energy and CHP electrical and furnace generation profiles. (Missing picture A.10c is due to absence of storage devices in the energy hub.)

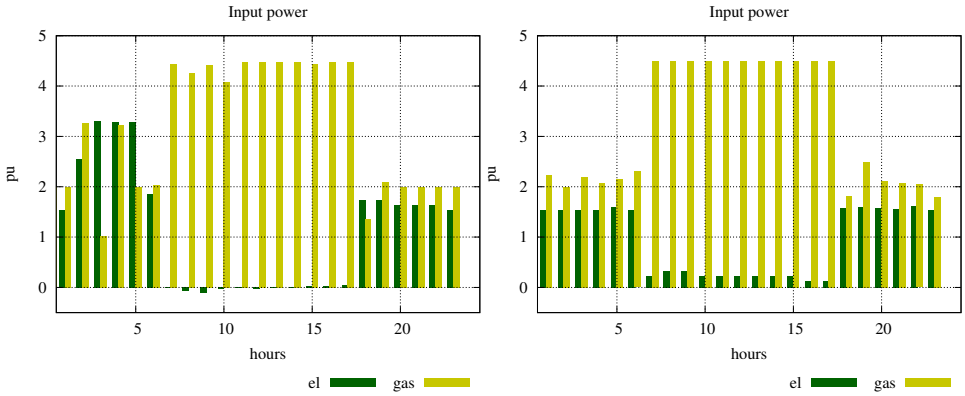

(a) Tariff B - both storage - input powers

(b) Tariff B - thermal storage - input powers

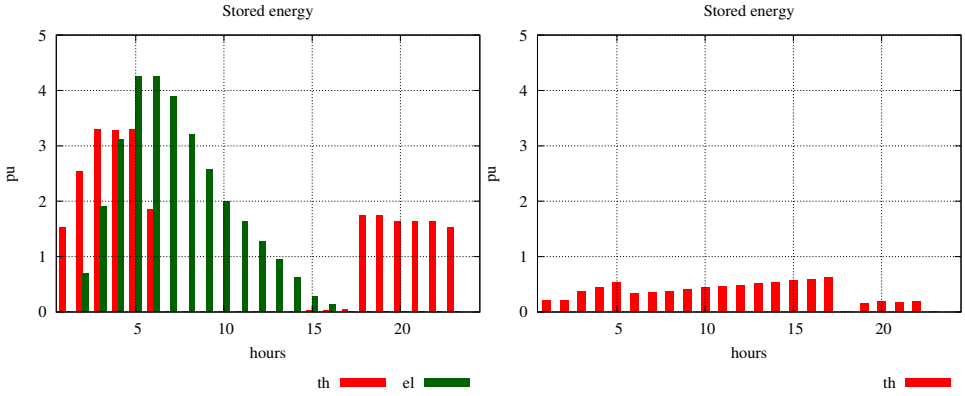

(c) Tariff B - both storages - stored energies

(d) Tariff B - thermal storage - stored energies

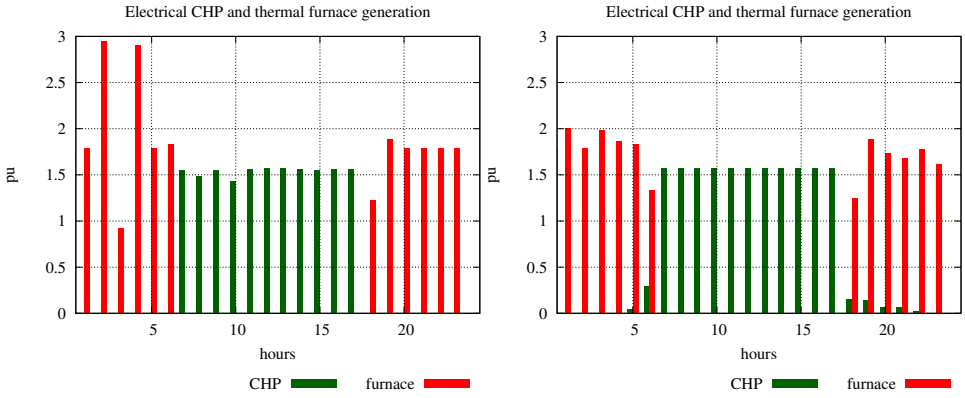

(e) Tariff B - both storages - P_{el}^{CHP}, P_{th}^{f}

(f) Tariff B - thermal storage - P_{el}^{CHP}, P_{th}^{f}

Figure A.11: Left hand side: tariff B scenario and both storage devices in the energy hub. Right hand side: tariff B scenario and thermal storage. From the top to the bottom: input powers, stored energies and CHP electrical and furnace generation profiles.

A.2.3 Tariff C scenario

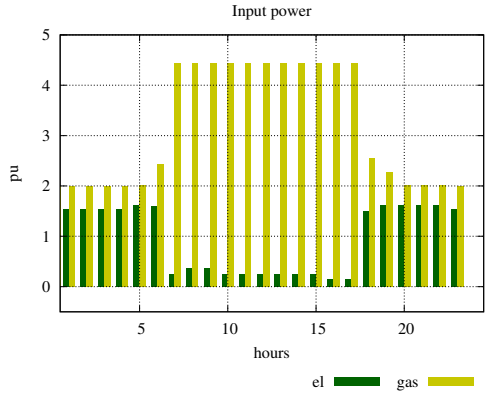

(a) Tariff C - without storage - input power

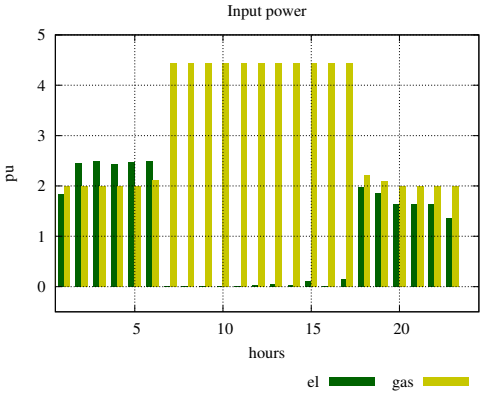

(b) Tariff C - electrical storage - input power

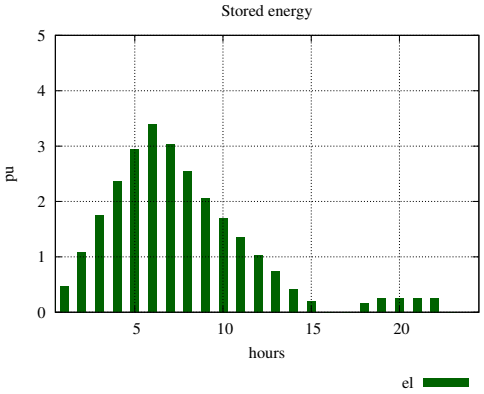

(c) Tariff C - without storage - stored energies

(d) Tariff C - electrical storage - stored energies

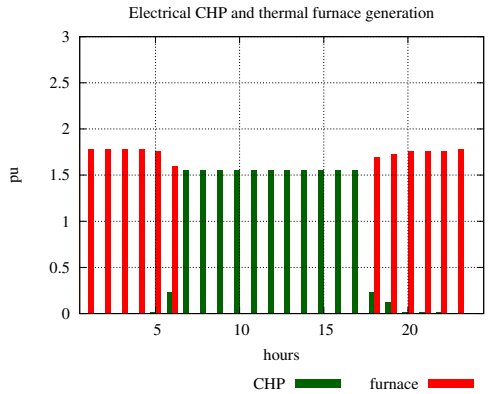

(e) Tariff C - without storage - P_{el}^{CHP}, P_{th}^{f}

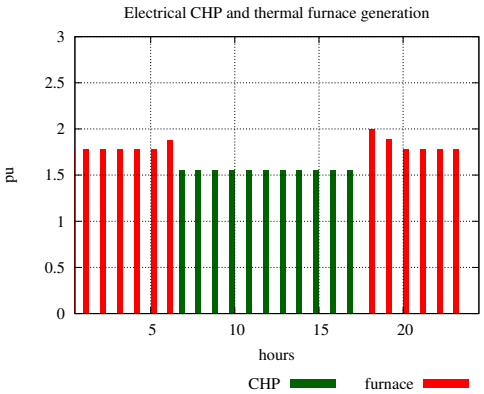

(f) Tariff C - electrical storage - P_{el}^{CHP}, P_{th}^{f}

Figure A.12: Left hand side: tariff C scenario and no storage devices in the energy hub. Right hand side: tariff C scenario and electrical storage. From the top to the bottom: input powers, stored energy and CHP electrical and furnace generation profiles. (Missing picture A.12c is due to absence of storage devices in the energy hub.)

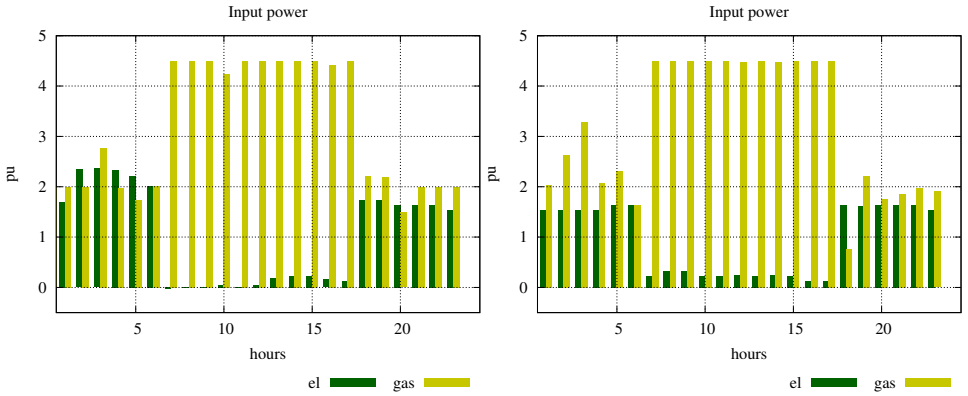

(a) Tariff C - both storage - input powers

(b) Tariff C - thermal storage - input powers

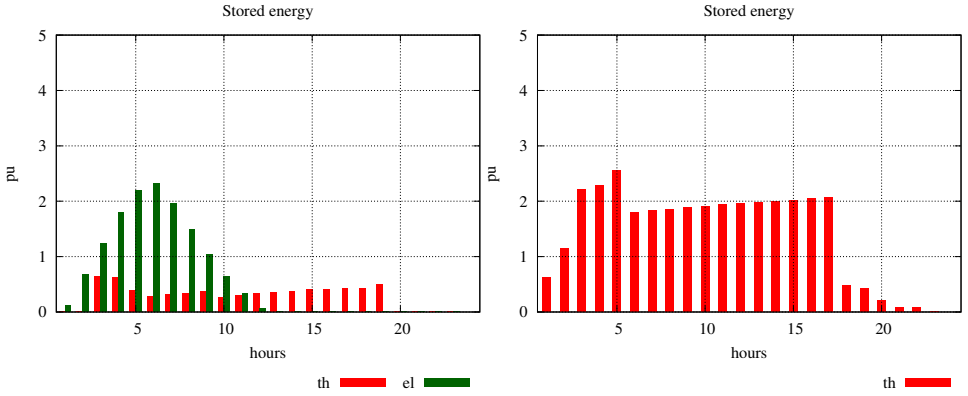

(c) Tariff C - both storages - stored energies

(d) Tariff C - thermal storage - stored energies

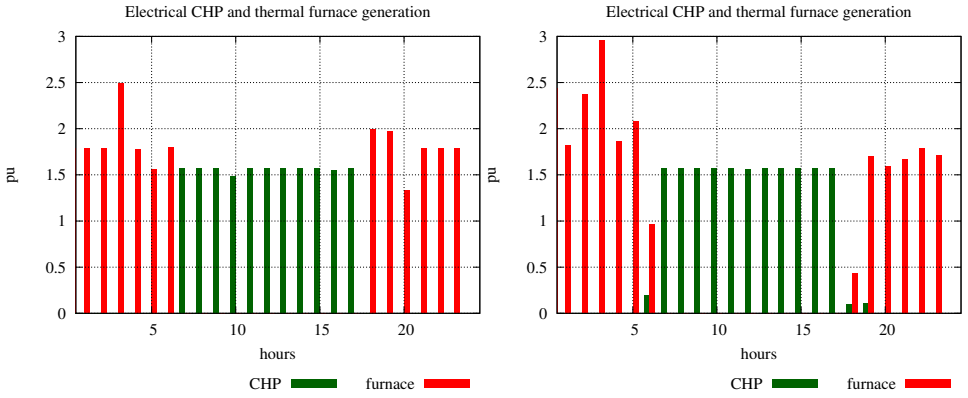

(e) Tariff C - both storages - P_{el}^{CHP}, P_{th}^{f}

(f) Tariff C - thermal storage - P_{el}^{CHP}, P_{th}^{f}

Figure A.13: Left hand side: tariff C scenario and both storage devices in the energy hub. Right hand side: tariff C scenario and thermal storage. From the top to the bottom: input powers, stored energies and CHP electrical and furnace generation profiles.

B Electrical and thermal networks system

In the following tables, data for electrical and thermal networks used as test case in chapter 4 are provided. In particular:

- efficiencies of devices in the energy hubs are shown in table B.1, where η_t, η_{ex}, $\eta_{CHP,el}$, $\eta_{CHP,th}$ and η_f are transformer, thermal exchanger, electrical and thermal CHP plant and furnace efficiency respectively;
- data of branches of electrical network are in table B.2. Water is the thermal vector (120° C forward and 60° C return) of the district heating network. To the sake of simplicity only hydraulic calculation has been done, disregarding temperature and temperature dependent behavior.
- Active (P_{el}) and reactive (Q_{el}) power absorption and generation of loads and generators data are shown in table B.3;
- data of pipelines of thermal network are in table B.4;
- in the thermal network, only loads have been considered as shown in table B.5 (P_{th} is the thermal power load).

Table B.1: Hubs coupling matric efficiencies.

name	η_t	η_{ex}	$\eta_{CHP,el}$	$\eta_{CHP,th}$	η_f
H3	0.98	0.7	0.35	0.45	–
H4	(1)	0.7	0.30	0.55	–
H5	(1)	0.7	–	–	–
H7	(1)	(1)	0.35	0.45	0.9

Table B.2: Electrical branches.

name	**length** [km]	**kilometric resistance** [Ω/km]	**kilometric inductance** [mH/km]	**kilometric capacitance** [nF/km]	max **current** [A]
L1	5.720	0.268	1.165	10	280
L2	4.100	0.320	0.406	290	200
L3	6.070	0.352	1.225	8.98	235
L4	3.740	0.125	0.335	360	400
L5	3.700	0.125	0.335	260	400
L6	4.495	0.206	0.380	340	280
L7	4.575	0.352	1.225	8.98	235

Table B.3: Electrical loads and generators (pu, $P_{base} = 1MW$).

bus	**loads**		**generators**			
			Scenario I		**Scenario II**	
	P_{el}	Q_{el}	P_{el}	Q_{el}	P_{el}	Q_{el}
N2	–	–	–	–	–	–
N3	1.630	0.824	–	–	3.50	0
N4	2.830	1.022	–	–	1.25	0
N5	2.920	1.615	3.0	0	2.25	0
N6	4.762	2.384	3.0	0	1.056 7.50	0 2.50
N7	0.570	0.323	–	–	7.50	2.50
N8	2.000	0.987	–	–	2.50	2.50
N9	0.252	0.170	–	–	1.05	0.07

Table B.4: Thermal branches.

name	**from**	**to**	**length [km]**	**diameter [km]**
L1	TH2	TH5	2.0	0.15
L2	TH3	TH5	1.5	0.15
L3	TH4	TH5	1.0	0.20
L4	TH6	TH4	1.0	0.18
L5	TH6	TH1	0.5	0.15

Table B.5: Thermal loads (pu, $P_{base} = 1MW$).

name	**bus**	P_{th}
C1	TH1	0.4081
C2	TH2	0.3150
C3	TH3	0.6270
C4	TH4	2.3358
C6	TH6	2.1205

C 9-bus 20-kV electrical network data

Data of test case used in chapter 4. Refer to tables in appendix H for component types data.

Table C.1: Branches data.

name	from	to	V_n[kV]	length [km]	type (ID)
L1	N2	N3	20	5.72	Cu 70 line
L2	N3	N4	20	4.1	AL 95 cable
L3	N3	N5	20	6.07	Cu 50 line
L4	N2	N6	20	3.74	AL 240 cable
L5	N6	N7	20	3.7	AL 240 cable
L6	N7	N8	20	4.5	AL 150 cable
L7	N7	N9	20	4.58	Cu 50 line

Table C.2: Transformer data.

name	from	to	V_1[kV]	V_2[kV]	type (ID)
trafo1	N1	N2	132	20	t_40_155_044

Table C.3: Generators data.

name	bus	SL, PQ, PV	type (ID)	V_n[kV]	daily chart (ID)
G1	N1	SL	sl	20	–
G3	N3	PQ	Pv_67	20	PV
G4	N4	PQ	H_gen	20	–
G5	N5	PQ	H_gen	20	–
G61	N6	PQ	In_42	20	MIDIDRO
G62	N6	PQ	Pv_67	20	PV
G71	N7	PQ	Eo_8	20	EO2
G72	N7	PQ	EH_gen	20	–
G8	N8	PQ	Id_42	20	IDROEL
G9	N9	PQ	Id_42	20	IDROEL

Table C.4: Loads data.

name	**bus**	**type (ID)**	V_n**[kV]**	**daily chart**
C3	N3	0759MVAR	20	BIGINDRES
C4	N4	2069MVAR	20	COMMER
C5	N5	3202MVAR	20	BIGIND
C6	N6	2823MVAR	20	COMMER
C7	N7	1714MVAR	20	INDreside
C8	N8	2238MVAR	20	BIGIND
C9	N9	0304MVAR	20	INDreside

D 11-bus 20-kV test case for swapping station

Data of test case used in chapter 5. Refer to tables in appendix H for component types data.

Table D.1: Branches data.

name	from	to	V_n[kV]	length [km]	type (ID)
L1_02_03	N2	N3	20	3.72	ARG7H1RX 185 mmq
L2_03_04	N3	N4	20	2.58	ARG7H1RX 185 mmq
L3_04_05	N4	N5	20	1.74	line Cu 70 mmq
L4_04_06	N4	N6	20	1.72	ARG7H1RX 70 mmq
L5_02_07	N2	N7	20	3.5	ARG7H1RX 120 mmq
L6_07_08	N7	N8	20	2.28	ARG7H1RX 70 mmq
L7_08_09	N8	N9	20	4.07	ARG7H1RX 70 mmq
L8_09_10	N9	N10	20	3.48	line Cu 70 mmq
L9_08_11	N8	N11	20	2.58	ARG7H1RX 70 mmq

Table D.2: Transformer data.

name	from	to	V_1[kV]	V_2[kV]	type (ID)
trafo1	N1	N2	132	20	t_40_155_044

Table D.3: Generators data.

name	bus	SL, PQ, PV	type (ID)	V_n[kV]	daily chart (ID)
AT	N1	SL	sl	20	–
G3	N3	PQ	G345_0	20	EO3
G5	N5	PQ	G42_0	20	IDROEL
G7	N7	PQ	G675_0	20	PV
G8	N8	PQ	G415_2	20	MIDIND
G9	N9	PQ	G53_0	20	IDROEL
G10	N10	PQ	G345_0	20	MIDIND
G11	N11	PQ	G42_0	20	COSTAN

Table D.4: Loads data.

name	**bus**	**type (ID)**	V_n**[kV]**	**daily chart (ID)**
L3	N3	L325162	20	INDreside
L4	N4	L252126	20	COMMER
L5	N5	L392196	20	INDreside
L6	N6	L384192	20	INDuffici
L7	N7	L1762092	20	INDreside
L8	N8	L392196	20	COMMER
L9	N9	L27621337	20	BIGIND
L10	N10	L1762092	20	TER
L11	N11	L2321112	20	TER

E 17-bus 20-kV test case for car parking

Data of test case used in chapter 5. Refer to tables in appendix H for component types data.

Table E.1: Branches data

name	from	to	V_n[kV]	length [km]	type (ID)
L1_02_03	N2	N3	20	5.72	ARG7H1RX 120 mmq
L1_03_04	N3	N4	20	4.1	ARG7H1RX 120 mmq
L1_04_05	N4	N5	20	3.38	line Cu 25 mmq
L1_03_06	N3	N6	20	6.07	ARG7H1RX 120 mmq
L1_06_07	N6	N7	20	2.75	line Cu 70 mmq
L2_02_08	N2	N8	20	3.74	ARG7H1RX 185 mmq
L2_08_09	N8	N9	20	4.31	ARG7H1RX 185 mmq
L2_09_10	N9	N10	20	4.7	ARG7H1RX 120 mmq
L2_10_11	N10	N11	20	6.5	line Cu 70 mmq
L2_10_12	N10	N12	20	4.58	line Cu 70 mmq
L3_02_13	N2	N13	20	2.35	ARG7H1RX 120 mmq
L3_13_14	N13	N14	20	3.1	ARG7H1RX 185 mmq
L3_14_15	N14	N15	20	2.45	line Cu 25 mmq
L3_14_16	N14	N16	20	1.9	line Cu 70 mmq
L3_16_17	N16	N17	20	1.2	line Cu 25 mmq

Table E.2: Transformer data

name	from	to	V_1[kV]	V_2[kV]	type (ID)
trafo1	N1	N2	132	20	t_40_155_044

Table E.3: Generators data

name	**bus**	**SL, PQ, PV**	**type (ID)**	V_n**[kV]**	**daily chart (ID)**
AT	N1	SL	sl	20	–
G3	N3	PQ	G675_0	20	PV
G4	N4	PQ	G42_0	20	MIDIND
G9	N9	PQ	EO	20	PV
G10	N10	PQ	G675_0	20	EO2
G11	N11	PQ	G42_0	20	IDROEL
G12	N12	PQ	G42_0	20	MIDIND

Table E.4: Loads data.

name	**bus**	**type (ID)**	V_n**[kV]**	daily chart (ID)
L3	N3	L1891_878	20	INDuffici
L4	N4	L122_091	20	BIGIND
L5	N5	L1891_878	20	INDuffici
L6	N6	L543_275	20	INDreside
L7	N7	L61_34	20	COMMER
L8	N8	L1891_878	20	INDuffici
L9	N9	L1891_878	20	INDuffici
L10	N10	L122_067	20	INDreside
L11	N11	L21_774	20	INDuffici
L12	N12	L21_774	20	INDuffici
L13	N13	L122_091	20	COMMER
L15	N15	L122_067	20	COMMER
L16	N16	L122_067	20	COMMER
L17	N17	L122_091	20	BIGIND

F 12-bus 20-kV test case for the token ring like procedure

Data of test case used in chapter 6. Refer to tables in appendix H for component types data.

Table F.1: Branches data.

name	from	to	V_n[kV]	length [km]	type (ID)
D1_02_03	N2	N3	20	5.72	ARG7H1RX 185 mmq
D1_03_04	N3	N4	20	4.1	ARG7H1RX 120 mmq
D1_04_05	N4	N5	20	2.3	line Cu 70 mmq
D1_05_06	N5	N6	20	3.2	line Cu 25 mmq
D2_02_07	N2	N7	20	4.3	ARG7H1RX 185 mmq
D2_07_08	N7	N8	20	4	ARG7H1RX 185 mmq
D2_08_09	N8	N9	20	3.9	ARG7H1RX 185 mmq
D2_09_10	N9	N10	20	4.2	line Cu 70 mmq
D2_10_11	N10	N11	20	3.4	line Cu 70 mmq
D2_11_12	N11	N12	20	4.3	line Cu 25 mmq

Table F.2: Transformer data.

name	from	to	V_1[kV]	V_2[kV]	type (ID)
trafo1	N1	N2	132	20	t_40_155_044

Table F.3: Generators data.

name	bus	type	type (ID)	V_n[kV]
AT	N1	SL	sl	20
GD4	N4	PQ	G55-0inv	20
GD5	N5	PQ	G31-0inv	20
GD8	N8	PQ	G67-0inv	20
GD9	N9	PQ	G31-0inv	20
GD10	N10	PQ	G31-0inv	20
GD11	N11	PQ	G31-0inv	20
GD12	N12	PQ	G55-0inv	20

Table F.4: Loads data.

name	bus	type (ID)	V_n[kV]
C03	N3	l_2009	20
C04	N4	l_1810	20
C05	N5	l_1007	20
C06	N6	l_1512	20
C07	N7	l_2009	20
C08	N8	l_3214	20
C09	N9	l_0904	20
C10	N10	l_1508	20
C11	N11	l_0904	20
C12	N12	l_1007	20

G 38-bus 20-kV test case for the token ring like procedure

Data of test case used in chapter 6. Refer to tables in appendix H for component types data.

Table G.1: Transformer data.

name	from	to	V_1[kV]	V_2[kV]	type (ID)
trafo1	N1	N2	132	20	t_40_13_1

Table G.2: Generators data.

name	bus	LS, PQ, PV	type (ID)	V_n[kV]
AT	N1	SL	sl	20
GD4	N4	PQ	G55-0inv	20
GD8	N8	PQ	G31-0inv	20
GD11	N11	PQ	G55-0inv	20
GD14	N14	PQ	G31-0inv	20
GD18	N18	PQ	G55-0inv	20
GD21	N21	PQ	G89-0	20
GD24	N24	PQ	G55-0inv	20

Table G.3: Branches data.

name	from	to	V_n[kV]	length [km]	type (ID)
D1_02_03	N2	N3	20	1.88	ARG7H1RX 185 mmq
D1_03_04	N3	N4	20	1.62	ARG7H1RX 185 mmq
D1_04_05	N4	N5	20	0.53	ARG7H1RX 185 mmq
D1_05_06	N5	N6	20	1.28	ARG7H1RX 185 mmq
D1_06_07	N6	N7	20	1.62	ARG7H1RX 185 mmq
D1_07_08	N7	N8	20	0.53	ARG7H1RX 185 mmq
D1_08_09	N8	N9	20	2	ARG7H1RX 185 mmq
D1_09_10	N9	N10	20	2.4	ARG7H1RX 185 mmq
D1_10_11	N10	N11	20	2.25	ARG7H1RX 185 mmq
D1_11_12	N11	N12	20	0.76	ARG7H1RX 185 mmq
D1_12_13	N12	N13	20	1.87	line Cu 25 mmq
D1_12_15	N12	N15	20	1.19	ARG7H1RX 120 mmq
D1_13_14	N13	N14	20	1.28	line Cu 25 mmq
D1_15_16	N15	N16	20	0.8	ARG7H1RX 120 mmq
D1_16_17	N16	N17	20	3	line Cu 25 mmq
D1_17_18	N17	N18	20	4	line Cu 25 mmq
D2_02_19	N2	N19	20	3.6	ARG7H1RX 185 mmq
D2_19_20	N19	N20	20	3.3	ARG7H1RX 185 mmq
D2_20_21	N20	N21	20	2.4	line Cu 70 mmq
D2_21_22	N21	N22	20	3.6	line Cu 70 mmq
D2_22_23	N22	N23	20	3	line Cu 70 mmq
D2_22_28	N22	N28	20	2.4	ARG7H1RX 70 mmq
D2_23_24	N23	N24	20	3.08	line Cu 70 mmq
D2_24_25	N24	N25	20	1.65	line Cu 25 mmq
D2_25_26	N25	N26	20	1.8	line Cu 25 mmq
D2_26_27	N26	N27	20	2.2	line Cu 70 mmq
D2_28_29	N28	N29	20	2.2	line Cu 25 mmq
D3_02_30	N2	N30	20	2.6	ARG7H1RX 185 mmq
D3_30_31	N30	N31	20	2.7	ARG7H1RX 185 mmq
D3_31_32	N31	N32	20	2.4	ARG7H1RX 185 mmq
D3_32_33	N32	N33	20	1.87	ARG7H1RX 120 mmq
D3_32_34	N32	N34	20	1.19	ARG7H1RX 120 mmq
D3_33_35	N33	N35	20	1.28	line Cu 70 mmq
D3_34_36	N34	N36	20	0.8	ARG7H1RX 120 mmq
D3_35_37	N35	N37	20	3	ARG7H1RX 120 mmq
D3_36_38	N36	N38	20	4	line Cu 25 mmq

Table G.4: Loads data.

name	bus	type (ID)	V_n[kV]	name	bus	type (ID)	V_n[kV]
C_1_03	N3	l_1	20	C_2_25	N25	l_21	20
C_1_04	N4	l_2	20	C_2_26	N26	l_2	20
C_1_05	N5	l_3	20	C_2_27a	N27	l_23	20
C_1_06	N6	l_4	20	C_2_27b	N27	l_24	20
C_1_07	N7	l_5	20	C_2_27c	N27	l_23	20
C_1_08	N8	l_6	20	C_2_28	N28	l_26	20
C_1_09	N9	l_7	20	C_2_29	N29	l_27	20
C_1_10	N10	l_8	20	C_3_30	N30	l_16	20
C_1_11	N11	l_7	20	C_3_31	N31	l_5	20
C_1_11b	N11	l_15	20	C_3_32	N32	l_20	20
C_1_13	N13	l_10	20	C_3_33	N33	l_7	20
C_1_14	N14	l_11	20	C_3_34	N34	l_15	20
C_1_15	N15	l_12	20	C_3_34b	N34	l_17	20
C_1_16b	N16	l_6	20	C_3_35	N35	l_21	20
C_1_17	N17	l_14	20	C_3_36	N36	l_24	20
C_1_18	N18	l_15	20	C_3_36b	N36	l_5	20
C_2_19	N19	l_16	20	C_3_37	N37	l_27	20
C_2_20	N20	l_17	20	C_3_37b	N37	l_2	20
C_2_21	N21	l_17	20	C_3_38	N38	l_3	20
C_2_23	N23	l_19	20	C_3_38b	N38	l_5	20
C_2_24	N24	l_20	20				

H Electric components data

Table H.1: Kilometric parameters of cables and lines.

ID	length [km]	kilometric resistance [Ω/km]	kilometric inductance [mH/km]	kilometric capacitance [nF/km]	max current [A]
Al 240 cable	0.125	0.335	360	0	400
Al 150 cable	0.206	0.382	340	0	280
Al 95 cable	0.320	0.406	290	0	200
Cu 35 line	0.519	1.229	9	0	180
Cu 70 line	0.268	1.165	10	0	280
Cu 50 line	0.352	1.225	9	0	235
ARG7H1RX 185 mmq	0.218	0.350	290	0	360
ARG7H1RX 120 mmq	0.333	0.382	250	0	280
line Cu 25 mmq	0.720	1.389	8	0	140
line Cu 70 mmq	0.268	1.286	9	0	280
ARG7H1RX 70 mmq	0.580	0.414	210	0	200

Table H.2: Transformers parameters.

ID	v_{cc}[%]	p_{cc}[%]	S [MVA]	OLTC
t_40_155_044	15.5	0.44	40	$\pm 12x0.75\%$
t_40_13_1	13.0	1.00	40	$\pm 8x0.02\%$

Table H.3: Generator types data (percentage values refer to the allowed variation depending on actual generation values).

ID	P [W]	Q [VAR]	P limits [W]	Q limits [VAR]
G55-0inv	4125000	0	±4125000	±4125000
G31-0inv	3100000	0	±3100000	±3100000
G89-0	8900000	0	±8900000	±8900000
G67-0inv	6750000	0	±6750000	±6750000
G675_0	6750000	0	±0	±0
G42_0	4200000	0	±0	±0
G415_2	4150000	2070000	±0	±0
G53_0	5300000	0	±0	±0
G345_0	3450000	0	±0	±0
EO	10000000	0	±0	±0
Eo_8	6000000	4000000	100%-0%	100%-95%
Id_42	4200000	1850000	100%-0%	100%-95%
Pv_67	6750000	0	100%-0%	100%-95%
In_42	3150000	2363000	100%-0%	100%-95%
EH_gen	0	0	100%-0%	100%-95%
sl	–	–	±∞	±∞

Table H.4: Loads types data.

ID	P [W]	Q [VAR]	ID	P [W]	Q [VAR]
l_1	2000000	968644.3	l_1810	1830000	1022000
l_2	500000	242161.1	l_1512	1500000	1230000
l_3	261800	175930.7	l_2009	2000000	960000
l_4	1400000	678051.1	l_3214	3200000	1420000
l_5	150000	100800.6	l_1508	1500000	824000
l_6	450000	217945	l_0904	970000	450000
l_7	125000	84000.51	l_1007	1000000	714000
l_8	320000	154983.1	L325_162	3250000	1620000
l_9	125000	84000.51	L252_126	2520000	1260000
l_10	132000	88704.5	L392_196	3920000	19600004
l_11	120000	80640.4	L384_192	3840000	19200009
l_12	100000	67200.4	L1762_092	1762000	9200001
l_13	550000	266377.	L2321_112	2321000	11200002
l_14	400000	193728.	L2762_1337	2762000	13370009
l_15	950000	460106	L122_091	1220000	910000
l_16	250000	168001	L122_067	1220000	670000
l_17	190000	127680.8	L97_438	970000	438000
l_18	190000	127680.8	L543_275	543000	275000
l_19	350000	169512.8	L61_34	610000	340000
l_20	180000	120960.7	L21_774	2100000	774000
l_21	190000	127680.8	L1891_878	1891000	878000
l_22	500000	242161.1	2069MVAR	1830000	1022000
l_23	350000	235201.4	0304MVAR	252000	170000
l_24	1000000	484322.2	0759MVAR	1630000	824000
l_25	350000	235201.4	1714MVAR	1252000	1170000
l_26	150000	99152.53	3202MVAR	2920000	1315000
l_27	200000	96864.44	2823MVAR	2762000	584000
l_28	250000	168001	2238MVAR	2100000	774000
l_29	150000	100800.6			
l_30	180000	120960.7			
l_31	900000	435889.9			

Table H.5: Load daily charts: for each daily chart, coefficients for both active and reactive power profiles are provided.

	COMMER		BIGINDRES		BIGIND		INDreside		INDoff		TER	
	P	Q	P	Q	P	Q	P	Q	P	Q	P	Q
0	0.10	0.10	0.63	0.51	0.85	0.85	0.40	0.16	0.04	0.04	0.17	0.17
1	0.10	0.10	0.48	0.45	0.85	0.85	0.10	0.04	0.04	0.04	0.17	0.17
2	0.10	0.10	0.49	0.46	0.87	0.87	0.10	0.04	0.04	0.04	0.17	0.17
3	0.10	0.10	0.49	0.46	0.88	0.88	0.10	0.04	0.04	0.04	0.17	0.17
4	0.10	0.10	0.50	0.47	0.89	0.89	0.10	0.04	0.04	0.04	0.17	0.17
5	0.14	0.14	0.66	0.54	0.91	0.91	0.40	0.16	0.04	0.04	0.17	0.17
6	0.18	0.18	0.76	0.58	0.92	0.92	0.60	0.24	0.08	0.08	0.17	0.17
7	0.60	0.60	0.97	0.67	0.94	0.94	1.00	0.40	0.18	0.18	0.44	0.44
8	0.80	0.80	0.94	0.67	0.97	0.97	0.90	0.36	0.40	0.40	0.70	0.70
9	0.92	0.92	0.70	0.58	1.00	1.00	0.40	0.16	0.48	0.48	0.87	0.87
10	1.00	1.00	0.65	0.56	1.00	1.00	0.30	0.12	0.50	0.50	0.87	0.87
11	1.00	1.00	0.65	0.56	1.00	1.00	0.30	0.12	0.50	0.50	0.83	0.83
12	0.99	0.99	0.65	0.56	1.00	1.00	0.30	0.12	0.49	0.49	0.78	0.78
13	0.99	0.99	0.65	0.56	1.00	1.00	0.30	0.12	0.48	0.48	0.78	0.78
14	0.99	0.99	0.64	0.55	0.98	0.98	0.30	0.12	0.44	0.44	0.79	0.79
15	0.98	0.98	0.64	0.55	0.97	0.97	0.30	0.12	0.32	0.32	0.83	0.83
16	0.82	0.82	0.65	0.56	1.00	1.00	0.30	0.12	0.20	0.20	0.87	0.87
17	0.66	0.66	0.68	0.57	1.00	1.00	0.35	0.14	0.16	0.16	0.87	0.87
18	0.50	0.50	0.70	0.58	0.99	0.99	0.40	0.16	0.16	0.16	0.87	0.87
19	0.40	0.40	0.97	0.69	0.99	0.99	0.95	0.38	0.12	0.12	0.78	0.78
20	0.15	0.15	1.00	0.70	1.00	1.00	1.00	0.40	0.08	0.08	0.61	0.61
21	0.13	0.13	1.00	0.70	1.00	1.00	1.00	0.40	0.04	0.04	0.35	0.35
22	0.12	0.12	0.96	0.66	0.91	0.91	1.00	0.40	0.04	0.04	0.26	0.26
23	0.10	0.10	0.91	0.64	0.91	0.91	0.90	0.36	0.04	0.04	0.17	0.17
24	0.10	0.10	0.63	0.51	0.85	0.85	0.40	0.16	0.04	0.04	0.17	0.17

Table H.6: Generator daily charts: for each daily chart, coefficients for both active and reactive power profiles are provided.

	PV		MIDIDRO		EO2		IDROEL		EO3		MIDIND	
	P	Q	P	Q	P	Q	P	Q	P	Q	P	Q
0	0.00	0	0.25	0.25	0.11	0.00	0.00	0.00	0.79	0.00	0.50	0.50
1	0.00	0	0.24	0.24	0.21	0.00	0.00	0.00	0.86	0.00	0.48	0.48
2	0.00	0	0.24	0.24	0.49	0.00	0.00	0.00	0.80	0.00	0.48	0.48
3	0.02	0	0.25	0.25	0.66	0.00	0.00	0.00	0.65	0.00	0.49	0.49
4	0.07	0	0.26	0.26	0.74	0.00	0.00	0.00	0.51	0.00	0.51	0.51
5	0.16	0	0.27	0.27	0.54	0.00	0.00	0.00	0.16	0.00	0.53	0.53
6	0.26	0	0.37	0.37	0.57	0.00	0.20	0.20	0.02	0.00	0.54	0.54
7	0.35	0	0.47	0.47	0.26	0.00	0.20	0.20	0.08	0.00	0.73	0.73
8	0.43	0	0.61	0.61	0.17	0.00	0.30	0.30	0.04	0.00	0.92	0.92
9	0.48	0	0.62	0.62	0.01	0.00	0.30	0.30	0.00	0.00	0.94	0.94
10	0.50	0	0.84	0.84	0.10	0.00	0.70	0.70	0.00	0.00	0.97	0.97
11	0.50	0	0.85	0.85	0.30	0.00	0.70	0.70	0.01	0.00	1.00	1.00
12	0.47	0	0.99	0.99	0.06	0.00	1.00	1.00	0.01	0.00	0.98	0.98
13	0.42	0	0.73	0.73	0.05	0.00	0.50	0.50	0.13	0.00	0.96	0.96
14	0.35	0	0.72	0.72	0.07	0.00	0.50	0.50	0.13	0.00	0.94	0.94
15	0.25	0	0.76	0.76	0.01	0.00	0.60	0.60	0.48	0.00	0.92	0.92
16	0.15	0	0.76	0.76	0.01	0.00	0.60	0.60	0.78	0.00	0.92	0.92
17	0.07	0	0.74	0.74	0.01	0.00	0.60	0.60	0.59	0.00	0.87	0.87
18	0.02	0	0.77	0.77	0.04	0.00	0.70	0.70	0.08	0.00	0.83	0.83
19	0.00	0	0.60	0.60	0.00	0.00	0.40	0.40	0.13	0.00	0.80	0.80
20	0.00	0	0.40	0.40	0.01	0.00	0.10	0.10	0.10	0.00	0.70	0.70
21	0.00	0	0.40	0.40	0.03	0.00	0.10	0.10	0.28	0.00	0.70	0.70
22	0.00	0	0.35	0.35	0.04	0.00	0.00	0.00	0.25	0.00	0.70	0.70
23	0.00	0	0.35	0.35	0.18	0.00	0.00	0.00	0.14	0.00	0.70	0.70
24	0.00	0	0.25	0.25	0.11	0.00	0.00	0.00	0.10	0.00	0.50	0.50

Bibliography

[1] Directorate-General for Research Sustainable Energy Systems. European smartgrids technology platform - vistion and strategy fro europe's electricity networks of the future. EUR 22040, 2006.

[2] M. Liserre, T. Sauter, and J.Y. Hung. Future energy systems: Integrating renewable energy sources into the smart power grid through industrial electronics. *Industrial Electronics Magazine, IEEE*, 4(1):18 –37, march 2010.

[3] H. Farhangi. The path of the smart grid. *Power and Energy Magazine, IEEE*, 8(1):18 –28, january-february 2010.

[4] G. Chicco and P. Mancarella. Trigeneration primary energy saving evaluation for energy planning and policy development. *Energy Policy*, 35(12):6132–6144, 2007.

[5] G. Andersson, G. Koeppel, and A.C. Zambroni de Souza. The influence of combined power, gas, and thermal networks in the reliability of supply. In *The Sixth World Energy System Conference*, Torino and Italy, 2006.

[6] G. Andersson, M. Geidl, K. Hemmes, and J.L. ZachariahWolff. Towards multisource multiproduct energy systems. *ScienceDirect and International Journal of Hydrogen Energy*, 32:1332–1338, 2007.

[7] P. Favre-Perrod, M. Geidl, B. Klöck, and G. Koeppel. A greenfield approach for future power systems. In *International Council on Large Electric Systems (CIGRÉ) 2006*, Paris and France, 2007.

[8] L. Carradore and F. Bignucolo. Distributed multi-generation and application of the energy hub concept in future networks. In *Universities Power Engineering Conference, 2008. UPEC 2008. 43rd International*, pages 1 –5, sept. 2008.

[9] G. Delille, B. François, G. Malarange, and J.L. Fraisse. Energy storage systems in distribution grids: new assets to upgrade distribution networks abilities. *IET Conference Publications*, 2009(CP550):493–493, 2009.

[10] G. Koeppel, M. Geidl, and G. Andersson. Value of storage devices in congestion constrained distribution networks. In *International Conference on Power System Technology*, Singapore, 2004.

[11] G. Koeppel and M. Korpas. Using storage devices for compensating uncertainties caused by non-dispatchable generators. In *Probabilistic Methods Applied to Power Systems, 2006. PMAPS 2006. International Conference on*, pages 1 –8, june 2006.

[12] A. Ter-Gazarian. *Energy Storage for Power Systems*. IET Energy Series 6, 2008.

[13] D. Linden and T.B. Reddy. *Handbook of batteries – 3rd edition*. McGraw-Hill Handbooks, 2001.

[14] Operating the electricity transmission networks in 2020. https://www.nationalgrid.com/, 2009.

[15] Federal Energy Regulatory Commission. Principles for efficient and reliable - reactive power supply and consumption.

[16] Inc. 1984-2008 The MathWorks. Matlab help.

[17] G. Andersson, P. Favre-Perrod, K. Fröhlich, M. Geidl, B. Klöckl, and G. Koeppel. The energy hub a powerful concept for future energy systems. In *Third annual Carnegie Mellon Conference on the Electricity Industry*, 2007.

[18] G. Andersson and M. Geidl. A modeling and optimization approach for multiple energy carrier power flow. In *PowerTech 2005*, St. Petersburg and Russia, 2005.

[19] G. Andersson and M. Geidl. Operational and structural optimization of multicarrier energy systems. *European Transactions on Electrical Power 2006*, 16:463–477, 2006.

[20] G. Andersson and M. Geidl. Optimal coupling of energy infrastructures. In *PowerTech Conference 2007*, 2007.

[21] B. Klöckl and P. Favre-Perrod. On the influence of demanded power upon the performance of energy storage devices. In *EPE-PEMC*, Riga, 2004.

[22] M. Geidl. *Integrated Modeling and Optimization of Multi-Carrier Energy Systems*. PhD thesis, ETH - Eidgenössische Technische Hochschule Zürich - Swiss Federal Institute of Technology Zurich, 2007.

[23] G. Andersson. Modelling and analysis of electric power systems. Lectures 35–526, ITET ETH Zürich, 2003.

[24] J.A. Momoh. *Electric Power System Applications of Optimization*. CRC Press: Taylor & Francis, 2009.

[25] A. Paolucci. *Lezioni di trasmissione dell'energia elettrica*. CLEUP Editore, 2000. in italian.

[26] C. Unsihuay, J.W. Marangon Lima, and A.C. Zambroni de Souza. Modeling the integrated natural gas and electricity optimal power flow. In *Power Engineering Society General Meeting*, 2007.

[27] E. Shashi Menon. *Gas pipeline hydraulics*. Boca Raton [etc.]: Taylor & Francis, 2005.

[28] Seungwon An, Qing Li, and T.W. Gedra. Natural gas and electricity optimal power flow. In *Transmission and Distribution Conference and Exposition, 2003 IEEE PES*, volume 1, pages 138 – 143 Vol.1, sept. 2003.

[29] B. Awad, M. Chaudry, J. Wu, and N. Jenkins. Integrated optimal power flow for electric power and heat in a microgrid. In *Electricity Distribution - Part 1, 2009. CIRED 2009. 20th International Conference and Exhibition on*, pages 1 –4, june 2009.

[30] T. Altman and P.F. Boulos. Convergence of newton method in nonlinear network analysis. *Mathl. Comput. Modelling*, 21:35–41, 1995.

[31] M. Geidl and G. Andersson. Optimal power flow of multiple energy carriers. *Power Systems, IEEE Transactions on*, 22(1):145 –155, feb. 2007.

[32] M. Geidl and G. Andersson. Optimal power dispatch and conversion in systems with multiple energy carriers. In *15th PSCC*, Liege, 2005.

[33] L. Carradore and R. Turri. Modeling and simulation of multi-vector energy systems. In *PowerTech, 2009 IEEE Bucharest*, pages 1 –7, 2009.

[34] L. Carradore, R. Turri, L.M. Cipcigan, and P. Papadopoulos. Electric vehicles as flexible energy storage systems in power distribution networks. In *Ecologic Vehicles Renewable Energies (EVER) 2010*, Monte Carlo, Monaco, 2010.

[35] F. Bignucolo, R. Caldon, L. Carradore, A. Sacco, and R. Turri. Role of storage systems and market based ancillary services in active distribution networks management. In *International Council on Large Electric Systems (CIGRÉ 2010*, Paris, France, 2010.

[36] M. Shahidehpour, Y. Fu, and T. Wiedman. Impact of natural gas infrastructure on electric power systems. In *Proceedings of the IEEE*, volume 93, may 2004.

[37] R. Caldon, A. Rossi Patria, and R. Turri. Optimization algorithm for a virtual power plant operation. In *Universities Power Engineering Conference*, 2004.

[38] J. Baker. New technology and possible advances in energy storage. *Energy Policy*, 36:4368–4373, 2008.

[39] M. Benini, M. Marracci, R. Martini, and D. Poli. Transmission tariffs in deregulated electric systems: a review of criteria for their definition. In *The Sixth World Energy System Conference*, Torino and Italy, 2006.

[40] G. Chicco and P. Mancarella. Distributed multi-generation: a comprehensive view. *ScienceDirect and Renewable and Sustainable Energy Reviews*, 13:535–551, 2009.

[41] J. Baker. New technology and possible advances in energy storage. *Energy Policy*, 36:4368–4373, 2008.

[42] T. Sels, C. Dragu, T. Van Craenenbroeck, and R. Belmans. Electrical energy storage systems: existing system versus newest systems - an overview. In *Power generation and sustainable development*, Liège and Belgium, 2001.

[43] D. Poli, S. Barsali, L. Carradore, R. Turri, and S. Scalari. Integration of process-side energy storage and active distribution networks: technical and economical optimisation. In *CIRED 2009*, Prague, 2009.

[44] El-Samahy, I., Bhattacharya, K., Canizares, and C.A. A unified framework for reactive power management in deregulated electricity markets. In *Power Systems Conference and Exposition and 2006. PSCE '06. 2006 IEEE PES*, pages 901 –907, nov. 2006.

[45] L. Carradore and R. Turri. Optimal co-ordinated operation of distributed multi-generation in active distribution networks. In *Universities Power Engineering Conference (UPEC), 2009 Proceedings of the 44th International*, Glasgow and Scotland and UK, 2009.

[46] L. Bano and A. Lorenzoni. Sostenere con efficienza le rinnovabili. *AIET*, 6:12 – 19, 2008. in italian.

[47] B. Kramer, S. Chakraborty, and B. Kroposki. A review of plug-in vehicles and vehicle-to-grid capability. In *Industrial Electronics and 2008. IECON 2008. 34th Annual Conference of IEEE*, 2008.

[48] M. Geidl and G. Andersson. How to avoid an electric shock. electric cars: from hype to reality. 2009 European Federation for Transport and Environment AISBL, 2009.

[49] G.A. Putrus, P. Suwanapingkarl, E.C. Bentley D. Johnson, and M. Narayana. Impacts of electric vehicles on power distribution networks. In *5th IEEE Vehicle Power and Propulsion Conference*, Michigan and Dearborn and USA, 2009.

[50] P. Papadopoulos, L.M. Cipcigan, N. Jenkins, and I. Grau. Distribution networks with electric vehicles. In *Universities Power Engineering Conference (UPEC), 2009 Proceedings of the 44th International*, Glasgow and Scotland and UK, 2009.

[51] Schneider K., Gerkensmeyer C., Kintner-Meyer M., and Fletcher R. Impact assessment of plug-in hybrid vehicles on pacific northwest distribution systems. In *Power and Energy Society General Meeting - Conversion and Delivery of Electrical Energy in the 21st Century*, Pittsburgh and PA, 2008.

[52] W. Kempton and J. Tomić. Vehicle-to-grid power fundamentals: Calculating capacity and net revenue. *Journal of Power Sources*, 144:268–279, feb. 2005.

[53] W. Kempton and J. Tomić. Vehicle-to-grid power implementation: From stabilizing the grid to supporting large-scale renewable energy. *Jurnal of power source*, 144(1):280–294, feb. 2005.

[54] M.C. Kisacikoglu, B. Ozpineci, and L.M. Tolbert. Examination of a PHEV bidirirectional charger system for V2G reactive power compensation. In *Twenty-Fifth Annual IEEE*, 2010.

[55] Assessment of plug-in electric vehicle integration with ISO/RTO systems, 2010. Produced for the ISO/RTO Council in conjunction with Taratec.

[56] Electrification Coalition. Electrification roadmap - revolutionizing transportation and achieving energy security. http://www.electrificationcoalition.org/, 2009.

[57] Coulomb technologies. http://www.coulombtech.com/.

[58] Nissan zero emission. http://www.nissan-zeroemission.com/.

[59] S.B. Peterson, J.F. Whitacre, and J. Apt. The economics of using plug-in hybrid electric vehicle battery packs for grid storage. *Journal of Power Sources*, 195:2377–2384, 2010.

[60] J. Taylor, A. Maitra, M. Alexander, D. Brooks, and M. Duvall. Evaluation of the impact of plug-in electric vehicle loading on distribution system operations. In *Power Energy Society General Meeting, 2009. PES '09. IEEE*, pages 1 –6, july 2009.

[61] M. De Nigris, I. Gianinoni, S. Grillo, S. Massucco, and F. Silvestro. Impact evaluation of plug-in electric vehicles (pev) on electric distribution networks. In *Harmonics and Quality of Power (ICHQP), 2010 14th International Conference on*, pages 1 –6, sept. 2010.

[62] J.C. Gómez and M.M. Morcos. Impact of EV battery chargers on the power quality of distribution systems. *IEEE Transactions on Power Delivery*, 18(3), 2003.

[63] P.H. Andersen, J.A. Mathews, and M. Rask. Integrating private transport into renewable energy policy: The strategy of creating intelligent recharging grids for electric vehicles. *Energy Policy*, 37:2481–2486, 2009.

[64] I. Cvetkov, T. Thacker, D. Dong, G. Francis, V. Podosinov, D. Boroyevich, F. Weng, R. Burgos, G. Skutt, and J. Lesko. Future home uninterruptible renewable energy system with vehicle-to-grid technology. In *Energy Conversion Congress and Exposition and 2009*, Sept 2009.

[65] Better place. http://www.betterplace.com/.

[66] Lithium force. http://www.lithiumforce.com/index.html.

[67] X. Zhong, A. Cruden, D. Infield, P. Holik, and S. Huang. Assessment of vehicle to grid power as power system support. In *Universities Power Engineering Conference (UPEC), 2009 Proceedings of the 44th International*, Glasgow and Scotland and UK, 2009.

[68] Is there still a (better) place for automotive battery swapping? http://m.rumors.automobilemag.com/6720849/green/is-there-still-a-better-place-for-automotive-battery-swapping/index.html.

[69] R. Pratt, M. Kintner-Meyer, K. Schneider, M. Scott, D. Elliott, and M. Warwick. Potential impacts of high penetration of plug-in hybrid plug-in vehicles on the u.s. power grid. In *DOE/EERE PHEV Stakeholder Workshop*, Washington DC and USA, 2007.

[70] Department for Business Enterprise and Regulatory Reform: Department for Transport. Investigation into the scope for the transport sector to switch to electric vehicles and plug-in hybrid vehicles, 2008.

[71] J. Goldman. http://archive.electricdrive.org/index.php?tg=fileman&idx=get&inl=1&id=3&gr=Y&path=Workshops%2FFlorida+Workshop&file=Goldman.PDF, 2002.

[72] A. Simpson. A new dimension for its: Plug in vehicles with smart grids. http://www.itssummit.com.au/Portals/58/Andrew%20Simpson.pdf and Australian ITS Summit, 2009.

[73] A.S. Tanenbaum. *Reti di calcolatori*. Pearson Education Italia, 2003. italian book.

[74] P. Lagonotte, J.C. Sabonnadière, J.Y. Léost, and J.P. Paul. Structural analysis of the electrical system: application to secondary voltage control in france. *IEEE Transactions on Power Systems*, 4, 1989.

[75] J. Zhong, E. Nobile, A. Bose, and K. Bhattachardya. Localized reactive power markets using the concept of voltage control areas. In *Power Engineering Society General Meeting and 2006. IEEE*, Montreal and Que, 2004.

[76] S.H. Song, H.C. Lee, Y.T. Yoon, and S.I. Moon. Cluster design compatible with market for effective reactive power management. In *Power Engineering Society General Meeting and 2006. IEEE*, Montreal and Que, 2004.

[77] A. Kumar, S.C. Srivastava, and S.N. Singh. A zonal congestion management approach using ac transmission congestion distribution factors. *Electric Power System Research*, 72:85–93, 2004.

[78] L. Carradore and R. Turri. A token ring procedure for distributed co-ordinated regulation of active mv networks. In *Harmonics and Quality of Power (ICHQP), 2010 14th International Conference on*, pages 1 –7, sept. 2010.